

---

---

# Efficient Method of Estimating Direction of Arrival (DOA) In Communications Systems

---

---

Masters Dissertation

**Bongani Prudence Nxumalo**

A dissertation submitted in fulfilment of the requirement for the  
degree of

**MASTERS OF SCIENCE IN ENGINEERING  
(ELECTRONIC ENGINEERING)**



Discipline of Electrical, Electronic & Computer Engineering  
Durban  
South Africa

Dissertation submitted August, 2021

---

---

# **Efficient Method of Estimating Direction of Arrival (DOA) In Communications Systems**

---

---

**Bongani Prudence Nxumalo**

**Supervisor:** Professor Tom Mmbasu Walingo

A dissertation submitted in fulfilment of the requirement for the  
degree of

**MASTERS OF SCIENCE IN ENGINEERING  
(ELECTRONIC ENGINEERING)**



Discipline of Electrical, Electronic & Computer Engineering  
University of KwaZulu-Natal  
South Africa

Dissertation submitted August, 2021

As the candidate's supervisor, I have approved this dissertation for submission.

Signed.....Date.....24/01/2022.....

Name: Professor Tom Mmbasu Walingo

# Declaration 1 - Plagiarism

I, **Bongani Prudence Nxumalo**, declare that;

1. The research reported in this dissertation, except where otherwise indicated, is my original research.
2. This dissertation has not been submitted for any degree or examination at any other university.
3. This dissertation does not contain other persons' data, pictures, graphs or other information, unless specifically acknowledged as being sourced from other persons.
4. This dissertation does not contain other persons' writing, unless specifically acknowledged as being sourced from other researchers. Where other written sources have been quoted, then:
  - (a) Their words have been re-written but the general information attributed to them has been referenced.
  - (b) Where their exact words have been used, then their writing has been placed in italics and inside quotation marks, and referenced.
5. This dissertation does not contain text, graphics or tables copied and pasted from the Internet, unless specifically acknowledged, and the source being detailed in the dissertation and in the references sections.

Signed.....Date.....24/01/2022.....

# Declaration 2 - Publication

The following papers emanating from this work have either been published or are under review:

1. **Bongani Prudence Nxumalo** and **Tom Walingo**, “Direction of Arrival (DOA) Estimation for Smart Antennas in Weather Impacted Environments ”, Progress In Electromagnetics Research (PIER), 2019
2. **Bongani Prudence Nxumalo** and **Tom Walingo**, “Performance Evaluation of DOA Algorithms for Non-uniform Linear Arrays in a Weather-Impacted Environment”, Earth and Space Science Open Archive (ESSOAr), (Under Review).

# Dedication

Above all, all thanks goes to the almighty God. I dedicate this research dissertation to my family, my late mother Goodness Jane Nyathi, my sister Ntwanano Nxumalo, my son Kevin Nxumalo and my wife Potlake Mathapelo Mokgoatsane.

# Acknowledgements

I wish to extend my sincere gratitude and appreciation to God and all the individuals who gave their full support and assistance in many ways during this work. I am greatly indebted to my supervisor, Prof Tom Walingo for his wise and expert guidance, constructive corrections, comments, and encouragement that contributed to the completion of the study. I would like to thank Prof James Okello for his support and opportunity to begin this study at first.

To my family, without their love, care and support, nothing would have been possible, no words can express the appreciation, love and thanks I have for you, you will forever reside in my heart. I would like to thank the University of KwaZulu Natal, CRART center and Armaments Corporation of South Africa (ARMSCOR) for all the financial support you provided me with, may you continue to support and empower many more to come. To all my friends, colleagues "Inkomu". To all the reviewers thank you for all the hard work you have invested into making this work a success. Finally, to my mother Goodness Nyathi, my sister Ntwanano Nxumalo and my son Kevin Nxumalo, thank you for believing in me and I dedicate this work to you.

# Abstract

In wireless communications systems, estimation of Direction of Arrival (DOA) has been used both for military and commercial purposes. The signal whose DOA is being estimated, could be a signal that has been reflected from a moving or stationary object, or a signal that has been generated from unwanted or illegal transmitter. When combined with estimating time of arrival, it is also possible to pinpoint the location of a target in space. Localization in space can also be achieved by estimating DOA using two receiving nodes with capability of estimating DOA. The beamforming pattern in smart antenna system is adjusted to emphasize the desired signal and to minimize the interference signal. Therefore, DOA estimation algorithms are critical for estimating the Angle of Arrival (AOA) and beamforming in smart antennas. This dissertation investigates the performance, angular accuracy and resolution of the Minimum Variance Distortionless Response (MVDR), Multiple Signal Classification (MUSIC) and our proposed method Advanced Multiple Signal Classification (A-MUSIC) as DOA algorithms on both Non-Uniform Array (NLA) and Uniform Linear Array (ULA). DOA is critical in antenna design for emphasizing the desired signal and minimizing interference.

The scarcity of radio spectrum has fuelled the migration of communication networks to higher frequencies. This has resulted into radio propagation challenges due to the adverse environmental elements otherwise unexperienced at lower frequencies. In rainfall-impacted environments, DOA estimation is greatly affected by signal attenuation and scattering at the higher frequencies. Therefore, new DOA algorithms cognisant of these factors need to be developed and the performance of the existing algorithms quantified. This work investigates the performance of the Conventional Minimum Variance Distortion-less Look (MVDL), Subspace DOA Estimation Methods of Multiple Signal Classification (MUSIC) and the developed hybrid DOA algorithm on a weather impacted wireless channel. The performance of the proposed Advanced-MUSIC (A-MUSIC) algorithm is compared to the conventional DOA estimation algorithms of Minimum Variance Distortionless Response (MVDR) and the Multiple Signal Classification (MUSIC) algorithms for both NLA and ULA antenna arrays. The developed simulation results show that A-MUSIC shows superior

performance compared to the two other algorithms in terms of Signal Noise Ratio (SNR) and the number of antenna elements. The results show performance degradation in a rainfall impacted communication network with the developed algorithm showing better performance degradation.

# Contents

<b>Declaration 1 - Plagiarism</b>	<b>ii</b>
<b>Declaration 2 - Publication</b>	<b>iii</b>
<b>Dedication</b>	<b>iv</b>
<b>Acknowledgements</b>	<b>v</b>
<b>Abstract</b>	<b>vi</b>
<b>List of Figures</b>	<b>xi</b>
List of Figures . . . . .	xi
<b>List of Tables</b>	<b>xiii</b>
List of Tables . . . . .	xiii
<b>List of Acronyms</b>	<b>xiv</b>
<b>Preface</b>	<b>xvii</b>
<b>I Introduction</b>	<b>1</b>
1 Evolution of Communication Networks . . . . .	4
1.1 Transmission Design of millimeter Wave (mmWave) Communication . . . . .	5
1.2 Challenges of millimeter Wave (mmWave) Communication . . . . .	6
2 Antenna Arrays . . . . .	6
2.1 Beamforming and Performance of Antenna Array Structure . . . . .	9
3 DOA Estimation Algorithms . . . . .	10
3.1 DOA Estimation Algorithm Challenges . . . . .	13
3.2 Proposed DOA Estimation Algorithm . . . . .	13

4	Radio Propagation Environment and Modelling . . . . .	14
4.1	Rain Attenuation over Communication Links . . . . .	16
4.2	Rain Attenuation model and Free Space Loss . . . . .	16
4.3	Diffraction Fading . . . . .	17
4.4	Multipath Propagation (Fading) . . . . .	18
5	Problem Statement and Motivation . . . . .	19
6	System Model . . . . .	19
7	Research Objectives . . . . .	21
8	Research Methodology . . . . .	21
9	Research Main Contributions . . . . .	22
9.1	Paper A: Direction of Arrival (DOA) Estimation for Smart Antennas in Weather Impacted Environments (Published in PIER). . . . .	22
9.2	Paper B: Performance Evaluation of DOA Algorithms for Non-uniform Linear Arrays (NLA) in a Weather Impacted Environment (Under Review in Earth and Space Science Open Archive (ESSOAr)). . . . .	22
	References . . . . .	24

**II Papers 31**

**A Direction of Arrival (DOA) Estimation for Smart Antennas in Weather Impacted Environments 32**

1	Introduction . . . . .	33
2	System Model . . . . .	35
3	Weather Channel Parameter Modelling . . . . .	37
3.1	Rainfall Modeling . . . . .	37
3.2	Attenuation Model . . . . .	40
3.3	Angle Deviation Model . . . . .	40
4	DOA Estimation Algorithms . . . . .	41
4.1	MVDR Algorithm . . . . .	41
4.2	MUSIC Algorithm . . . . .	42
4.3	Proposed A-MUSIC Algorithm . . . . .	42
5	Performance Measures . . . . .	44
6	Results and Discussion . . . . .	45
7	Conclusion . . . . .	57

References . . . . .	58
<b>B Performance Evaluation of DOA Algorithms for Non-uniform Linear Arrays in a Weather-Impacted Environment</b>	<b>61</b>
1 Introduction . . . . .	62
2 System Model . . . . .	64
3 NLA methods . . . . .	66
3.1 Co-prime Array Scheme . . . . .	67
3.2 Modified Array Interpolation Scheme . . . . .	68
4 Weather channel parameter modelling . . . . .	69
4.1 Rainfall modelling . . . . .	69
4.2 Attenuation Model . . . . .	72
4.3 Angle Deviation Model . . . . .	72
5 DOA Estimation Algorithms . . . . .	72
5.1 MVDR Algorithm . . . . .	72
5.1.1 MVDR Co-prime NLA . . . . .	73
5.1.2 MVDR Interpolation NLA . . . . .	73
5.2 MUSIC Algorithm . . . . .	74
5.2.1 MUSIC Co-prime NLA . . . . .	74
5.2.2 MUSIC Interpolation NLA . . . . .	75
5.3 A-MUSIC Algorithm . . . . .	75
5.3.1 A-MUSIC Co-prime NLA . . . . .	75
5.3.2 A-MUSIC Interpolation NLA . . . . .	77
6 Performance Measures . . . . .	78
6.1 Root Mean Square Error (RMSE) . . . . .	79
6.2 Cramer Rao Bound (CRB) . . . . .	79
6.3 DOA Estimation Algorithm complexity . . . . .	80
7 Simulation Results . . . . .	80
8 Conclusion . . . . .	92
References . . . . .	93
<b>III Conclusion</b>	<b>96</b>
1 Summary of research contribution . . . . .	97
2 Possible Future Work . . . . .	98

# List of Figures

## List of Figures

1	System model . . . . .	20
A.1	Non-uniform Linear Array (NLA) with $d = \frac{\lambda}{2} * [0, d_2, \dots, d_{(M-1)}]$ . . . . .	36
A.2	Widespread rainfall. . . . .	38
A.3	Shower rainfall. . . . .	38
A.4	Thunderstorm rainfall. . . . .	39
A.5	DOA estimation attenuation with rain rate $r = 0\text{mm/hr}$ for $N = 5$ . . . . .	46
A.6	DOA estimation attenuation at drizzle rain rate $r = 2\text{mm/hr}$ for $N = 5$ . . . . .	47
A.7	DOA estimation attenuation at widespread rain rate $r = 8\text{mm/hr}$ for $N = 5$ . . . . .	47
A.8	DOA estimation attenuation at shower rain rate $r = 20\text{mm/hr}$ for $N = 5$ . . . . .	48
A.9	DOA attenuation with rain rate $r=0\text{mm/hr}$ for $N=15$ . . . . .	49
A.10	DOA attenuation in light rain rate of $r=2\text{mm/hr}$ for $N=15$ . . . . .	50
A.11	DOA attenuation in moderate rain rate of $r=8\text{mm/hr}$ for $N=15$ . . . . .	50
A.12	DOA attenuation in heavy rain rate of $r=20\text{mm/hr}$ for $N=15$ . . . . .	51
A.13	MUSIC, MVDR and A-MUSIC Accuracy Comparison at $-20\text{dB}$ and $-40\text{dB}$ with DOA = $[20^0, 40^0, 50^0]$ . . . . .	52
A.14	DOA estimation attenuation error comparison for $N=5$ . . . . .	53
A.15	DOA estimation attenuation error comparison for $N=10$ . . . . .	54
A.16	DOA estimation attenuation error comparison for $N=20$ . . . . .	54
A.17	Comparison of DOA estimation algorithms in Non-weather and weather impacted environment. . . . .	55
A.18	Error comparison in various rain rates vs SNR. . . . .	56
A.19	Error comparison in RMSE vs number of snapshots. . . . .	57
B.1	Non-uniform Linear Array (NLA). . . . .	66

B.2	Co-prime array. . . . .	67
B.3	Widespread rainfall. . . . .	69
B.4	Shower rainfall. . . . .	70
B.5	Thunderstorm rainfall. . . . .	71
B.6	DOA estimation attenuation using Co-prime array with no rain. . . . .	82
B.7	DOA estimation attenuation using Co-prime array for widespread rainfall. . . . .	82
B.8	DOA estimation attenuation using Co-prime array for shower rainfall. . . . .	83
B.9	DOA estimation attenuation using Co-prime array for thunderstorm rainfall. . . . .	83
B.10	DOA estimation attenuation using array interpolation with no rain. . . . .	84
B.11	DOA estimation attenuation using array interpolation for widespread rainfall. . . . .	84
B.12	DOA estimation attenuation using array interpolation for shower rainfall. . . . .	85
B.13	DOA estimation attenuation using array interpolation for thunderstorm rainfall. . . . .	85
B.14	MVDR RMSE vs rain rate for coprime and array interpolation at $L=7, 10, 20$ . . . . .	86
B.15	MUSIC RMSE vs rain rate for coprime and array interpolation at $L=7, 10, 20$ . . . . .	86
B.16	A-MUSIC RMSE vs rain rate for coprime and array interpolation at $L=7, 10, 20$ . . . . .	87
B.17	DOA estimation attenuation error comparison for $L = 7$ . . . . .	88
B.18	DOA estimation attenuation error comparison for $L = 10$ . . . . .	88
B.19	DOA estimation attenuation error comparison for $L = 20$ . . . . .	89
B.20	DOA estimation using co-prime array error comparison vs SNR. . . . .	90
B.21	DOA estimation using array interpolation error comparison vs SNR. . . . .	90
B.22	DOA estimation CRB error comparison vs number of snapshots. . . . .	91
B.23	Comparison of computational complexity. . . . .	91

# List of Tables

## List of Tables

A.1	Rain Rates Categories. . . . .	37
A.2	Computational Complexity of DOA Estimation Algorithms. . . . .	45
A.3	Simulation Parameters for MVDR, MUSIC and A-MUSIC Algorithm. . . . .	45
A.4	Spectrum Performance for actual DOA = $[0^0, 10^0, 35^0, 60^0]$ . . . . .	49
A.5	Spectrum Performance for actual DOA = $[0^0, 10^0, 35^0, 60^0]$ . . . . .	52
B.1	Rain Rates Categories. . . . .	69
B.2	Computational Complexity of DOA Estimation Algorithms. . . . .	80
B.3	Simulation parameters . . . . .	81

# List of Acronyms

<b>1D</b>	<b>One-Dimensional</b>
<b>1G</b>	<b>First Generation</b>
<b>2D</b>	<b>Two-Dimensional</b>
<b>2G</b>	<b>Second Generation</b>
<b>3G</b>	<b>Third Generation</b>
<b>4G</b>	<b>Fourth Generation</b>
<b>5G</b>	<b>Fifth Generation</b>
<b>AI</b>	<b>Array Interpolation</b>
<b>AOA</b>	<b>Angle Of Arrival</b>
<b>A-MUSIC</b>	<b>Advanced Multiple Signal Classification</b>
<b>BER</b>	<b>Bit Error Rate</b>
<b>CH</b>	<b>Channel</b>
<b>CRB</b>	<b>Cramer-Rao Bound</b>
<b>DECOM</b>	<b>DOA Estimation with Combined MUSIC</b>
<b>DF</b>	<b>Direction Finding</b>
<b>DFT</b>	<b>Discrete Fourier Transform</b>
<b>DOA</b>	<b>Direction Of Arrival</b>
<b>DOAE</b>	<b>Direction Of Arrival Estimation</b>
<b>DTFT</b>	<b>Discrete Time Fourier Transform</b>

<b>ESPRIT</b>	<b>Estimation Of Signal Parameters via Rotational Invariance Technique</b>
<b>EVD</b>	<b>Eigen-Value Decomposition</b>
<b>FFT</b>	<b>Fast Fourier Transform</b>
<b>IP</b>	<b>Internet Protocol</b>
<b>ITU</b>	<b>International Telecommunication Union</b>
<b>ITU-R</b>	<b>International Telecommunication Union-Radio communication</b>
<b>LTE</b>	<b>Long Term Evolution</b>
<b>MAC</b>	<b>Meduim Access Control</b>
<b>MIMO</b>	<b>Multiple Iput Multiple Output</b>
<b>mmW</b>	<b>milimetre-Wave</b>
<b>MSE</b>	<b>Mean Square Error</b>
<b>MUSIC</b>	<b>Multiple Signal Classification</b>
<b>MVDR</b>	<b>Minimum Variance Distortionless Response</b>
<b>NLA</b>	<b>Non-Uniform Linear Array</b>
<b>NOMA</b>	<b>Non-Orthogonal Multiple Access</b>
<b>OFDMA</b>	<b>Orthogonal Frequency Division Multiple Access</b>
<b>OTHR</b>	<b>Over-The-Horizon-Radar</b>
<b>PHY</b>	<b>Physical</b>
<b>PM</b>	<b>Propagation Method</b>
<b>QoS</b>	<b>Quaity of Service</b>
<b>RDF</b>	<b>Radio Direction Finding</b>
<b>RF</b>	<b>Radio Frequency</b>
<b>RMSE</b>	<b>Root Mean Square Error</b>
<b>SNR</b>	<b>Signal to Noise Ratio</b>
<b>SVD</b>	<b>Singular -Value Decomposition</b>
<b>SWIPT</b>	<b>Simultaneous Wireless Information and Power Transfer</b>

**ULA**                    **Uniform Linear Array**

**UMTS**                **Universal Mobile Telecommunications System**

# Preface

*"We cannot seek achievement for ourselves and forget about progress and prosperity of our community. Our ambitions must be broad enough to include the aspirations and needs of others, for their sakes and for our own"*

— Cesar Chavez

Bongani Prudence Nxumalo

University of KwaZulu-Natal, January 24, 2022

# **Part I**

## **Introduction**

## **Introduction and Background**

In wireless communication systems, estimation of Direction of Arrival (DOA) has been used both for military and commercial purposes. The signal whose DOA is being estimated, could be a signal that has been reflected from a moving or stationary object, or a signal that has been generated from unwanted or illegal transmitter. When combined with estimating time of arrival, it is also possible to pinpoint the location of a target in space. Localization in space can also be achieved by estimating DOA using two receiving nodes with capability of estimating DOA. Estimation of DOA angles from multiple sources plays an important role in array processing because both the base and mobile stations can employ multiple antenna array elements and their array signal processing can increase the capacity and throughput of the system significantly. In most applications, the first task is to estimate the DOAs of incoming signals. This information can be used to localize the signal sources. DOA estimation is considered a key issue in array signal processing and thus the focus of this work.

Antenna array processing has received much attention in the last two decades. Research in this area has been applied in many fields, such as seismology [1], acoustics [2], sonar [3], radar [4], and mobile communication systems [5-7]. Signal parameter estimation using an antenna array has attracted research in mobile communications. For example, the estimation of Direction of Arrival (DOA) is an important issue in many applications, especially in cellular communications. The Direction of Arrival (DOA) estimation determines the angle at which an electromagnetic or acoustic wave arrives at an array of antennas or sensors [8]. Using an array of antennas has an advantage over single antenna in achieving an improved performance in; the overall gain, provision of diversity reception, reduction of interference from a particular direction, steering the antenna array at desired direction, and determining the DOA of the incoming signals. Furthermore, estimating the DOA of multiple source signals is very important in extracting the useful signal from a noisy and interference-prone environment. Through smart antenna systems based on appropriate spatial filtering, direction finding techniques can be used to separate the direction of the desired signal and interference signal [9]. In the last few decades, the DOA estimation has been among the most active areas of research in signal processing. Practically, it has found many applications in the field of sonar

---

and navigation, radar, radio astronomy, tracking of various objects, rescue missions, mobile communication, internet broadcasting, conferencing and other emergency assistance activities [10]. Due to its convenience and flexibility, DOA estimation has contributed a lot in the popularity of wireless communication systems. Indeed, the need of increasing the wireless capacity is very important because of over usage of low end of the spectrum which has led to the higher frequency band exploitation. With higher frequencies, higher data rate and higher user density, multipath fading and interference pose severe limitations in data transmission [11]. Thus, the localization of a signal source by DOA estimation is vital in the attempt to increase the wireless network capacity by the reduction of multipath effects and other interferences.

DOA algorithms can be classified into non-parametric methods and the high resolution classical subspace methods [12-23]. Non-parametric algorithms includes conventional beamforming and Capon's method whereas subspace-based algorithms include the MUSIC method. Most of these algorithms are based on the eigenvalue decomposition (EVD) of the cross-spectral matrix or the singular value decomposition (SVD) of the received data. These algorithms were first introduced to find the one-dimensional (1-D) DOA and further extended for the two-dimensional (2-D) DOA estimation of finding the azimuth and elevation angles for incident sources. Other algorithms have been developed to perform the 2-D estimation [24-30, 17]. The problem with these methods is finding the correct pair of azimuth and elevation angles for the multiple incident sources. To overcome this problem, many algorithms were proposed [31-34, 24], but the computational complexity for these algorithms is high. Therefore, pair matching problems are considered a key concern in 2-D DOA estimation. A new subspace method suggested by Marcos and co-workers [35-38] called the "propagator method" (PM) for array signal processing estimates of DOA does not require any EVD for the cross-spectral matrix or SVD for the received data. The goal of using 2-D, the PM is to reduce the computational complexity with only a small degradation in performance. The PM proposed for the 2-D estimation [28] based on the ESPRIT algorithm [13] requires a pair matching for azimuth, elevation angles and has failure estimation for a region of practical interest in mobile communication systems. Most of the Eigen subspace methods for estimating angles of arrival for multiple sources must know the noise covariance matrix explicitly. Moreover, most authors assume that the noise is white Gaussian noise. For non-white, they propose the prewhitening approach with the knowledge of the covariance matrix. On the other hand, some algorithms [39-41] are proposed to estimate the DOA for an unknown covariance matrix under different assumptions. In this work we focus on the signal source DOA estimation, especially on Uniform Linear Array (ULA) and Non-uniform Linear Array (NLA) configuration, with the aim of increasing its angle accuracy and its resolution. Furthermore, the performance of several DOA algorithms is investigated and the

factors that affect the accuracy and resolution of the system checked. Advanced-MUSIC (A-MUSIC) which employs the signal subspace, and the noise subspace is proposed. The proposed method, A-MUSIC, takes advantage of the signal subspace and the noise subspace, by making them orthogonal to each other through repeatedly reconstructing covariance matrix, to obtain the two noise subspaces and signal subspaces. By averaging previous results and reconstructing covariance matrixes of signals and noise, DOA is estimated through the spectrum function. The evolution of communication networks, antenna arrays, DOA estimation algorithms, challenges, radio propagation environment and modelling, problem statement and motivation, system model and contributions of this research are widely discussed in the following sections.

### **1 Evolution of Communication Networks**

Communication network technologies have evolved through different paths targeting improved performance, high efficiency, and full guaranteed Quality of Service (QoS). The first generation (1G) network used analog technologies to fulfil the fundamental basics of mobile voice, while the second generation (2G) introduced the concept of network capacity and extended coverage. The radio signals used by the 1G network were analog, while 2G networks were digital. 2G capabilities were achieved by allowing multiple users on a single channel via multiplexing. The third generation (3G) standard utilizes Universal Mobile Telecommunications System (UMTS) as its core network architecture. 3G network combines aspects of the 2G network with new technologies and protocols to deliver a significantly faster data rates. The fourth generation (4G) is a pure data wireless connection network, providing access to a wide range of end-to-end internet protocol (IP) communication services, which includes advanced services such as mobility, flexibility, reliability, and affordability. The main difference between 3G and 4G is the data rate. The key technologies that have made 4G possible are MIMO (Multiple Input Multiple Output) and OFDM (Orthogonal Frequency Division Multiplexing). The most important 4G standards are WiMAX and LTE where 4G LTE is a major improvement over 3G speeds. The fifth generation (5G) is highly anticipated to offer low-latency, high throughput and massive connectivity of billions of devices around the world. For its realization, the 5G faces the challenges of proliferation of data traffic, high energy consumption, increasing spectral resource efficiency, and power optimization. 5G uses a scalable orthogonal frequency-division multiplexing (OFDM) framework. 5G benefits greatly from this and can have latency as low as one millisecond with realistic estimates to be around 1-10 seconds. The explosive growth of new communication services such as the internet, rapid widespread proliferation of mobile communications, and the global alliance of communication carriers, following

communication deregulation in many countries, suggest that we are entering an advanced information age of true substance. The implementation of infrastructure technologies which support the basis of communication networks, such as transmission and switching, has been promoted to match the changes in social needs at good cost-performance, based on the evolution of semiconductor devices, computers and software technology [42]. The incredible demand for wireless data bandwidth shows no sign of slowing down in the foreseeable future. At the same time, the mobile data experience for users continues to expand and develop, putting an increasing strain on network use of the available wireless spectrum. With this projected growth in mind, the cellular industry looked to other frequency bands that could possibly be utilized in the development of new 5G wireless technologies. The high-frequency bands in the spectrum above 24 GHz were targeted as having the potential to support large bandwidths and high data rates, ideal for increasing the capacity of wireless networks. These high-frequency bands are often referred to as “mmWave” due to the short wavelengths that can be measured in millimeters. Although the mmWave bands extend all the way up 300 GHz, it is the bands from 24 GHz up to 100 GHz that are expected to be used for 5G. The mmWave bands up to 100 GHz are capable of supporting bandwidths up to 2 GHz, without the need to aggregate bands together for higher data throughput. These higher frequency band pose a serious challenge to signal propagation making the determination of DOA tricky.

### **1.1 Transmission Design of millimeter Wave (mmWave) Communication**

In recent years [43], millimeter wave (mmWave) communication systems have attracted significant interest regarding meeting the capacity requirements of the future 5G network. The mmWave systems have frequency ranges in between 30 GHz and 300 GHz where a total of around 250 GHz bandwidths are available. Although the available bandwidth of mmWave frequencies is promising, the propagation characteristics are significantly different from microwave frequency bands in terms of path loss, diffraction and blockage, rain attenuation, atmospheric absorption, and foliage loss behaviors. In general, the overall loss of mmWave systems is significantly larger than that of microwave systems for a point-to-point link. Fortunately, the small wavelength of mmWave frequencies enable large number of antenna elements to be deployed in the same form factor, thereby providing high spatial processing gains that can theoretically compensate for at least the isotropic path loss. Nevertheless, as mmWave systems are equipped with several antennas, a number of computation and implementation challenges arise to maintain the anticipated performance gain of mmWave systems.

### 1.2 Challenges of millimeter Wave (mmWave) Communication

There are fundamental differences between mmWave communications and existing other communication systems, in terms of high propagation loss, directivity, and sensitivity to blockage. These characteristics of mmWave communications pose several challenges towards exploiting their full potential and include; integrated circuits and system design, interference management, spatial reuse, anti-blockage, and dynamics control [44] among others. This challenges directly impact on DOA estimation. Due to the fundamental differences between mmWave communications and existing other communication systems operating in the microwaves band (e.g., 2.4 GHz and 5 GHz), there are many challenges in physical (PHY), medium access control (MAC), and routing layers for mmWave communications to make a big impact in the 5G wireless networks. The high propagation loss, directivity, sensitivity to blockage, and dynamics due to mobility of mmWave communications require new thoughts and insights in architectures and protocols to cope with these challenges and affect DOA estimation.

The challenges on the integrated circuits and system design include the nonlinear distortion of power amplifiers, phase noise, IQ imbalance, highly directional antenna design, etc. Due to the directivity of transmission, coordination mechanism becomes the key to the MAC design, and concurrent transmission (spatial reuse) should be exploited fully to improve network capacity. Typically, there are two essential challenges in mmWave DOA beamforming for mobile scenarios. Firstly, narrow beams in mmWave systems focus their transmitted power in the set direction, yet less robust to the movement as beam misalignment causes sharp connectivity loss. Secondly, the low-efficiency and time-consuming beam training scheme that appropriates network resources utilized for communication. To effectively support system design, deployment, and to tackle these challenges the following has emerged in literature; new emerging technologies for 5G systems e.g massive multiple-input multiple-output (MIMO) technologies, multiple access technologies, hybrid analog-digital precoding and combining non-orthogonal multiple access (NOMA), cell-free massive MIMO, and simultaneous wireless information and power transfer (SWIPT) technologies. New DOA estimation algorithm is another way of one way of combating the challenges on a lower scale.

## 2 Antenna Arrays

Modern antennas use a geometric arrangement of a set of two or more antenna elements for transmitting and/or receiving electromagnetic waves. These antennas are systematically connected in

such a way that their individual currents are in specific amplitude and phase relationship [45]. Smart antenna arrays allow the antenna system to be electronically directed to receive or transmit information primarily from a particular direction without mechanically moving the structure. As the field of signal processing improved, arrays could be utilized to receive energy (or information) from a particular direction while denying information or nulling out the energy in unwanted directions. Consequently, the arrays could be used to decrease the intentional interference such as jamming or unintentional interference. The main source of unintentional interference is the radiation from other sources not meant for the system in question [46]. Furthermore, the growth in signal processing led to the concept of adaptive antenna arrays. These arrays adapted their radiation or reception pattern based on the operational environment. This significantly raised the capacity available in wireless communication systems [47]. While there has been a large amount of work and development on the signal processing aspects, the physical geometry has had relatively little attention. The reason for this is in mathematical complexity when dealing with the optimization of the element positions for various situations. Array geometry optimization can be therefore expected to support the ongoing advancement performance of wireless communication system [48].

Using the array antenna has an advantage over single antenna of achieving an improved performance when applying DOA estimation algorithm. The improved performance involves an increase in the overall gain, improvement of the spatial resolution, provision of diversity reception, reduction of interference from a particular direction, steering the antenna array at desired direction, and determining the DOA of the incoming signals. Antennas with a given radiation pattern may be arranged in a pattern (line, circle, plane, etc.) to yield a different radiation pattern. For an antenna array, a configuration of multiple antennas (elements) is arranged to achieve a given radiation pattern. Some of the common geometric arrays are:

- (i) Linear array: The antenna elements are arranged along a straight line with equal spacing distance between two adjacent antenna elements.
- (ii) Non-linear array: The antenna elements arranged along a straight line with spacing distance between two adjacent antenna elements and phase difference.
- (iii) Circular array: The antenna elements arranged around a circular ring.
- (iv) Planar array - antenna elements arranged over some planar surface (example - rectangular array).
- (v) Conformal array - antenna elements arranged to conform to some non-planar surface (such as an aircraft skin). An investigation of DOA on some of the antenna configuration at migrating frequencies is important and subject of this work.

Beamforming is used along with an array of antennas sensors to transmit or receive signals to or from a specified spatial direction in the presence of interference and noise. Hence, it acts as a spatial filter [49]. It is a classic yet continuously developing field that has enormous practical applications. In the last decade, there has been renewed interest in beamforming driven by applications in wireless communications, where multiantenna techniques have emerged as one of the key technologies to accommodate the explosive growth of the number of users and rapidly increasing demands for new high data-rate services. The techniques for estimating the DOA of signals using an antenna array have been booming in recent years. Many methods exist and are classified according to the technique used, the information they require (external or not) and finally the criterion used conventional methods, projection on the noise or source subspace, maximum likelihood method. A receive beamformer is commonly used to estimate the signal arriving from a specific direction in the presence of noise and interfering signals. In a receive beamformer, the output of the array of sensors are linearly combined using spatial filter coefficients weight vector so that the signals coming from a desired direction are passed to the beamformer output undistorted, while signals from other directions are attenuated.

With a central focus on bearing estimation, the prime objective here is to locate the source of transmitted communication/ radar signal. DOA estimation algorithms in the literature [50][51] have different capabilities and limitations. The DOA estimation problem in some cases, is first solved by estimation methods of the number of sources [52][53][54] and then applying a high-resolution method to estimate the angular position of these sources. These high-resolution methods are known to be more robust than conventional techniques. The most general beamforming techniques include conventional as well as adaptive beamformers. For the conventional non-adaptive beamformers, the weight vector for a specific Direction of Arrival (DOA) depends on the array response alone and can be pre-calculated, independent of the received data. Hence, they are data independent beamformers and they present a constant response for all signal/interference scenarios. The adaptive beamformers are data-dependent since the weight vectors are calculated as a function of the incoming data to optimize the performance subject to various constraints [50]. They have better resolution and much better interference rejection capability than the data-independent beamformers and hence are used in this work

However, in practical array systems, traditional adaptive beamforming algorithms are known to degrade, if some of exploited assumptions on the environment, sources, or sensor array become wrong or imprecise. Similar types of degradation can occur when the signal array response is known exactly, but the training sample size is small. Therefore, the robustness of adaptive beamforming

techniques against environmental and array imperfections and uncertainties remains one of the key issues that needs investigation. The commonly used algorithms acquire the source signals at the Nyquist rate and transmits all measurements to a central processor in order to estimate just a small number of source bearings. The communication load between sensors can be drastically reduced, however, by exploiting spatial sparsity, i.e., the fact that the number of sources we are trying to find is much less than the total number of possible source bearings.

### **2.1 Beamforming and Performance of Antenna Array Structure**

Array beam forming techniques exist that can yield multiple, simultaneously available beams. The beams can be made to have high gain and low sidelobes, or controlled beamwidth. Adaptive beam forming techniques dynamically adjust the array pattern to optimize some characteristic of the received signal. In beam scanning, a single main beam of an array is steered and the direction can be varied either continuously or in small discrete steps. Antenna arrays using adaptive beamforming techniques can reject interfering signals having a Direction of Arrival (DOA) different from that of a desired signal [55]. Multipolarized arrays can also reject interfering signals having different polarization states from the desired signal, even if the signals have the same DOA. These capabilities can be exploited to improve the capacity of wireless communication systems. An array consists of two or more antenna elements that are spatially arranged and electrically interconnected can be used to produce a directional radiation pattern. The interconnection between elements, called the feed network, can provide fixed phase to each element or can form a phased array. In optimum and adaptive beamforming, the phases (and usually the amplitudes) of the feed network are adjusted to optimize the received signal. The geometry of an array and the patterns, orientations, and polarizations of the elements influence the performance of the array [56]. Antenna array signal Direction of Arrival (DOA) estimation is a key task of array signal processing. Array signal processing emerged in the recent few decades as an active area and was centred on the ability of using and combining data from different antenna arrays to deal with specific spatial and temporal estimation tasks.

The challenge of estimating the wave number or angle of arrival of a plane wave is referred to as direction finding challenge. It has a large application in radar, sonar, seismic systems, electronic surveillance, medical diagnosis and treatment, radio astrology and other areas. The application of the array processing requires either the knowledge of a reference signal or the direction of the desired signal source to achieve its desired objectives. Antenna arrays are widely used to solve direction finding. The main objective of this research investigation is to build on Direction of Arrival (DOA) estimation measurement system using Uniform Linear Array (ULA) and Non-uniform Linear Array

(NLA). The evaluation of sub-space-based techniques implementation is given by underlying the factors that affect the accuracy and resolution of the DOA estimation. Those factors include the number of array elements, number of snapshots, number of signal sources, and signal to noise ratio. Due to some applications in wireless communication systems that need more than a half wavelength of the distance between the adjacent array elements, the Non-uniform Linear Array (NLA) in a form of DOA estimation with combined MUSIC for Co-prime Array (DECOM) was proposed. Its most remarkable property is that it increases the degrees of freedom. In addition, the autocorrelation of signals can be estimated in a much denser spacing other than the physically sparse sampling spacing, and sinusoids in noise can be estimated in a more effective way. These obviously contribute to improving wireless network capacity.

### **3 DOA Estimation Algorithms**

The Direction of Arrival (DOA) algorithms applied in this dissertation are the conventional Minimum Variance Distortion-less Response (MVDR), subspace DOA estimation methods of Multiple Signal Classification (MUSIC), and the developed estimation algorithm Advanced-MUSIC (A-MUSIC). They are known as subspace techniques which use the eigenvectors obtained by an eigen decomposition of sample covariance matrix of the data matrix. These techniques have shown to be effective and high resolution of the system compared to other techniques. They are popular and the most promising to give an accurate DOA estimation with limited sensors, low complexity of computation and with the capacity of identifying multiple targets [10]. These algorithms allow the systems to get the desired angle of arrival of the incoming narrow band radio signal from the far field source to the receiver arrays. They have the ability to produce a high precision measurement for multiple signals sources and can be implemented in real time using digital signal processing technology [57].

The uniform and non-uniform linear array based MVDR and MUSIC algorithms are used to prove the accuracy and the effectiveness of the DOA estimation. For uniform linear array, the MVDR algorithm and MUSIC algorithm are used to find a Direction of Arrival (DOA) spectrum. The signal is sent at 2.4GHz frequency band, the same frequency used in wireless communication [58] with the angle interval in the range:  $[-\pi/2, \pi/2]$ . Then, the DOA estimation method using non-uniform linear array is given. At first, the decomposition of non-uniform linear array into two uniform linear arrays for the corresponding co-prime arrays is done, then the combined MUSIC results of the two decomposed uniform linear arrays is done to get DOA estimation [59][60]. A mathematical model is given and the

performance of the DOA estimation based on MVDR, MUSIC and the proposed A-MUSIC algorithm simulation are presented in papers section of dissertation.

Several methods have been applied in DOA estimation; among them the maximum likelihood method of Capon [61], many researchers take the first category of estimators to consist of the spectral estimation method that covers MVDR estimator, linear prediction method, maximum entropy method, Maximum Likelihood method (ML) and beamforming. The second category consists of the eigen structure methods that includes the min-norm method, the estimation of Signal Parameters via Rotational Invariance Technique (ESPRIT) algorithm, and Burg's maximum entropy method which is among the non-subspace techniques [61]. Although they have been often successful and widely used, these methods have some major limitations especially bias and sensitivity in parameter estimates, generally due to the incorrect model of the measurements. Then, Schmidt in 1979 revised and corrected the measurement model in case of the sensor arrays of arbitrary form and proposes a new subspace technique called Multiple Signal Classification (MUSIC) algorithm [62]. MUSIC technique is based on exploiting the Eigen structure of input covariance matrix. According to MUSIC spatial spectrum, DOA of the multiple source signals can be easily estimated by identifying the peaks.

Huang and Lee proposed the adaptive array beamforming in the presence of errors due to steering vector mismatch and finite sample effect [63]. The method proposed a fully data-dependent loading to overcome the difficulties. No additional sophisticated scheme is needed to choose the required loading. The loading factor can be completely obtained from the received array data. In [64] a comprehensive survey on beamforming techniques for DOA estimation has been given. The survey was based on studying various beamforming techniques and algorithms to estimate the Direction of Arrival (DOA) of a signal. An assessment on the background robust algorithms using Nyquist sampling rate and its compressive sensing alternative was made. Hence, the methods that specifically exploit the spatial sparsity property are advantageous because they use very small number of measurements in the form of random projections of the sensor data along with one full waveform recording at one of the sensors. The researchers in [65], have worked with DOA using MUSIC algorithm in uniform linear array antennas. This literature showed how the performance of smart antenna greatly depends on the effectiveness of DOA estimation algorithm. It analysed the performance of MUSIC (Multiple Signal Classification) algorithm for DOA estimation and simulation results showed that MUSIC provides better angular resolution for increasing number of array element, distance between array element and number of samples. All the simulations were done using MATLAB. A new algorithm for improving DOA estimation accuracy has been carried out. Two contributions are introduced. First, Doppler frequency shift that resulted from the target

movement is estimated using the displacement invariance technique (DIT). Second, the effect of doppler frequency is modelled and incorporated into ESPRIT algorithm in order to increase the estimation accuracy. It is worth mentioning that the subspace approach has been employed by ESPRIT and DIT methods to reduce the computational complexity and the model's nonlinearity effect. The simulation results of the proposed algorithm are better than those of the previous estimation techniques leading to the estimator performance enhancement [66]. Most of the methods used to locate the DOA in uniform linear array considered the spacing distance between two adjacent array elements to be a half wavelength. However, in wireless communication, there are some cases where such half wavelength minimum spacing is not applicable; for instance many parabola antennas, their physical size are designed to have a large size for enhanced directivity. Also, in an array that operates over a wide spectrum. For example, over-the-horizon radar (OTHR) is a unique radar system that performs wide-area surveillance by exploiting the reflective and refractive nature of high-frequency radio wave propagation through the ionosphere [67].

Recently, Non-uniform Linear Array (NLA) in a form of co-prime array has been proposed. Its most remarkable property is that it increases the degree of freedom. In addition, the autocorrelation of signals can be estimated in a much denser spacing other than the physically sparse sampling spacing, and sinusoids in noise can be estimated in a more effective way. Due to the useful properties of the NLA, its importance has been realized and many research from different aspects of it have been run in recent four years. The interest has shifted to the super resolution using the co-prime arrays. Many researchers have discovered many methods to improve on the Direction of Arrival (DOA) estimation. For example, in [67], the authors have proposed a novel array structure for the DOA estimation with increased degrees of freedom. This was a new method for a super resolution spectral estimation from the perspective of degree of freedom. In [68], the authors proposed a new search free DOA estimation for co-prime arrays by using a projection-like method to eliminate the phase ambiguities for obtaining the unique estimation of DOA. In [69], the researcher proposed a DECOM DOA Estimation with Combined MUSIC for Co-prime Array. They proposed a combination scheme to obtain the unique, DOA estimation for co-prime array from the MUSIC of the decomposed uniform linear arrays and give prove of the existence and uniqueness of the solution. They also designed a two-phase adaptive spectrum search scheme to obtain the accurate DOA estimation with low computational complexity.

Multiple signal classification is a subspace technique based on exploiting the eigen structure of input covariance matrix suggested by Schmidt in 1979 [70]. The eigenvectors are easily obtained by either an eigen decomposition of sample covariance matrix or a singular value decomposition of the data matrix [68]. MUSIC algorithm, the powers and cross correlations between the various input signals

with a set of input parameters such as number of array elements, number of snapshots, element spacing, angular separation, signal-to-noise ratio can be readily obtained. The Direction of Arrival (DOA) of the multiple incident signals can be estimated by locating the peaks of a MUSIC spatial spectrum at a high resolution. This leads to high quality wireless communication. The multiple signal classification algorithm is normally of high performance in DOA estimation; however, at a very small difference of angle of arrival between two adjacent signals and close array elements, it fails to perform well.

#### **3.1 DOA Estimation Algorithm Challenges**

The Direction of Arrival (DOA) estimation is not only affected by the incident signal coming from the transmitter but also by the sparse complex environment [47], [71]. The DOA estimation is affected by many factors such as signal to noise ratio, number of array elements, number of snapshots and number of signal source. The Signal to Noise Ratio (SNR) can be increased by providing the source with a higher level of signal output power if necessary. In wireless systems, it is always important to optimize the performance of the transmitting and receiving antennas. Thus, the signal to noise ratio directly affects the performance of super-resolution DOA estimation algorithm [9], [72].

Basically, the number of array elements can affect the estimation performance for super resolution algorithm. Generally, if the remaining array parameters are the same, the greater number of array elements, the better estimation performance for super resolution algorithm. In the time domain, the number of snapshots is defined as the number of samples. In the frequency domain, the number of snapshots is defined as the number of time sub-segments of Discrete Fourier Transform (DFT). The estimation of Direction of Arrival (DOA) gives better estimation performance for super resolution algorithm when the number of snapshots is high and other array parameters remain constant [73]. Briefly, there are many factors that affects the performance of DOA estimation in practical applications such as the array element amplitude and phase inconsistencies, mutual coupling between array elements, multipath environment and the wrong position of sensors.

#### **3.2 Proposed DOA Estimation Algorithm**

The main idea in the Direction of Arrival (DOA) estimation is to use an array of antennas to receive a narrowband signal from a far field sources in the diverse directions. The signal received is then processed using a sub-space method that has a high resolution and an accurate DOA estimation. In the past, many directions of arrival (DOA) estimation algorithms have been proposed. Among them

are non-subspace methods and subspace methods. In this work, the attention has been on Minimum Variance Distortion-less Response (MVDR) and Multiple Signal Classification (MUSIC) algorithms because of their popularity, their high performance and mostly their low computational complexity compared to other techniques. Therefore, these algorithms were applied to Uniform Linear Array (ULA) and to Non-uniform Linear Array (NLA) to check their performance on the accuracy issue. Although the DOA estimation theory and other technologies in array antennas settings have become well established some further investigations can be conducted:

(i) Currently, one-dimension (1D) of Non-uniform Linear Array (NLA) setup issues is in place, but little research on two-dimension (2D) arrays has been done. The two-dimension investigation is more in accordance with the real-time environments where both elevation and azimuth angles are needed.

(ii) Direction of Arrival (DOA) estimation and array calibration can all contribute to the parameters optimization problems. Therefore, a faster algorithm for solving optimization functions is worthy of further research.

(iii) In the spatial spectrum algorithms, most of researchers are concerned with the reception of the narrowband, though there are other applications of the spatial spectrum estimation techniques such as the DOA estimation for wideband signal, correction of path in multi-array conditions and error correction for broadband arrays. Particularly, for the array calibration and angle joint estimation of the parameters.

(iv) Multiple signal classification algorithm as one of the super high algorithms plays a big role in DOA estimation computation, but it still has a large amount of computation complexity. Also, enhancing the real time character and robustness will be an important part of the link for spatial spectrum estimation technology.

(v) Current research efforts have paid more attention in removing errors and ambiguities in the spatial spectrum from array amplitude, phase difference, mutual coupling, and positions errors. There are other factors such as near field scattering, electromagnetic interference, channel bandwidth inconsistency, non-uniform linear channel amplifier, quantization and quadrature sampling errors which impact on the estimated errors.

## **4 Radio Propagation Environment and Modelling**

Propagation mechanisms are very complex and diverse. First, due to the separation between the receiver and the transmitter, attenuation of the signal strength occurs. In addition, the signal

propagates by means of diffraction, scattering, reflection, transmission, refraction, etc. Diffraction occurs when the direct line of the sight propagation between the transmitter and the receiver is obstructed by an opaque obstacle whose dimensions are considerably larger than the signal wavelength [74]. The diffraction occurs at the obstacle edges where the radio waves are scattered, and, as a result they are additionally attenuated. The diffraction mechanism allows the reception of radio signals when the line-of-sight (LoS) conditions are not satisfied, whether in urban or rural environments. Scattering occurs when the propagation path contains the obstacles whose dimensions are comparable to the wavelength [75]. The nature of this phenomenon is similar to the diffraction, except that the radio waves are scattered in a greater number of directions. Out of all the mentioned effects, the scattering is the most difficult to be predicted. Reflection occurs when the radio wave impinges the obstacle whose dimensions are considerably larger than the wavelength of the incident wave. A reflected wave can either decrease or increase the signal level at the reception point. In cases when many reflected waves exist, the received signal level tends to be very unstable. This phenomenon is commonly referred to as multipath fading, and the signal is often Rayleigh distributed. Transmission occurs when the radio wave encounters an obstacle which is to some extent transparent for the radio waves. This mechanism allows the reception of radio signals inside of buildings in cases when the actual transmitter locations are either outdoor or indoor. This phenomenon is very important in the macrocell radio system design. Due to an inconstant refractive index of the atmosphere, the radio waves do not propagate along a straight line, but rather along a curved one. Therefore, the coverage area of an actual transmitter is usually larger. As a result of the fluctuations of the atmosphere parameters, the received signal strength level is fluctuating as well. Since there is frequently no LoS between the transmitter and the receiver, the received signal is a sum of components which often stem from several previously described phenomena. Therefore, the received signal level is quite variable with respect to time and especially with respect to the receiver or transmitter displacement. Even a displacement of just a fraction of the wavelength can cause the signal level to change by more than 30 dB. These fluctuations are known as short-term (or multipath) fading. On the other hand, the local average of the signal varies slowly with the displacement. These slow fluctuations depend mostly on environmental characteristics and they are known as long-term fading. Furthermore, most of these parameters are frequency dependent and affected by the migration to higher frequencies.

### 4.1 Rain Attenuation over Communication Links

Transmission of a radio signal through a wireless radio channel is affected by refraction, diffraction and reflection, free space loss, object penetration, and absorption that corrupt the originally transmitted signal before radio wave arrives at a receiver antenna. The propagation of electromagnetic wave occurs when energy transference from local antenna system is allowed to travel through free space. Once in free space, the forward travelling component of the electromagnetic wave interacts with different media often consisting of gases, microscopic granules, and rainfall. The rainfall media is usually of great concern as it is highly sensitive to the frequency of the travelling wave energy, as well as its amplitude. Thus, in a rainy medium, the attenuated portion of this wave is approximately equal to the exponential factor of distance, and propagation constant [76].

### 4.2 Rain Attenuation model and Free Space Loss

Most communication systems at microwave and millimetre bands may experience a loss due to rain attenuation which temporarily makes the link unavailable for use at a given time. Rain attenuation depends on rain rate characteristics, rain shape, rain drop size, and volume density. In instances where the rain attenuation measurements are not available, the rain rate becomes an important parameter for estimating the level of fade due to the rain. An empirical relationship between the rain rate  $R(mm/hr)$  and the  $\alpha_r$  rain attenuation is denoted below. The total attenuation  $A_T$  is given by

$$A_T = \alpha_r + L_{fs}, \quad (1)$$

where  $\alpha_r$  is the rain attenuation. The ITU rainfall model [77] is used for attenuation as

$$\alpha_r = cr^a, \quad (2)$$

where  $r$  is the expected rain rate. The parameter  $c$  and exponent  $a$  depend on the frequency,  $f(\text{GHz})$ , the polarization state, and the elevation angle of the signal path. In wireless communications, as the signal propagates through the medium, it disperses with distance [78]. This type of attenuation, known as free space loss ( $L_{fs}$ ), can be expressed as the ratio of the signal power between the transmitter and the receiver in dB as

$$L_{fs} = 10 * \log_{10} \left( \frac{P_t}{P_r} \right) = 20 * \log_{10} \left( \frac{4\pi d}{\lambda} \right), \quad (3)$$

where  $P_t$  is the transmitted signal power,  $P_r$  is the received signal power, and  $d$  is the distance between transmitter and receiver and  $\lambda$  is the signal wavelength in metres. The free space loss is proportional to the square of the distance between the transmitter and the receiver. Thus, as this distance is increased, the free space attenuation becomes very large.

### 4.3 Diffraction Fading

Diffraction fading (k-factor fading) takes place when the signal travelling from the transmitting antenna to the receiving antenna is intercepted by any obstacle. This kind of fading is a direct consequence of the refraction of radio wave as they traverse the lower atmosphere. As such, the radio path should be clear of any obstacles or a minimum path clearance criterion should be adhered to during terrestrial line of sight link planning as outlined in ITU-R Recommendation P.530-14 [79]. The degree of wave bending will determine whether or not electromagnetic waves are likely to be intercepted by obstacles along the radio link path. The degree of bending is usually modelled through the effective earth radius factor (k-factor). However, other quantities like the atmospheric radio refractivity, the atmospheric refractive index or the vertical refractivity gradient can also be used to characterize the refractive properties of the atmosphere. The refractive index,  $n$ , is the primary parameter used to describe refraction in the atmosphere. It is defined as the ratio of the velocity of an electromagnetic wave travelling in air to that in a vacuum (free space) [80]:

$$n = \frac{c}{v} = \sqrt{\mu\varepsilon} \quad (4)$$

where  $c$  is the velocity of an electromagnetic wave in a vacuum (free space),  $v$  is the speed of a radio wave in air,  $\mu$  is the relative permeability of air,  $\varepsilon$  is the relative permittivity of air. Since the refractive index is very close to unity in the troposphere,  $n = 1.000312$ , the atmospheric radio refractivity,  $N$  which defines the refractive index in parts per million is usually used to define the refraction and is given by [81, 82]:

$$N = (n - 1)10^6 = \frac{77.6}{T}P + 3.3 \times 10^5 \frac{e}{T^2} \quad (5)$$

where  $P$  is the atmospheric pressure (hPa),  $e$  is the water vapour pressure (hPa),  $T$  and is the absolute temperature (K). From the foregoing equations, the point k-factor,  $k$  is obtained from the following expression [83]:

$$k = \left[ 1 + \frac{\frac{dN}{dh}}{157} \right]^{-1} \quad (6)$$

where  $\frac{dN}{dh}$  is the vertical refractivity gradient. Atmospheric pressure, temperature, and water vapour content decrease with height above the earth's surface in the troposphere, but temperature will also increase with height in layers with temperature inversion in the troposphere. The decrease in dry air pressure and water vapour pressure is usually approximated as an exponential function of height. The variation of the tropospheric refractivity can also, as a result of these approximations, be approximated by an exponential function of height, as follows [84]:

$$N = N_s e^{-\frac{h}{H}} \quad (7)$$

where  $h$  is the height above the ground level,  $N_s$  is the surface level refractivity and  $H$  is the applicable scale height.

#### 4.4 Multipath Propagation (Fading)

Multipath propagation occurs when a signal travelling from the transmitter to the receiver takes different paths. The main signal, that is the straight path signal, is then received together with other multiple copies that are delayed and attenuated. The delays and attenuations suffered will vary from one copy of the signal to the other depending on the route taken to the receiver, which at times could involve multiple reflections arising from the signal encountering obstacles along the path that are much greater than its wavelength. Depending on the way the signals superimpose at the receiver, the net effect could be destructive (multipath fading) or constructive (multipath enhancement).

In [79], the ITU-R proposes three methods for the determination of multipath fading and enhancement in terrestrial line of sight links. The methods include; small percentages of time, all percentages of time and predicting enhancement. For the small percentages method, both gross and detailed planning cases are considered. For the gross planning case, the percentage of time,  $\rho_w$ , a fade depth,  $A$ , that is exceeded in the average worst month is given by [79]:

$$\rho_w = K d^{3.1} (1 + |\varepsilon_p|)^{-1.29} f^{0.8} \times 10^{-0.00089h_L - \frac{A}{10}} \quad (8)$$

where  $\varepsilon_p$  is the path inclination factor in radians,  $f$  is the frequency in GHz,  $h_L$  is the altitude of the smaller of the transmitting antenna and the receiving antenna and  $K$  is the geoclimatic factor, and is obtained using the following equation [79]:

$$K = 10^{-(4.6+0.0027dN_1)} \quad (9)$$

where  $dN_1$  is the refractivity gradient in the lowest 65m of the atmosphere not exceeded for 0.01% of the time of an average year. For detailed link design, the percentage of time,  $\rho_w$  a fade depth,  $A$  is exceeded in the average worst month is given by [79]:

$$\rho_w = K d^{3.4} (1 + |\varepsilon_p|)^{-1.03} f^{0.8} \times 10^{-0.00076h_L - \frac{A}{10}} \quad (10)$$

where all parameters are as defined in equation (8), except  $K$ , the geoclimatic factor, which is obtained using the following equation [85]:

$$K = 10^{-(4.4+0.0027dN_1)} (10 + S_a)^{-0.46} \quad (11)$$

where  $dN_1$  is as defined in equation (9) and  $S_a$  is the terrain roughness factor. Large signal enhancements are usually experienced under ducting conditions and for cases where the value is

above 10dB, the following equation is used [79]:

$$\rho_w = 100 - 10^{\frac{(-1.7-0.2A_{0.01}-E)}{3.5}} \quad (12)$$

where  $E$  is the enhancement in dB,  $w$  is as defined in (8) and  $A_{0.01}$  is the attenuation exceeded for 0.01% of the time. Thus, we can conclude that multipath fading is affected by the following [79, 86]; point atmospheric refractivity gradient, frequency of operation, percentage of time a particular fade depth is exceeded, the height of the antennas, the terrain roughness factor and the inclination of the path among others. Most of these factors are affected by the migration of communication networks to higher frequencies.

## 5 Problem Statement and Motivation

Spectrum scarcity has necessitated the migration of radio frequencies from the lower to the higher frequencies. This has resulted in radio propagation challenges due to the adverse environmental elements otherwise unexperienced at lower frequencies. A re-design and re-evaluation of the performance of traditional lower frequency technologies and algorithms for implementation at higher frequencies especially for both Uniform Linear Array (ULA) and Non-uniform Linear Arrays (NLA) antenna are therefore necessary. Specifically, the performance of Direction of Arrival (DOA) algorithms for ULA and NLA on weather impacted environments needs to be quantified and new algorithms developed to counteract the migration challenges. This work investigates the performance of Minimum Variance Distortionless Response (MVDR), Multiple Signal Classification (MUSIC) and the proposed Advanced-MUSIC (A-MUSIC) for ULA and NLA algorithms on a weather-impacted wireless channel. The Multiple Signal Classification (MUSIC) algorithm and its variants is applied directly to the ULA and NLA geometry resulting in high computational complexity due to the multiple searches for the maximum. This work proposes the Advanced-MUSIC (A-MUSIC) DOA algorithm that employs forward-backward averaging pre-processing technique on the cross correlation of array output to improve the performance of the DOA techniques. The application of these techniques in a weather impacted radio propagation scenario for ULA and NLA is challenging and is the focus of this work.

## 6 System Model

The system model of Fig. 1 is used in this work. It illustrates the uniform spaced linear array antenna with transmitting and N receiving antenna array. A source transmits signals  $s(t)$  that after passing

through a weather-impacted environment arrives at the antenna at an angle  $\theta$ . The signals  $x(t)$  induced on the antenna arrays are multiplied by adjustable complex weights  $w$  and then combined to form the system output  $y(t)$ . The processor receives array signals, system output, and direction of the desired signal as additional information. In our model for a wave front narrow band signal  $s_i(t)$ , the received signal at antenna  $i = 1, 2, \dots, N$ ,  $x_i(t)$ , is given by

$$x_i(t) = \sum_{i=1}^N \alpha_i s_i(t) a_i(\theta_i + \Delta\theta_i) + v_i(t), \quad (13)$$

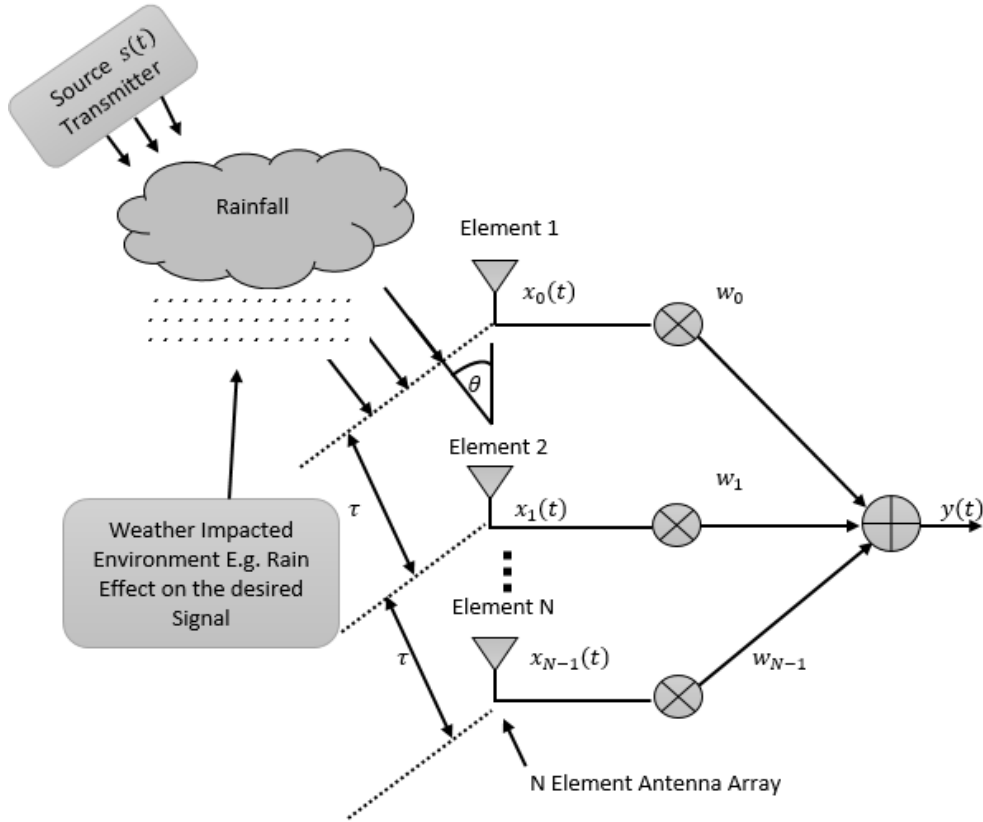


Fig. 1: System model

where  $\alpha_i$  is the rainfall attenuation,  $\theta_i$  the angle of arrival,  $\Delta\theta_i$  the rainfall angle deviation and  $v_i(t)$  the measured noise at antenna  $i$ . The response function of the array element  $i$  to the signal source  $a_i(\hat{\theta}_i)$  is

$$a_i(\hat{\theta}_i) = \exp[-j(i-1) \frac{2\pi d \sin \hat{\theta}_i}{\lambda}], \quad (14)$$

where  $\lambda$  is the wavelength and  $d$  is the spacing difference between array elements. The total received signal vector  $X(t)$  is expressed as:

$$X(t) = A(\hat{\theta}) \tilde{S}(t) + V(t), \quad (15)$$

where

$$\begin{aligned} X(t) &= [x_1(t), x_2(t), \dots, x_N(t)]^T, \\ A(\hat{\theta}) &= [a_1(\hat{\theta}_1), a_2(\hat{\theta}_2), \dots, a_N(\hat{\theta}_I)]^T, \\ \tilde{S}(t) &= [\tilde{s}_1(t), \tilde{s}_2(t), \dots, \tilde{s}_N(t)]^T, \\ V(t) &= [v_1(t), v_2(t), \dots, v_N(t)]^T. \end{aligned} \tag{16}$$

where  $\tilde{s}_i(t) = \alpha_i s_i(t)$  and  $\hat{\theta}_i = \theta_i + \Delta\theta_i$ . The modelling and investigation of the rainfall attenuation  $\alpha_i$  and angle deviation  $\Delta\theta_i$  due to the weather impacted rainfall channel is the focus of this investigation. Furthermore, the performance of the DOA algorithms and development of a better algorithm is done in this work.

## 7 Research Objectives

The dissertation aims to achieve the following main objectives:

1. To develop, model and investigate the performance of the conventional Minimum Variance Distortion-less Look (MVDL), subspace DOA Estimation Methods of Multiple Signal Classification (MUSIC) and the proposed estimation algorithm on a weather impacted wireless channel, Advanced-MUSIC (A-MUSIC).
2. To develop, model and investigate the performance Multiple Signal Classification (MUSIC), Root-MUSIC and the proposed Advanced-MUSIC (A-MUSIC) Non-uniform Linear Array (NLA) algorithms on a weather impacted wireless channel.
3. To conduct the investigations of 1) and 2) above on different channel models and at higher frequencies and develop practical results.

## 8 Research Methodology

This work was done through mathematical analysis and computer simulation, and verification is done through development of a simple prototype. DOA estimation method for both uniform and non-uniform linear array under various weather conditions is done through MATLAB simulation.

## 9 Research Main Contributions

The work done in this dissertation has resulted into several publications outlined below:

### 9.1 Paper A: Direction of Arrival (DOA) Estimation for Smart Antennas in Weather Impacted Environments (Published in PIER).

**Abstract:** Direction of Arrival estimation (DOA) is critical in antenna design for emphasizing the desired signal and minimizing interference. The scarcity of radio spectrum has fuelled the migration of communication networks to higher frequencies. This has resulted in radio propagation challenges due to the adverse environmental elements otherwise unexperienced at lower frequencies. In rainfall-impacted environments, DOA estimation is greatly affected by signal attenuation and scattering at the higher frequencies. Therefore, new DOA algorithms cognisant of these factors need to be developed and the performance of the existing algorithms quantified. This work investigates the performance of the conventional Minimum Variance Distortion-less Look (MVDL), subspace DOA Estimation Methods of Multiple Signal Classification (MUSIC) and the developed estimation algorithm on a weather impacted wireless channel, Advanced-MUSIC (A-MUSIC). The results show performance degradation in a rainfall impacted communication network with the developed algorithm showing better performance degradation.

### 9.2 Paper B: Performance Evaluation of DOA Algorithms for Non-uniform Linear Arrays (NLA) in a Weather Impacted Environment (Under Review in Earth and Space Science Open Archive (ESSOAr)).

**Abstract:** Spectrum scarcity has necessitated the migration of radio frequencies from the lower to the higher frequencies. This has resulted in radio propagation challenges due to the adverse environmental elements otherwise unexperienced at lower frequencies. This necessitates a rethink and re-evaluation on the performance of the traditional lower frequency technologies and algorithms at the higher frequencies, especially for non-uniform linear antenna arrays. A redesign or modification of the technologies for the higher frequencies is required. Specifically, the performance of Direction of Arrival (DOA) algorithms for non-linear antenna arrays on weather impacted environments need to be quantified and new algorithms developed to counter the migration challenges. This work investigates the performance Multiple Signal Classification (MUSIC), Root-MUSIC and the proposed Advanced-MUSIC (A-MUSIC) Non-uniform Linear array (NLA)

algorithms on a weather impacted wireless channel. The results indicate that the developed NLA achieves better DOA estimation than the conventional NLA with all at reduced performance in a weather impacted scenario.

## References

- [1] J. Green, P. E., J. Kelly, E. J., and M. J. Levin, "A Comparison of Seismic Array Processing Methods," *Geophysical Journal International*, vol. 11, no. 1, pp. 67–84, 1966. [Online]. Available: <https://doi.org/10.1111/j.1365-246X.1966.tb03493.x>
- [2] W. Vanderkulk, "Optimum Processing for Acoustic Arrays," *Radio and Electronic Engineer*, vol. 26, no. 4, pp. 285–292, 1963.
- [3] J. W. R. Griffiths and J. E. Hudson, "An Introduction to Adaptive Processing In a Passive Sonar System," *Aspects of Signal Processing*, pp. 299–308, 1977.
- [4] L. Brennan and L. Reed, "Theory of Adaptive Radar," *IEEE Transactions on Aerospace and Electronic Systems*, vol. AES-9, no. 2, pp. 237–252, 1973.
- [5] J. Winters, "Optimum Combining In Digital Mobile Radio with Co-channel Interference," *IEEE Transactions on Vehicular Technology*, vol. 33, no. 3, pp. 144–155, 1984.
- [6] B. Suard, A. Naguib, G. Xu, and A. Paulraj, "Performance of CDMA Mobile Communication Systems Using Antenna Arrays," in *1993 IEEE International Conference on Acoustics, Speech, and Signal Processing*, vol. 4, 1993, pp. 153–156.
- [7] A. Flieller, P. Larzabal, and H. Clergeot, "Applications of High Resolution Array Processing Techniques for Mobile Communication System," in *Proceedings of the Intelligent Vehicles '94 Symposium*, 1994, pp. 606–611.
- [8] M. M. Abdalla, M. B. Abuitbel, and M. A. Hassan, "Performance Evaluation of Direction of Arrival (DOA) Estimation Using MUSIC and ESPRIT Algorithms for Mobile Communication Systems," in *6th Joint IFIP Wireless and Mobile Networking Conference (WMNC)*, 2013, pp. 1–7.
- [9] A. Tennant, "Array pattern Nulling by Element Position Perturbations Using a Genetic Algorithm," *Electronics Letters*, vol. 30, pp. 174–176, 1994. [Online]. Available: [https://digital-library.theiet.org/content/journals/10.1049/el\\_19940139](https://digital-library.theiet.org/content/journals/10.1049/el_19940139)
- [10] N. A. Dheringe and B. N. Bansode, "Performance Evaluation and Analysis of Direction of Arrival (DOA) Estimation Using MUSIC, TLS ESPRIT and Pro ESPRIT Algorithms," *International Journal of Advanced Research in Electrical, Electronics and Instrumentation Engineering*, vol. 04, no. 06, pp. 4948–4958, 2015.
- [11] A. Goldsmith, *Wireless Communications*. Cambridge University Press, 2005.
- [12] R. Schmidt, *A Signal Subspace Approach to Multiple Emitter Location and Spectral Estimation*. Stanford University, 1981. [Online]. Available: <https://books.google.co.za/books?id=mLKUnQEACAAJ>
- [13] R. O. Schmidt, "Multiple Emitter Location and Signal Parameter Estimation," *IEEE Transactions on Antennas and Propagation*, vol. 34, pp. 276–280, Mar. 1986.

## REFERENCES

---

- [14] K. L. Bienvenu, G., "Principle De La Gonionmetrie Passive Adaptive," *InProc. 7'eme Colloque GRESIT Nice, France*, vol. 34, p. 106/1–106/10, 1979.
- [15] R. Schmidt, "Multiple Emitter Location and Signal Parameter Estimation," 1979.
- [16] R. Roy and T. Kailath, "ESPRIT-Estimation of Signal Parameters Via Rotational Invariance Techniques," *Ph.D. Dissertation, Dept. Elect. Eng., Stanford Univ.*, 1987.
- [17] A. Swindlehurst and T. Kailath, "Azimuth/Elevation Direction Finding Using Regular Array Geometries," *IEEE Transactions on Aerospace and Electronic Systems*, vol. 29, no. 1, pp. 145–156, 1993.
- [18] R. Roy and T. Kailath, "ESPRIT-Estimation of Signal Parameters Via Rotational Invariance Techniques," *IEEE Transactions on Acoustics, Speech, and Signal Processing*, vol. 37, no. 7, pp. 984–995, 1989.
- [19] R. H. R. III and T. Kailath, "ESPRIT-Estimation of Signal Parameters via Rotational Invariance Techniques," *Optical Engineering*, vol. 29, no. 4, pp. 296 – 313, 1990. [Online]. Available: <https://doi.org/10.1117/12.55606>
- [20] R. Roy, A. Paulraj, and T. Kailath, "ESPRIT-A Subspace Rotation Approach To Estimation of Parameters of Cisoids In Noise," *IEEE Transactions on Acoustics, Speech, and Signal Processing*, vol. 34, no. 5, pp. 1340–1342, 1986.
- [21] A. Paulraj, R. Roy, and T. Kailath, "Estimation Of Signal Parameters Via Rotational Invariance Techniques- Esprit," *Nineteenth Asilomar Conference on Circuits, Systems and Computers, 1985.*, 1985.
- [22] A. Paulraj, R. Roy, and T. Kailath, "A Subspace Rotation Approach To Signal Parameter Estimation," *IEEE Proceedings*, vol. 74, pp. 1044–1046, Jul. 1986.
- [23] G. Xu, S. Silverstein, R. Roy, and T. Kailath, "Beamspace ESPRIT," *IEEE Transactions on Signal Processing*, vol. 42, no. 2, pp. 349–356, 1994.
- [24] P. Krekel and E. Deprettere, "A Two-Dimensional Version of The Matrix Pencil Method to Solve The DOA Problem," in *1989 European Conference on Circuit Theory and Design*, 1989, pp. 435–439.
- [25] Q. Yin, R. Newcomb, and L. Zou, "Estimating 2-D Angles of Arrival Via Two Parallel Linear Arrays," in *International Conference on Acoustics, Speech, and Signal Processing.*, 1989, pp. 2803–2806 vol.4.
- [26] F. Sakarya and M. Hayes, "Estimating 2-D DOA Angles Using Nonlinear Array Configurations," *IEEE Transactions on Signal Processing*, vol. 43, no. 9, pp. 2212–2216, 1995.
- [27] A. Swindlehurst and T. Kailath, "2-D Parameter Estimation Using Arrays with Multidimensional Invariance Structure," in *Twenty-Third Asilomar Conference on Signals, Systems and Computers, 1989.*, vol. 2. Los Alamitos, CA, USA: IEEE Computer Society, nov 1989, pp. 950–954. [Online]. Available: <https://doi.ieeecomputersociety.org/10.1109/ACSSC.1989.1201038>
- [28] Y. Wu, G. Liao, and H. So, "A Fast Algorithm for 2-D Direction-of-Arrival (DOA) Estimation," *Signal Processing*, vol. 83, no. 8, pp. 1827–1831, 2003. [Online]. Available: <https://www.sciencedirect.com/science/article/pii/S016516840300118X>

- [29] J. Fernandez del Rio and M. Catedra-Perez, "The Matrix Pencil Method for Two-Dimensional Direction of Arrival (DOA) Estimation Employing An L-Shaped Array," *IEEE Transactions on Antennas and Propagation*, vol. 45, no. 11, pp. 1693–1694, 1997.
- [30] T.-H. Liu and J. Mendel, "Azimuth and Elevation Direction Finding Using Arbitrary Array Geometries," *IEEE Transactions on Signal Processing*, vol. 46, no. 7, pp. 2061–2065, 1998.
- [31] M. Zoltowski and D. Stavrinos, "Sensor Array Signal Processing Via a Procrustes Rotations Based Eigenanalysis of The ESPRIT Data Pencil," *IEEE Transactions on Acoustics, Speech, and Signal Processing*, vol. 37, no. 6, pp. 832–861, 1989.
- [32] P. Bas Ober, E. Deprettere, and A.-J. van der Veen, "Efficient Methods to Compute Azimuth and Elevation In High Resolution DOA Estimation," in *[Proceedings] ICASSP 91: 1991 International Conference on Acoustics, Speech, and Signal Processing*, 1991, pp. 3349–3352 vol.5.
- [33] A. Swindlehurst and T. Kailath, "2-D Parameter Estimation Using Arrays with Multidimensional Invariance Structure," *Twenty-Third Asilomar Conference on Signals, Systems and Computers*, 1989.
- [34] A. van der Veen, P. Ober, and E. Deprettere, "Azimuth and Elevation Computation In High Resolution DOA Estimation," *IEEE Transactions on Signal Processing*, vol. 40, no. 7, pp. 1828–1832, 1992.
- [35] S. Marcos, A. Marsal, and M. Benidir, "The Propagator Method for Source Bearing Estimation," *Signal Processing*, vol. 42, no. 2, pp. 121–138, 1995.
- [36] S. Marcos, "Calibration of A Distorted Towed Array Using A Propagation Operator," *The Journal of the Acoustical Society of America*, vol. 93, no. 4, pp. 1987–1994, 1993.
- [37] S. Marcos and M. Benidir, "On A High Resolution Array Processing Method Non-Based On The Eigenanalysis Approach," in *International Conference on Acoustics, Speech, and Signal Processing*, 1990, pp. 2955–2958 vol.5.
- [38] S. Marcos, A. Marsal, and M. Benidir, "Performances Analysis of The Propagator Method for Source Bearing Estimation," in *Proceedings of ICASSP '94. IEEE International Conference on Acoustics, Speech and Signal Processing*, vol. iv, 1994, pp. IV/237–IV/240 vol.4.
- [39] S. Prasad, R. Williams, A. Mahalanabis, and L. Sibul, "A Transform-Based Covariance Differencing Approach for Some Classes of Parameter Estimation Problems," *IEEE Transactions on Acoustics, Speech, and Signal Processing*, vol. 36, no. 5, pp. 631–641, 1988.
- [40] A. Paulraj and T. Kailath, "Eigenstructure Methods for Direction of Arrival (DOA) Estimation In The Presence of Unknown Noise Fields," *IEEE Transactions on Acoustics, Speech, and Signal Processing*, vol. 34, no. 1, pp. 13–20, 1986.
- [41] A. Moghaddamjoo, "Transform-Based Covariance Differencing Approach To The Array with Spatially Nonstationary Noise," *IEEE Transactions on Signal Processing*, vol. 39, no. 1, pp. 219–221, 1991.
- [42] T. Tanaka, D. E., M. Inayoshi, and N. Mizuhara, "Overview of Communication Network Evolution," 1998.

- [43] T. Bogale, X. Wang, and L. Le, "Chapter 9 - MmWave Communication Enabling Techniques for 5G Wireless Systems: A Link Level Perspective," in *mmWave Massive MIMO*, S. Mumtaz, J. Rodriguez, and L. Dai, Eds. Academic Press, 2017, pp. 195–225. [Online]. Available: <https://www.sciencedirect.com/science/article/pii/B9780128044186000091>
- [44] Y. Niu, Y. Li, D. Jin, L. Su, and A. Vasilakos, "A Survey of Millimeter Wave (mmWave) Communications for 5G: Opportunities and Challenges," *Wireless Networks*, vol. 21, 02 2015.
- [45] C. Balanis, *Antenna Theory: Analysis and Design, 3RD ED.* Wiley India Pvt. Limited, 2009. [Online]. Available: <https://books.google.co.za/books?id=2SJ0CgAAQBAJ>
- [46] S.-S. Jeon, Y. Wang, Y. Qian, and T. Itoh, "A Novel Smart Antenna System Implementation for Broad-Band Wireless Communications," *Antennas and Propagation, IEEE Transactions on*, vol. 50, pp. 600 – 606, 06 2002.
- [47] H. Hourani, "An Overview of Adaptive Antenna Systems," January 2004.
- [48] K. A. Keerthi, "Adaptive Beamforming Smart Antenna for Wireless Communication System," *International Research Journal of Engineering and Technology (IRJET)*, vol. 02, no. 03, pp. 2038–2043, 2015.
- [49] B. Van Veen and K. Buckley, "Beamforming: A Versatile Approach To Spatial Filtering," *IEEE ASSP Magazine*, vol. 5, no. 2, pp. 4–24, 1988.
- [50] H. Trees, *Optimum Array Processing – Part IV of Detection, Estimation, and Modulation Theory*, 05 2002.
- [51] X. Mestre and M. Lagunas, "Finite Sample Size Effect on Minimum Variance Beamformers: Optimum Diagonal Loading Factor for Large Arrays," *IEEE Transactions on Signal Processing*, vol. 54, no. 1, pp. 69–82, 2006.
- [52] H. Cox, R. Zeskind, and M. Owen, "Robust Adaptive Beamforming," *IEEE Transactions on Acoustics, Speech, and Signal Processing*, vol. 35, no. 10, pp. 1365–1376, 1987.
- [53] B. Carlson, "Covariance Matrix Estimation Errors and Diagonal Loading In Adaptive Arrays," *IEEE Transactions on Aerospace and Electronic Systems*, vol. 24, no. 4, pp. 397–401, 1988.
- [54] L. Chang and C.-C. Yeh, "Performance of DMI and Eigenspace-Based Beamformers," *IEEE Transactions on Antennas and Propagation*, vol. 40, no. 11, pp. 1336–1347, 1992.
- [55] T. Roy, D. Meena, and L. Prakasam, "FPGA Based Digital Beam Forming for Radars," in *2009 IEEE Radar Conference*, 2009, pp. 1–5.
- [56] C. Dietrich, W. Stutzman, B.-K. Kim, and K. Dietze, "Smart Antennas In Wireless Communications: Base-Station Diversity and Handset Beamforming," *IEEE Antennas and Propagation Magazine*, vol. 42, no. 5, pp. 142–151, 2000.

- [57] T. Dhope, "Application of MUSIC , ESPRIT and ROOT MUSIC in DOA Estimation," in *Faculty of Electrical Engineering and Computing, University of Zagreb, Croatia*, 2010, pp. 1–5.
- [58] T. Rappaport, *Wireless Communications: Principles and Practice, 2nd Edition*, December 2001, vol. 2.
- [59] Z. Tan, Y. C. Eldar, and A. Nehorai, "Direction of Arrival (DOA) Estimation Using Co-Prime Arrays: A Super Resolution Viewpoint," *IEEE Transactions on Signal Processing*, vol. 62, no. 21, pp. 5565–5576, 2014.
- [60] P. T. Eswar and K. T. Yaswanth, "Performance Analysis of Direction of Arrival (DOA) Estimation Algorithms In Smart Antennas," *International Journal of Advanced Research in Electronics and Communication Engineering*, vol. 03, no. 06, pp. 664–670, 2014.
- [61] Y. Khmou, S. Safi, and M. Frikel, "Comparative Study Between Several Direction of Arrival (DOA) Estimation Methods," *Journal of Telecommunications and Information Technology*, vol. 1, pp. 41–48, 2014. [Online]. Available: <https://hal.archives-ouvertes.fr/hal-01057828>
- [62] G.-G. D. Aniket, K. R. and S. A. Wagh, "Subspace Based DOA Estimation Techniques," *IJRET: International Journal of Research in Engineering and Technology*, vol. 4, no. 06, pp. 560–564, 2015.
- [63] C.-C. Huang and J.-H. Lee, "Robust Adaptive Beamforming Using A Fully Data-Dependent Loading Technique," *Progress In Electromagnetics Research B*, vol. 37, pp. 307–325, 2012.
- [64] T. Kesavamurthy, V. Krishnaveni, and A. B, "Beamforming for Direction-of-Arrival (DOA) Estimation-A Survey," *International Journal of Computer Applications*, vol. 61, no. 11, pp. 4–11, 2013.
- [65] V. Krishnaveni, T. Kesavamurthy, and A. B, "Direction of Arrival (DOA) Estimation Using MUSIC Algorithm," *IJRET: International Journal of Research in Engineering and Technology*, vol. 61, no. 11, pp. 633 – 636, 2014.
- [66] Y. Fayad, C. Wang, Q. Cao, and A. E.-D. S. Hafez, "Direction of Arrival (DOA) Estimation Accuracy Enhancement Via Using Displacement Invariance Technique," *International Journal of Antennas and Propagation*, vol. 2015, pp. 1–10, 2015.
- [67] P. Pal and P. P. Vaidyanathan, "A novel Array Structure for Directions-of-Arrival Estimation with Increased Degrees of Freedom," in *2010 IEEE International Conference on Acoustics, Speech and Signal Processing*, 2010, pp. 2606–2609.
- [68] Z. Weng and P. M. Djurić, "A Search-Free DOA Estimation Algorithm for Co-prime Arrays," *Digital Signal Processing*, vol. 24, pp. 27–33, 2014. [Online]. Available: <https://www.sciencedirect.com/science/article/pii/S105120041300225X>
- [69] C. Zhou, Z. Shi, Y. Gu, and X. Shen, "DECOM: DOA Estimation with Combined MUSIC for Co-prime Array," in *2013 International Conference on Wireless Communications and Signal Processing*, 2013, pp. 1–5.

## REFERENCES

---

- [70] K. Lee, "Sensor Array Processing for High Resolution of DOA Estimation of Spatial Subspace Using Smoothing Technique of BeamSpace MUSIC in Coherent Channels," *International Journal of Control and Automation*, vol. 8, pp. 167–174, December 2015.
- [71] P. Gupta and S. Kar, "MUSIC and Improved MUSIC Algorithm To Estimate Direction of Arrival (DOA)," in *2015 International Conference on Communications and Signal Processing (ICCSP)*, 2015, pp. 0757–0761.
- [72] S. Vaidyanath and S. D., "Performance Evaluation of Smart Antenna DOA Estimation Using MUSIC Improved MUSIC Algorithm," *International Journal of Innovative Technology and Research*, vol. 0, no. 0, 2015. [Online]. Available: <https://www.ijitr.com/index.php/ojs/article/view/541>
- [73] P. Gerstoft, A. Xenaki, and C. F. Mecklenbräuker, "Multiple and Single Snapshot Compressive Beamforming," *The Journal of the Acoustical Society of America*, vol. 138, no. 4, pp. 2003–2014, Oct 2015. [Online]. Available: <http://dx.doi.org/10.1121/1.4929941>
- [74] A. Neskovic, N. Neskovic, and G. Paunovic, "Modern Approaches In Modeling of Mobile Radio Systems Propagation Environment," *IEEE Communications Surveys Tutorials*, vol. 3, no. 3, pp. 2–12, 2000.
- [75] G. Joshi, C. Dietrich, C. Anderson, W. Newhall, W. Davis, J. Isaacs, and G. Barnett, "Near-Ground Channel Measurements Over Line-of-Sight and Forested Paths," *IEE Proceedings - Microwaves, Antennas and Propagation*, vol. 152, no. 6, pp. 589–596, 2005.
- [76] H. C. Van de Hulst, "Light Scattering By Small Particles," *Quarterly Journal of the Royal Meteorological Society*, vol. 84, no. 360, pp. 198–199, 1958. [Online]. Available: <https://rmets.onlinelibrary.wiley.com/doi/abs/10.1002/qj.49708436025>
- [77] I. T. U. ITU-R, "Specific Attenuation Model for Rain for Use In Prediction Methods," *Recommendation*, pp. 838–3, 2005.
- [78] W. Stallings, *Wireless Communications and Networks*, 1st ed. Prentice Hall Professional Technical Reference, 2001.
- [79] I. T. U. ITU-R, "Propagation Data and Prediction Methods Required for The Design of Terrestrial Line-of-Sight Systems," *Recommendation*, pp. 530–12, 2012.
- [80] R. Freeman, *Radio System Design for Telecommunications, Third Edition*, WILEY- INTERSCIENCE, 3rd ed. John Wiley Sons Inc, 2007.
- [81] S. M. Babin, "A Case Study of Subrefractive Conditions at Wallops Island, Virginia," *Journal of Applied Meteorology*, vol. 34, no. 5, pp. 1028–1038, 1995.
- [82] R. A. Harris, "Cost Action 255: Radiowave Propagation Modelling for SatCom Services at Ku-Band and Above : Final Report." *ESA Publications Division*, 2002.
- [83] N. Chaudhary, D. Trivedi, and R. Gupta, "The Impact of K-Factor on Wireless Link in Indian Semi-desert Terrain," vol. 2, no. 4, 2011, pp. 776–779.

## REFERENCES

---

- [84] B. G. Ayantunji, P. Okeke, J. Urama, and Y. Najib, "A Semi-Empirical Model for Vertical Extrapolation of Surface Refractivity Over Nigeria," *African Review of Physics*, vol. 6, 2011.
- [85] L. Castanet, J. Lemorton, T. Konefal, A. K. Shukla, P. A. Watson, and C. L. Wrench, "Comparison of Various Methods for Combining Propagation Effects and Predicting Loss In Low-Availability Systems In The 20–50 GHz Frequency Range," *International Journal of Satellite Communications*, vol. 19, no. 3, pp. 317–334, 2001. [Online]. Available: <https://onlinelibrary.wiley.com/doi/abs/10.1002/sat.703>
- [86] P. Odedina and T. Afullo, "Multipath Propagation Modeling and Measurement In Clear-air Environment for LOS Link Design Application," *Southern Africa Telecommunication Networks and Applications Conference Proceedings*, 2009.

**Part II**

**Papers**

# Paper A

## Direction of Arrival (DOA) Estimation for Smart Antennas in Weather Impacted Environments

Bongani Prudence Nxumalo and Tom Walingo

*Progress In Electromagnetics Research (PIER)*

© 2021

*The layout has been revised.*

### **Abstract**

*Direction of Arrival (DOA) estimation is critical in antenna design for emphasizing the desired signal and minimizing interference. The scarcity of radio spectrum has fuelled the migration of communication networks to higher frequencies. This has resulted in radio propagation challenges due to the adverse environmental elements otherwise unexperienced at lower frequencies. In rainfall impacted environments, DOA estimation is greatly affected by signal attenuation and scattering at the higher frequencies. Therefore, new DOA algorithms cognisant of these factors need to be developed and the performance of the existing algorithms quantified. This work investigates the performance of the Conventional Minimum Variance Distortion-less Look (MVDL), Subspace DOA Estimation Methods of Multiple Signal Classification (MUSIC), and the developed estimation algorithm on a weather impacted wireless channel, Advanced-MUSIC (A-MUSIC). The results show performance degradation in a rainfall impacted communication network with the developed algorithm showing better performance degradation.*

### **1 Introduction**

Smart antenna systems merge antenna arrays with intelligent digital signal processing ability in order to transmit and receive in a versatile and spatially delicate way. Different users are served with narrow beam radiation patterns, thus reducing multipath and co-channel interference and enhancing frequency reuse. They determine spatial signal signature, Direction of Arrival (DOA) or Angle of Arrival (AOA), and use it to estimate the beamforming vectors, to track and identify the antenna beam. Thus, the most critical parts of smart antennas are DOA estimation and beamforming [1]. The accurate estimation of the DOA of all signals transmitted to the adaptive array antenna enables the maximization of its performance with respect to recovering the required transmitted signal and suppressing any presence of interfering signals. The beamforming technique also ensures less interference to the system, thus increasing the overall system performance. The development of efficient DOA algorithms is critical for the performance of the communication networks. Traditionally, the developed DOA algorithms are popularly classified into two main categories: the conventional Beamforming [2,3], e.g., Bartlett and Capon (Minimum Variance Distortionless Response (MVDR)) and the Subspace DOA Estimation Methods such as the Multiple Signal Classification (MUSIC) and Estimation of Signal Parameters via Rotational Invariance Techniques (ESPRIT). In the conventional MVDR technique, the Bartlett algorithm, Fourier based spectral

analytical techniques are applied to the spatio-temporally sampled data of mostly a single signal. It was extended to multiple signals by Capon to contain signal contributions from the desired angle as well as the undesired angle as the Minimum Variance Algorithm [4]. The Bartlett algorithm maximises the power of beamforming output for a given input signal whereas the Capon algorithm attempts to minimize the power contributed by noise and any signals coming from other direction than desired. Both methods involve spectrum evaluation followed by finding the local maxima that give the estimated DOA. However, these methods are highly dependent on physical antenna aperture array size resulting in poor resolution and accuracy [2,4]. In addition, they do not exploit the structure of the narrowband input data model of the measurements.

Subspace techniques conduct characteristic decomposition of the covariance matrix for any array output data, resulting in a signal subspace orthogonal with to noise subspace corresponding to the signal components. Estimation of DOA is performed from one of these subspaces, assuming that noise in each channel is highly uncorrelated. The popularity of the MUSIC algorithm [5] is due to its generality. It is applicable to arrays of arbitrary but known configuration and response, used to estimate multiple parameters per source. MUSIC algorithm has the ability to simultaneously measure multiple signals with high precision and resolution among others. However, the conventional MUSIC algorithm requires a priori knowledge of the second-order spatial statistics of the background noise and interference field. It also involves a computationally demanding spectral search over the angle, therefore, expensive in implementation. The ESPRIT [6] is a computationally efficient and robust subspace method of DOA estimation. It uses two identical matched array pairs aiding it in reducing complexity. Although ESPRIT alleviates the computational complexity of MUSIC algorithm, it is more prone to errors [7]. Other algorithms also exist for DOA estimation. The development and performance evaluation of these algorithms and their variants has been exhaustively done for the legacy communication network environments [4,7–10] and need not be reemphasised.

The increasing demand on mobile broadband services has led to the scarcity of radio spectrum due to spectrum exhaustion [11]. This has led to migration to higher frequency millimetre-wave (mmW) bands, which range from 30GHz to 300GHz, for mmW communication with additional large bandwidths. Apart from the merits of expanded bandwidth and high frequency reuse packing due to shorter wavelengths, mmW communication, possess its own challenges including large path loss suffered by mmW signals, and the effect of the weather effectors to signals in this band. Rainfall is a common weather phenomenon that affects signal transmission at this band. In link budget planning and design at lower frequencies, rainfall is considered as a fixed propagation attenuation [12]. The transmitted signal suffers from absorption from the rain causing signal attenuation. In mmW

systems, the wavelengths of the signals are comparable to the raindrop size from 0.1mm to 10mm [13]. Hence, apart from attenuation, the signals undergo scattering when being transmitted through rain leading to both amplitude attenuation and phase fluctuation [14]. Rain attenuation and scattering are a function of the rain rate, polarization, physical size of drops and operating frequency [15, 16]. Rainfall attenuation, frequency attenuation, and phase distortion affect the received signal. For these mmW systems, DOA algorithms that do not consider the effect of the weather are not realistic. This work is among the first that investigates the performance of the DOA algorithms in a rainfall-impacted network and develops a hybrid algorithm to combat the rainfall effects in DOA estimation. A realistic Markovian rainfall channel model is used to accurately capture the rainfall variations in three cases; widespread, shower and thunderstorm rain events.

The rest of the paper is organized as follows. In Section 2, the system model is presented. Section 3, represents the weather channel parameter modelling. The proposed method of efficiently estimating the DOA and other conventional and subspace DOA estimation algorithms are presented in Section 4. In Section 5, the performance measures and overall performance evaluation algorithm is done while simulation results and discussion are presented in Section 6. The paper concludes in Section 7.

Notation: The bold upper and lower-case letters represent the matrices and column vectors, respectively.  $I$  is an identity matrix. The following superscripts  $(\bullet)^*$ ,  $(\bullet)^H$ ,  $(\bullet)^{-1}$  and  $(\bullet)^T$  represent optimality, Hermitian, inverse and transpose operators, respectively and  $E(\bullet)$  is the mathematical expectation,  $d$  is the spacing difference between array elements,  $c$  is the speed of light and  $\lambda$  is the wavelength.

## 2 System Model

The DOA algorithms estimate the angle of arrival of all incoming signals. In Fig. A.1 a Uniform Linear Array (ULA) of  $N$  equally spaced sensors is shown. A source transmits signals  $s(t)$  that after passing through a weather-impacted environment arrives at the antenna at an angle  $\theta$ . The signals  $x(t)$  induced on the antenna arrays are multiplied by adjustable complex weights  $w$  and then combined to form the system output  $y(t)$ . The processor receives array signals, system output, and direction of the desired signal as additional information. In our model, for a wavefront narrow band signal  $s_i(t)$ , the received signal  $x_i(t)$  at antenna element,  $i = 1, 2, \dots, N$ , is given by

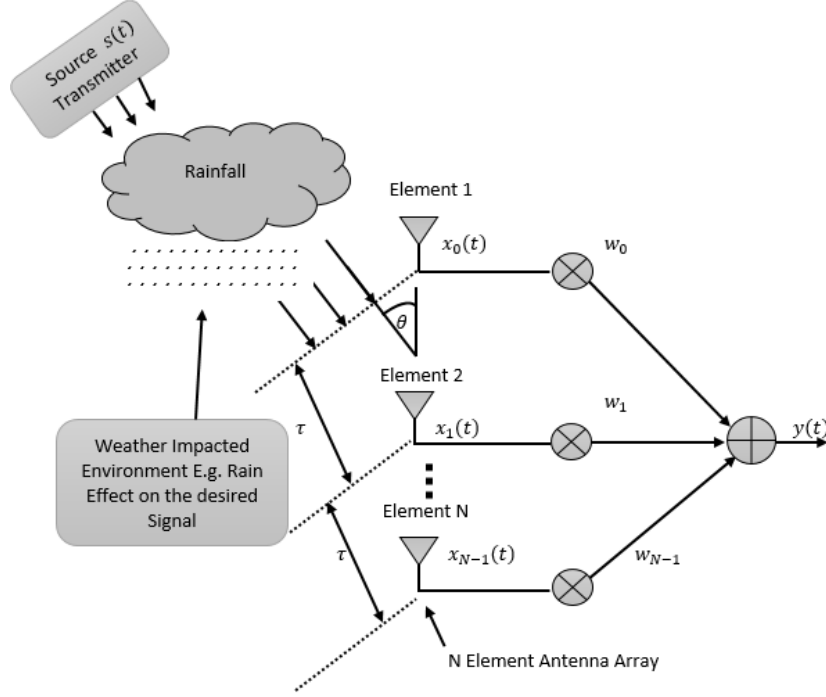


**Fig. A.1:** Non-uniform Linear Array (NLA) with  $d = \frac{\lambda}{2} * [0, d_2, \dots, d_{(M-1)}]$ .

$$x_i(t) = \sum_{i=1}^N \alpha_i s_i(t) a_i(\theta_i + \Delta\theta_i) + v_i(t), \quad (\text{A.1})$$

where  $\alpha_i$  is the rainfall attenuation,  $\theta_i$  the angle of arrival,  $\Delta\theta_i$  the rainfall angle deviation, and  $v_i$  the measured noise at antenna  $i$ . The response function of the array element  $i$  to the signal source  $a_i(\hat{\theta}_i)$  is

$$a_i(\hat{\theta}_i) = \exp[-j(i-1) \frac{2\pi d \sin \hat{\theta}_i}{\lambda}] \quad (\text{A.2})$$

where  $\lambda$  is the wavelength, and  $d$  is the spacing difference between array elements. The total received signal vector  $X(t)$  is expressed as

$$X(t) = A(\hat{\theta}) \tilde{S}(t) + V(t), \quad (\text{A.3})$$

where

$$\begin{aligned} X(t) &= [x_1(t), x_2(t), \dots, x_N(t)]^T, \\ A(\hat{\theta}) &= [a_1(\hat{\theta}_1), a_2(\hat{\theta}_2), \dots, a_N(\hat{\theta}_N)]^T, \\ \tilde{S}(t) &= [\tilde{s}_1(t), \tilde{s}_2(t), \dots, \tilde{s}_N(t)]^T, \\ V(t) &= [n_1(t), n_2(t), \dots, n_N(t)]^T. \end{aligned} \quad (\text{A.4})$$

In Equation (A.4),  $\tilde{S}(t) = \alpha_i s_i(t)$  and  $\hat{\theta} = \theta_i + \Delta\theta_i$ . The modelling and investigation of the rainfall attenuation  $\alpha_i$  and angle deviation  $\Delta\theta_i$  due to the weather impacted rainfall channel are done in the next section.

### 3 Weather Channel Parameter Modelling

#### 3.1 Rainfall Modeling

The magnitude of attenuation experienced by signals depends on the rain intensity. Based on its intensity, a rain event may be classified as drizzle (D), widespread (W), shower (S) or thunderstorm (T). The rainfall is modelled by four or fewer states of a Markov Chain,  $R$ , given by

$$R = \{D, W, S, T\}, \quad (\text{A.5})$$

Table A.1 presents the rain event intensities.

**Table A.1:** Rain Rates Categories.

Description	Rain rate (mm/hr)	Steady state ( $\pi_n$ )
Drizzle	1-5	$\pi_D$
Widespread	5-10	$\pi_W$
Shower	10-40	$\pi_S$
Thunderstorm	>40	$\pi_T$

Practical rainfall, widespread, shower and thunderstorm events consists of a mix of the different rain events [17]. This work utilizes Markov models developed from actual rain data to model practical rain events, with the transition diagram and state transition probabilities as given bellow:

i) Widespread rainfall: Consists of drizzle and widespread events. The transition diagram shown in Fig. A.2, with the transitional probabilities,  $P_{i,j}^W$ , from state  $i$  to  $j$ , with  $i, j \in R$ , given by equation (A.6)

$$P_{i,j}^W = \begin{bmatrix} P_{DD} & P_{DW} \\ P_{WD} & P_{WW} \end{bmatrix}, \quad (\text{A.6})$$

where  $P_{DW}$  is the probability of transitioning from drizzle to widespread,  $P_{WD}$  is the probability of transitioning from widespread to drizzle,  $P_{DD}$  is the probability of no transition from drizzle and  $P_{WW}$  is the probability of no transition from widespread.

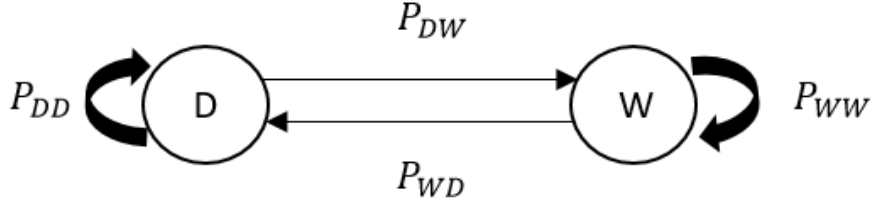


Fig. A.2: Widespread rainfall.

ii) Shower rainfall consists of drizzle, widespread and shower events. The transition diagram shown in Fig. A.3, with the transitional probabilities,  $P_{i,j}^S$ , from state  $i$  to  $j$ , with  $i, j \in R$ , given by equation (A.7)

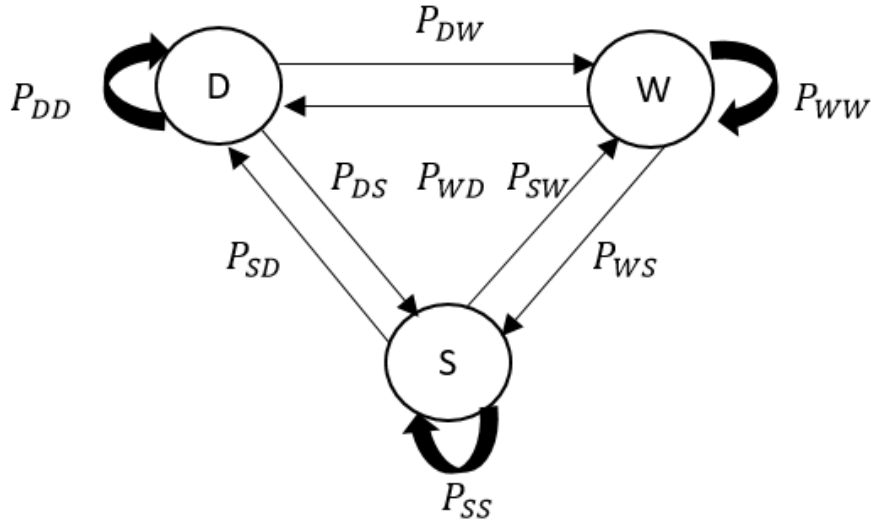


Fig. A.3: Shower rainfall.

$$P_{i,j}^S = \begin{bmatrix} P_{DD} & P_{DW} & P_{DS} \\ P_{WD} & P_{WW} & P_{WS} \\ P_{SD} & P_{SW} & P_{SS} \end{bmatrix}, \quad (\text{A.7})$$

where  $P_{DS}$  is the transition probability from drizzle to shower,  $P_{WS}$  is the transition probability from widespread to shower,  $P_{SD}$  is the transition probability from shower to drizzle,  $P_{SW}$  is the transition probability from shower to widespread and  $P_{SS}$  is the no transition probability from shower.

iii) Thunderstorm rainfall consists of drizzle, widespread, shower and thunderstorm events. The transition diagram shown in Fig. A.4, with the transitional probabilities,  $P_{i,j}^T$ , from state  $i$  to  $j$ , with  $i, j \in R$ , given by equation (A.8)

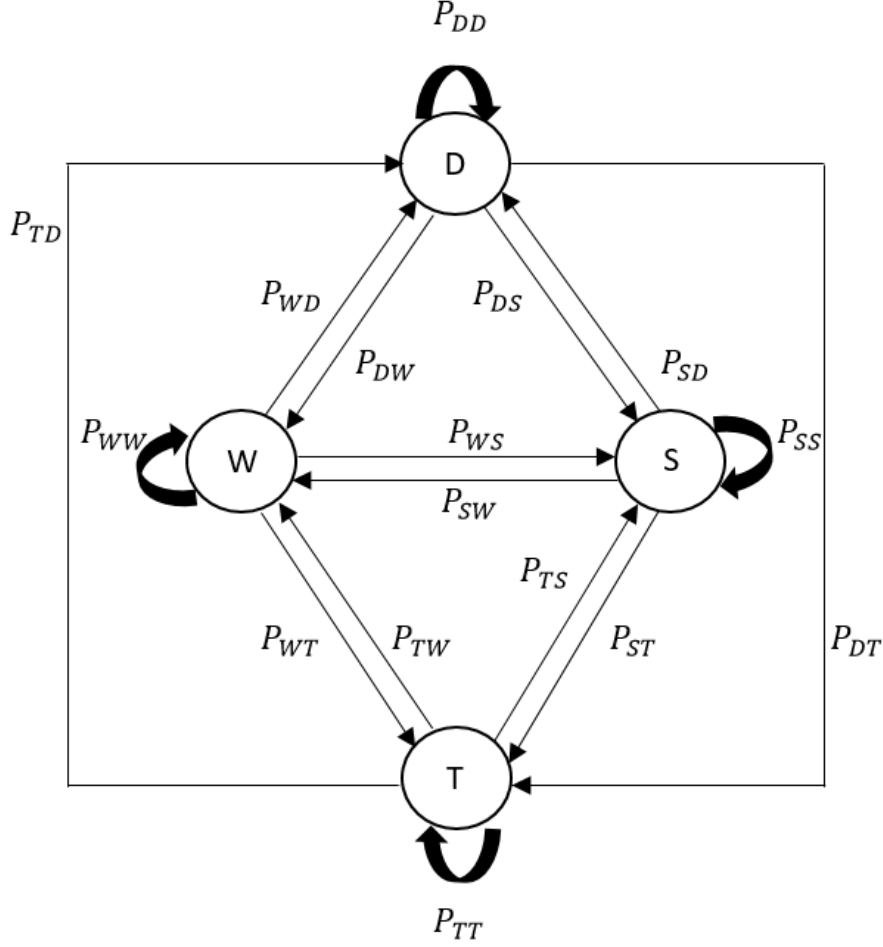


Fig. A.4: Thunderstorm rainfall.

$$P_{i,j}^T = \begin{bmatrix} P_{DD} & P_{DW} & P_{DS} & P_{DT} \\ P_{WD} & P_{WW} & P_{WS} & P_{WT} \\ P_{SD} & P_{SW} & P_{SS} & P_{ST} \\ P_{TD} & P_{TW} & P_{TS} & P_{TT} \end{bmatrix}, \quad (\text{A.8})$$

where  $P_{DT}$  is the probability of transitioning from drizzle to thunderstorm,  $P_{WT}$  is the probability of transitioning from widespread to thunderstorm,  $P_{ST}$  is the probability of transitioning from shower to thunderstorm,  $P_{TD}$  is the probability of transitioning from thunderstorm to drizzle,  $P_{TW}$  is the probability of transitioning from thunderstorm to widespread,  $P_{TS}$  is the probability of transitioning from thunderstorm to shower and  $P_{TT}$  is the no transition probability from thunderstorm. The transitional probabilities used are practically obtained from [17]. The steady state probability of an event  $n$ ,  $\pi_n = \{\pi_D, \pi_W, \pi_S, \pi_T\}$ , is solved by the standard Markov chain solution methods. The expected rate for a rainfall occurrence is derived from the probabilities as

$$E[r] = \sum_n r_n \pi_n, \quad (\text{A.9})$$

where  $r_n$  is the median rain event and  $\pi_n$  is the steady state probability of the  $n^{th}$  state of the Markov model. The actual rain rate  $r$  is computed from a lognormal distribution with the given mean [17][18]19].

### 3.2 Attenuation Model

We consider a radio propagation environment where the signal is affected by attenuation due to the weather-impacted factors. The total attenuation  $A_T$  is given by

$$A_T = \alpha_i + L_{fs}, \quad (\text{A.10})$$

where  $\alpha_i$  is the rain attenuation. The ITU rainfall model [20] is used for attenuation as

$$\alpha_i = kr^a, \quad (\text{A.11})$$

where  $r$  is the rain rate in mm/hr, of section 3.1. The constant parameter  $k$  and exponent  $a$  depend on the frequency  $f$ (GHz), the polarization state, and the elevation angle of the signal path. Free space loss attenuation,  $L_{fs}$ , is given by

$$L_{fs} = 20 * \log_{10} \frac{4\pi d}{\lambda}, \quad (\text{A.12})$$

where  $\lambda$  is the signal wavelength in metres, and  $d$  is the distance from the transmitter.

### 3.3 Angle Deviation Model

The weather related factors result in the delay and scattering of the transmitted signal as well as phase angle, and angle deviation change. The angle deviation,  $\Delta\theta_i$ , is modelled as a normal distributed random variable with a mean  $\mu_\theta$  bounded as follows

$$\Delta\theta_{min} \leq \Delta\theta_i \leq \Delta\theta_{max}, \quad (\text{A.13})$$

where  $\Delta\theta_{min}$  and  $\Delta\theta_{max}$  are the minimum and maximum angle deviations respectively. The mean  $\mu_\theta$  is derived from the normalised rain rate

$$\mu_\theta = \frac{r}{r_{max}}, \quad (\text{A.14})$$

and  $r_{max}$  is the maximum rain rate. The assumption is reasonable as the heavier the rain the more the scattering. Though the weather elements affect the mean and the standard deviation, we keep the standard deviation constant.

## 4 DOA Estimation Algorithms

### 4.1 MVDR Algorithm

The MVDR algorithm minimizes the output power and constraints the gain of the direction of desired signal to unity [21] as follows,

$$\min E\{|y_n(t)|^2\} = \min\{w^H \sigma(x, x) w\}, \quad (\text{A.15})$$

subject to  $w \cdot a(\hat{\theta}) = 1$  where

$$y_n(t) = w^H \sigma(x, x) w, \quad (\text{A.16})$$

is the output of the array system,  $w$  is the weight vector,  $H$  is the Hermitian matrix,  $a(\hat{\theta})$  is the steering vector and  $\sigma(x, x)$  is covariance matrix of the received signal  $x$ . The covariance matrix  $\sigma(x, x)$  is given by

$$\sigma(x, x) = \frac{1}{N} \sum_{i=1}^N x x^H, \quad (\text{A.17})$$

where  $N$  is the number of elements. From the block diagram of Fig. A.1, the signal vector  $x(t)$  defined at different angles  $\hat{\theta}_i$  induced on the antenna arrays is multiplied by weight vectors  $w$  and then combined to form the system output  $y(t)$ . The weighted vector  $w$  is obtained by using Lagrange multiplier in (A.15) as

$$w = \frac{(\sigma(x, x))^{-1} a(\hat{\theta})}{a^H(\hat{\theta}) (\sigma(x, x))^{-1} a(\hat{\theta})}. \quad (\text{A.18})$$

Thus, MVDR computed as a Capon's output power spectrum is given by

$$P_{MVDR}(\hat{\theta}) = \frac{1}{a^H(\hat{\theta}) (\sigma(x, x))^{-1} a(\hat{\theta})}. \quad (\text{A.19})$$

The MVDR technique is summarized in Algorithm 1.

---

#### Algorithm 1 MVDR algorithm

---

- 1: **Input:**  $x = \{x_i(t)\} = f(\alpha_i, \hat{\theta}_i)$ ,  $N$ ,  $d$ ,  $\lambda$ ,  $K$  and  $\mu \leftarrow$  step size
  - 2: Compute the weight vector  $w$ , equation (A.18)
  - 3: Compute covariance matrix  $\sigma(x, x)$ , equation (A.17)
  - 4: Compute the output array system, equation (A.16)
  - 5: Minimize the output power, equation (A.15), subject to  $w \cdot a(\hat{\theta}) = 1$
  - 6: Compute spectrum function, equation (A.19), spanning  $\theta$
-

## 4.2 MUSIC Algorithm

MUSIC is a high-resolution subspace DOA algorithm where an estimate  $\sigma(x, x)$  of the covariance matrix is obtained and its eigenvectors decomposed into orthogonal signal and noise subspace [22]. The DOA is estimated from one of these subspaces. The noise in each channel is assumed uncorrelated. The algorithm searches through the set of all possible steering vectors to find those orthogonal to the noise subspace. The diagonal covariance matrix  $\sigma(x, x)$  is given by (A.17). The covariance matrix is decomposed to

$$\sigma(x, x) = A(\hat{\theta}_i)\tilde{S}_i(t)A(\hat{\theta}_i)^H + \sigma^2I = Q\Lambda Q^H, \quad (\text{A.20})$$

where  $A(\hat{\theta}_i) = [a_1(\hat{\theta}_1), a_2(\hat{\theta}_2), \dots, a_N(\hat{\theta}_I)]^T$  is a  $M \times D$  array steering matrix,  $\sigma^2$  is the noise variance,  $I$  is an identity matrix of size  $M \times M$  and  $\tilde{S}_i(t)$  the received signal with  $Q$  unitary and a diagonal matrix  $\Lambda = \text{diag}\{\lambda_1, \lambda_2, \dots, \lambda_M\}$ , of real eigenvalue ordered as  $\lambda_1 \geq \lambda_2 \geq \dots \geq \lambda_M \geq 0$ . The vector that is orthogonal to  $A$  is the eigenvector of  $R$  having the eigenvalues of  $\Lambda$ . The MUSIC spatial spectrum is defined by

$$P_{MUSIC}(\hat{\theta}) = \frac{1}{a^H(\hat{\theta})Q_nQ_n^H a(\hat{\theta})}, \quad (\text{A.21})$$

where  $a(\hat{\theta})$  is the steering vector corresponding to one of the incoming signals and  $Q_n$  is the signal subspace. The MUSIC technique is summarized in Algorithm 2.

---

### Algorithm 2 MUSIC algorithm

---

- 1: **Input:**  $x = \{x_i(t)\} = f(\alpha_i, \hat{\theta}_i)$ ,  $N$ ,  $d$ ,  $\lambda$ ,  $K$
  - 2: Compute covariance matrix  $\sigma(x, x)$ , equation (A.17)
  - 3: Decomposition  $\sigma(x, x)$  into eigenvectors and eigenvalues in equation (A.20)
  - 4: Rearrange the eigenvectors and eigenvalues into the signal subspace and noise subspace.
  - 5: Compute the spectrum function (A.21) by spanning  $\theta$ .
  - 6: Determine the substantial peaks of  $P_{MUSIC}(\theta)$  to acquire estimates of the angle of arrival.
- 

## 4.3 Proposed A-MUSIC Algorithm

In rain impacted mmW systems, the SNR is low leading to small signal intervals. The existing MVDR and MUSIC algorithms are adversely affected and need modifications. We propose an A-MUSIC algorithm that repeatedly reconstructs the covariance matrix to continuously obtain two noise and signal subspaces averaged over several iterations. The reconstructed covariance matrix  $\hat{\sigma}(x, x)$  is given by

$$\hat{\sigma}(x, x) = \sigma(x, x) + J\sigma(x, x)^*J, \quad (\text{A.22})$$

where  $J$  is MATLAB constructions given as  $J = \text{fliplr}(\text{eye}(N))$  which returns columns flipped in the left-right direction and  $N$  is the number of elements. The eigen decomposition on reconstructed covariance matrix  $\hat{\sigma}(x, x)$  is

$$\hat{\sigma}(x, x) = \hat{Q}\Lambda\hat{Q}^H = Q_{S1}\Lambda_{S1}Q_{S1}^H + Q_{N1}\Lambda_{N1}Q_{N1}^H, \quad (\text{A.23})$$

where  $\hat{\sigma}(x, x)$  is divided into signal subspace  $Q_S$  and noise subspace  $Q_N$ . Using low rank of matrix instead of full rank matrix  $\hat{\sigma}(x, x)$  can be reconstructed into  $\omega_x$  as

$$\omega_x = Q_{S2}\Lambda_{S2}Q_{S2}^H + Q_{N2}\Lambda_{N2}Q_{N2}^H. \quad (\text{A.24})$$

The average signal subspace ( $Q_S$ ), signal eigenvalue ( $\Lambda_S$ ), noise subspace ( $Q_N$ ), and the noise eigenvalue ( $\Lambda_N$ ) are given by

$$\begin{aligned} Q_S &= \frac{Q_{S1} + Q_{S2}}{2}, \\ Q_N &= \frac{Q_{N1} + Q_{N2}}{2}, \\ \Lambda_S &= \frac{\Lambda_{S1} + \Lambda_{S2}}{2}, \\ \Lambda_N &= \frac{\Lambda_{N1} + \Lambda_{N2}}{2}. \end{aligned} \quad (\text{A.25})$$

The A-MUSIC spectrum is then defined by

$$P_{(A-MUSIC)}(\hat{\theta}) = \frac{a^H(\hat{\theta})[\frac{(\sigma(s,s))(\sigma(s,s))^H}{N}]a(\hat{\theta})}{a^H(\hat{\theta})\sigma(n, n)a(\hat{\theta})}, \quad (\text{A.26})$$

where  $\sigma(s, s) = Q_S\Lambda_S^{-1}Q_S^H$ , and  $\sigma(n, n) = Q_N\Lambda_N^{-1}Q_N^H$  are signal and noise subspace covariance matrix. The A-MUSIC technique is summarized in Algorithm 3.

---

**Algorithm 3** Proposed A-MUSIC Algorithm

---

- 1: **Input:**  $x = \{x_i(t)\} = f(\alpha_i, \hat{\theta}_i), N, d, \lambda, K$
  - 2: Compute the covariance matrix, equation (A.20)
  - 3: Compute reconstructed covariance matrix  $\hat{\sigma}(x, x)$ , equation (A.22)
  - 4: Compute the Eigen decomposition on reconstructed covariance matrix  $\hat{\sigma}(x, x)$
  - 5: Compute reconstructed covariance matrix  $\omega_x$ , for equation (A.24)
  - 6: Compute the average signal subspace, noise subspace, signal eigenvalues, and the noise eigenvalue,  $Q_S, Q_N, \Lambda_S, \Lambda_N$  equation (A.25)
  - 7: Determine signal and noise subspace averaged covariance matrix  $\sigma(s, s)$  and  $\sigma(n, n)$
  - 8: Compute the spectrum function, equation (A.26), spanning  $\theta$
-

## 5 Performance Measures

The performance of the DOA estimation algorithms is evaluated in terms of spectrum functions, equations (A.19), (A.21) and (A.26), the Root Mean Square Error (RMSE) and the signal to noise ratios. The RMSE is given by

$$RMSE = \sqrt{\frac{1}{K * N} \sum_{j=1}^K \sum_{i=1}^N (\tilde{\theta}_{ij} - \theta_i)^2}, \quad (\text{A.27})$$

where  $K$  is the number of simulation trials,  $N$  is the number of elements and the estimate of the  $i^{th}$  angle of arrival in the  $j^{th}$  trial is  $\tilde{\theta}_{ij}$ . Where utilised, the signal to noise ratio (SNR) is given by

$$SNR = 20 \log_{10}\left(\frac{x}{v}\right), \quad (\text{A.28})$$

where  $x$  is the received signal strength in dB and  $v$  is the noise strength in dB. The overall performance evaluation is done as in algorithm 4.

---

### Algorithm 4 System Algorithm

---

- 1: **Input:** Required rainfall
  - 2: Compute expected rain rate, equation
  - 3: Compute the actual rain rate  $r$  from lognormal distribution with given mean
  - 4: **for**  $i$  number of antennas  $< N_{max}$
  - 5:     Compute the rain attenuation  $\alpha_r$ , total attenuation given
  - 6:      $A_T$  and the angle  $\hat{\theta}_i$ . find the angle deviation  $\Delta\theta_i$  as shown
  - 7:     in (A.13) and the mean  $\mu_\theta$ .
  - 8:     Determine the received signal  $x_i(t)$ .
  - 9: **end for**
  - 10: Determine DOA, Algorithm 1,2 and 3.
- 

The complexity of MVDR and MUSIC algorithm has been derived as shown in Table A.2 [23][24]. For A-MUSIC, there are three major computational steps needed to estimate the DOA. The complexity of the first step is the covariance function and reconstruction of the covariance matrix,  $O(N^2K)$ . The second step is the eigen value decomposition operation, which has a complexity of  $O(N^3)$ . The third step is obtaining the spatial pseudo spectrum, which has a complexity of  $\mathcal{O}(J_\theta \cdot J_{\Delta\theta}(N+1)(N-K)/2)$ , with  $J$  being the number of spectral points of the total angular field of view. Therefore, the total complexity of A-MUSIC is given by  $\mathcal{O}(N^2K + N^3) + \mathcal{O}(J_\theta \cdot J_{\Delta\theta}(N+1)(N-K)/2)$ .

**Table A.2:** Computational Complexity of DOA Estimation Algorithms.

DOA algorithm	Computational Complexity
MVDR	$\mathcal{O}(N^2K + N^3 + (2N^2 + 3N))$
MUSIC	$\mathcal{O}(N^2K + N^3 + JN)$
A-MUSIC	$\mathcal{O}(N^2K + N^3) + \mathcal{O}(J_\theta \cdot J_{\Delta\theta}(N + 1)(N - K)/2)$

## 6 Results and Discussion

The performances of the general MVDR, MUSIC and the proposed algorithm A-MUSIC are investigated and discussed in this section. The performance of the algorithms for different number of array elements, rain rates and SNR is investigated. Unless otherwise specified for a particular result the simulation parameters are as given in Table A.3. The developed results are for a case where four signals impinge on the ULA sensors from the same signal source. The signal consists of the first direct path signal and the scaled and delayed replicas of the first signal representing multipath signals known priori. The background noise is modelled as a stationary Gaussian white random process. The

**Table A.3:** Simulation Parameters for MVDR, MUSIC and A-MUSIC Algorithm.

Simulation Parameters	Values
Input $\theta$	$[0^0, 10^0, 35^0, 60^0]$
Number of elements	$N = 5, N = 15$
Spacing difference	$d = 0.5\lambda$
Signal-to-noise ratio	$SNR = 20dB$
Snapshots	$K = 100$
Rain rate in (mm/hr)	$[0, 2.5, 6, 12, 20]$
$a$ at f(GHz)	0.7103
$k$ at f(GHz)	1.16995
$\Delta\theta_{min}, \Delta\theta_{max}$	$[0^0 - 65^0]$

results of Fig. A.5-A.8 show the spatial output spectrum in dB's of the MVDR, MUSIC and the proposed A-MUSIC for different rain rates from zero to 20mm/hr representing the following cases;

no rain, widespread, shower and thunderstorm rain conditions with the number of elements  $N = 5$  for 100 snapshots. Note that without rain the spectrum results for MVDR and MUSIC are similar to the ones in [25] respectively. From the results, the following can be observed; the accuracy of DOA estimation reduces with increasing rain rate and the performance of the A-MUSIC is better than MUSIC followed by MVDR. This is because of the multiple averaging nature of A-MUSIC algorithm. It can also be observed that at a higher rain rate of 20mm/hr MVDR and MUSIC fail to estimate the Direction of Arrival (DOA).

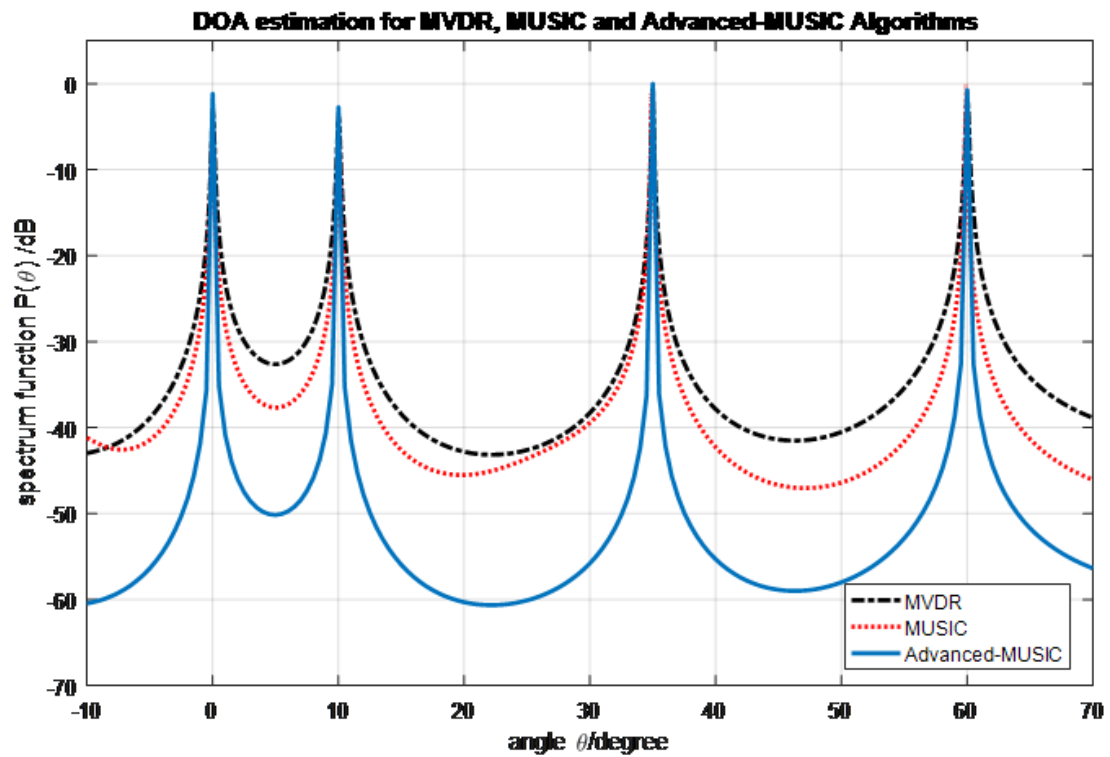


Fig. A.5: DOA estimation attenuation with rain rate  $r = 0\text{mm/hr}$  for  $N = 5$ .

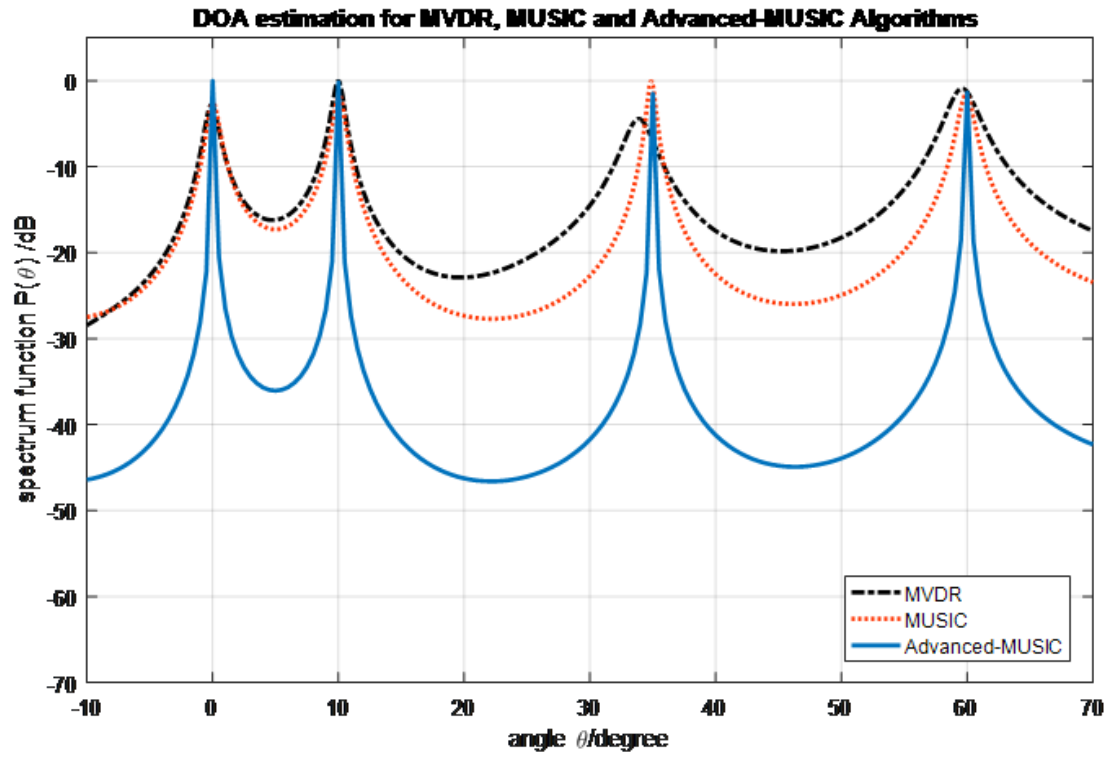


Fig. A.6: DOA estimation attenuation at drizzle rain rate  $r = 2\text{mm/hr}$  for  $N = 5$ .

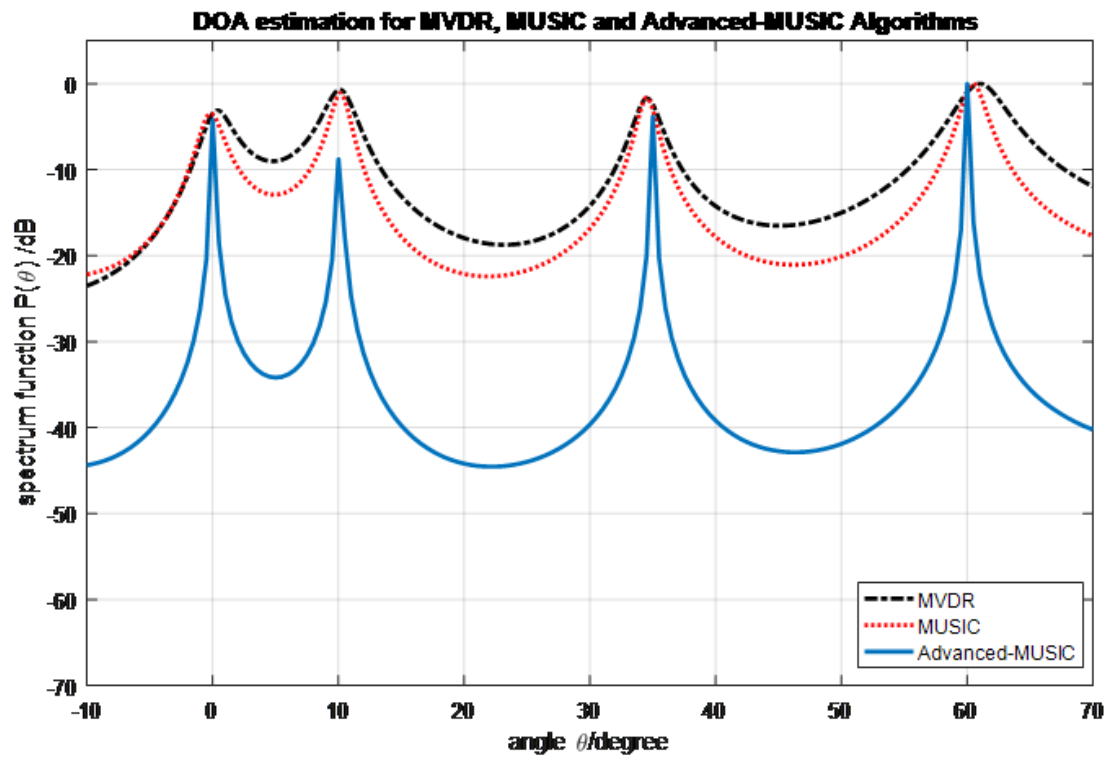


Fig. A.7: DOA estimation attenuation at widespread rain rate  $r = 8\text{mm/hr}$  for  $N = 5$ .

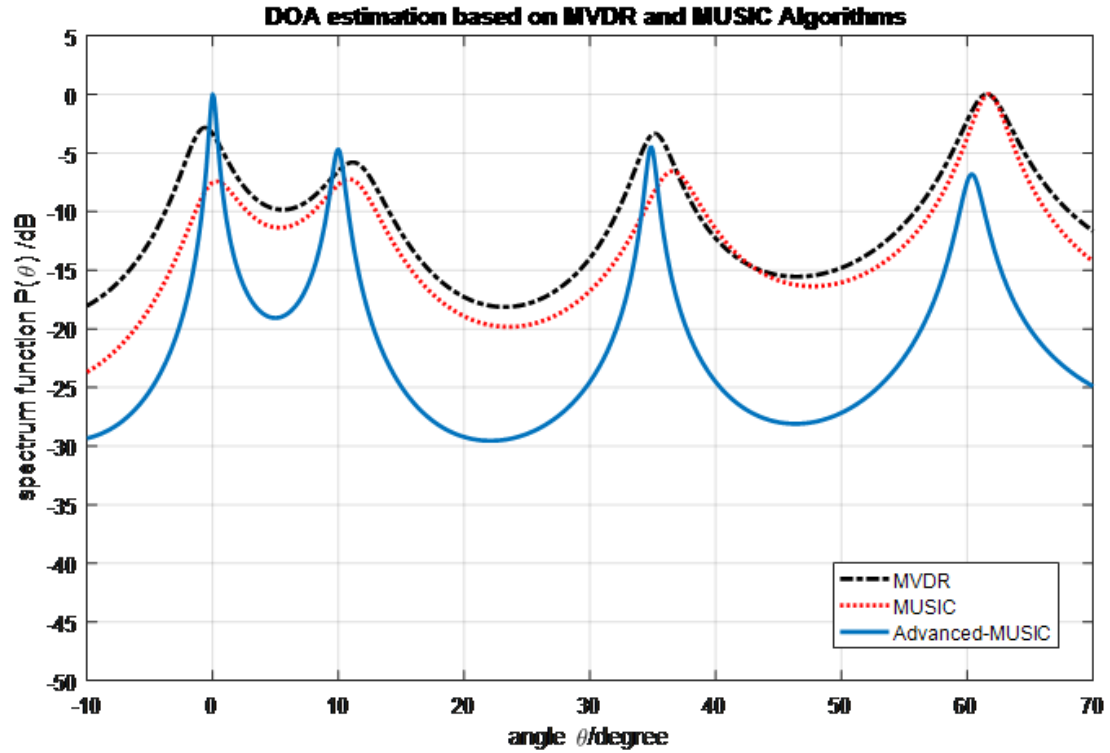
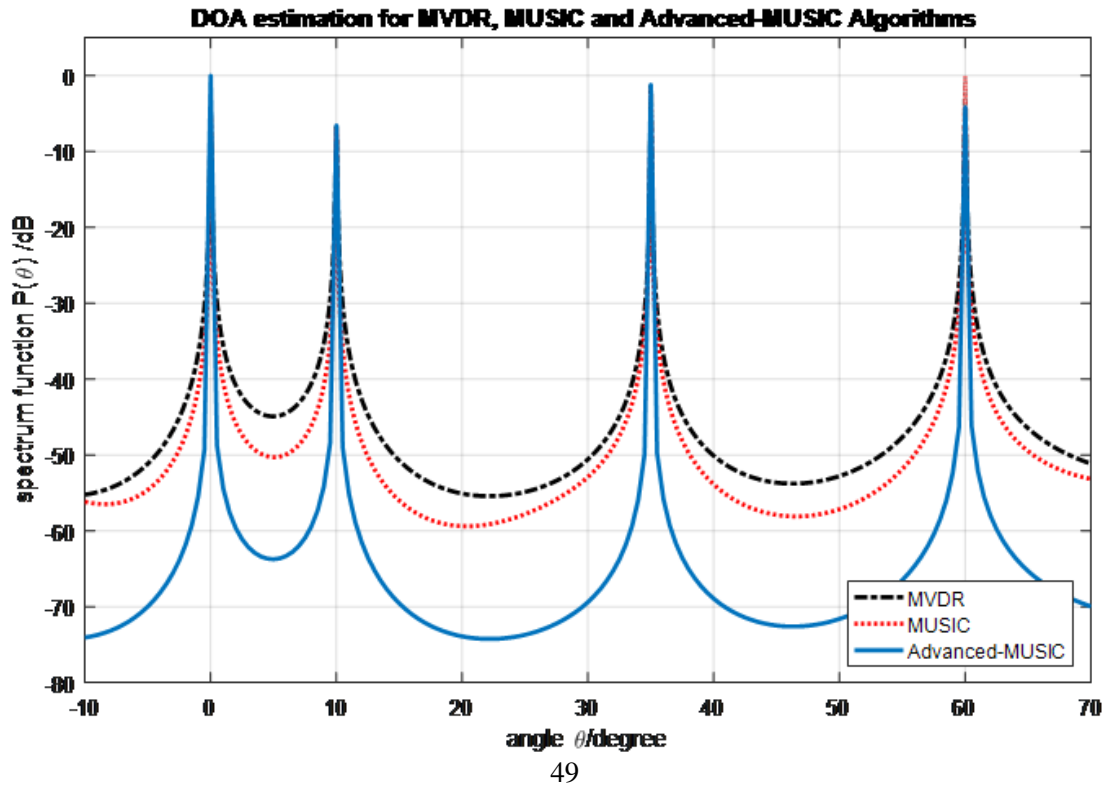


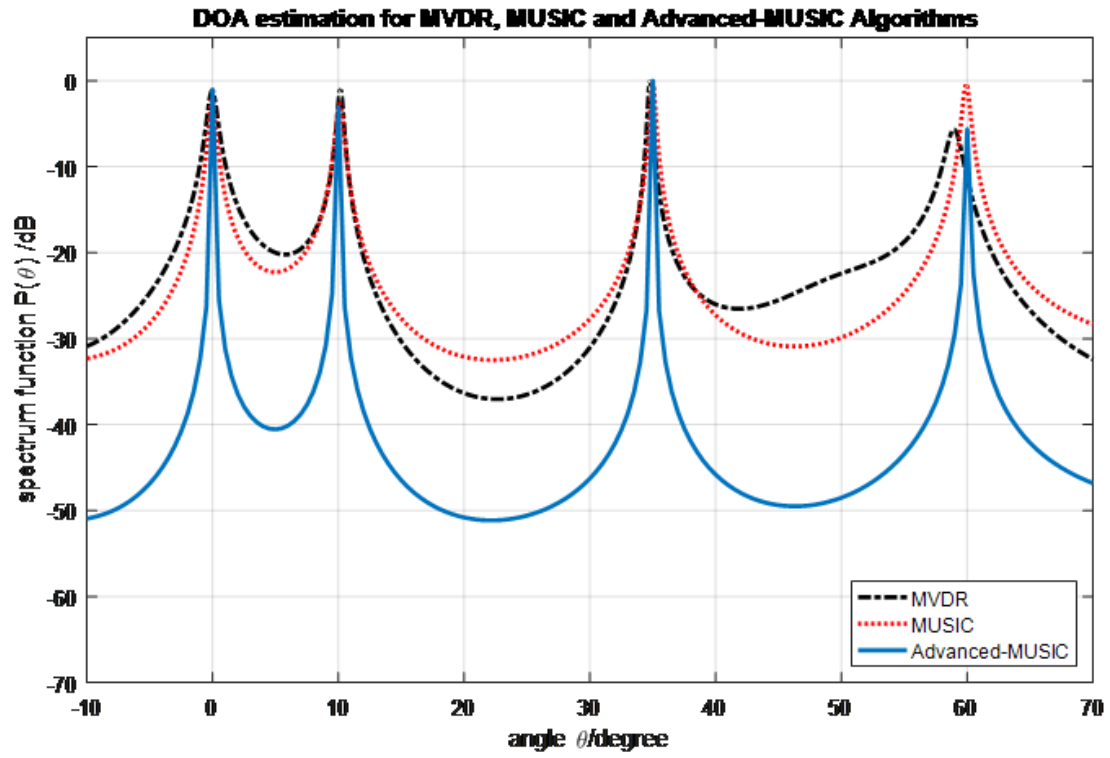
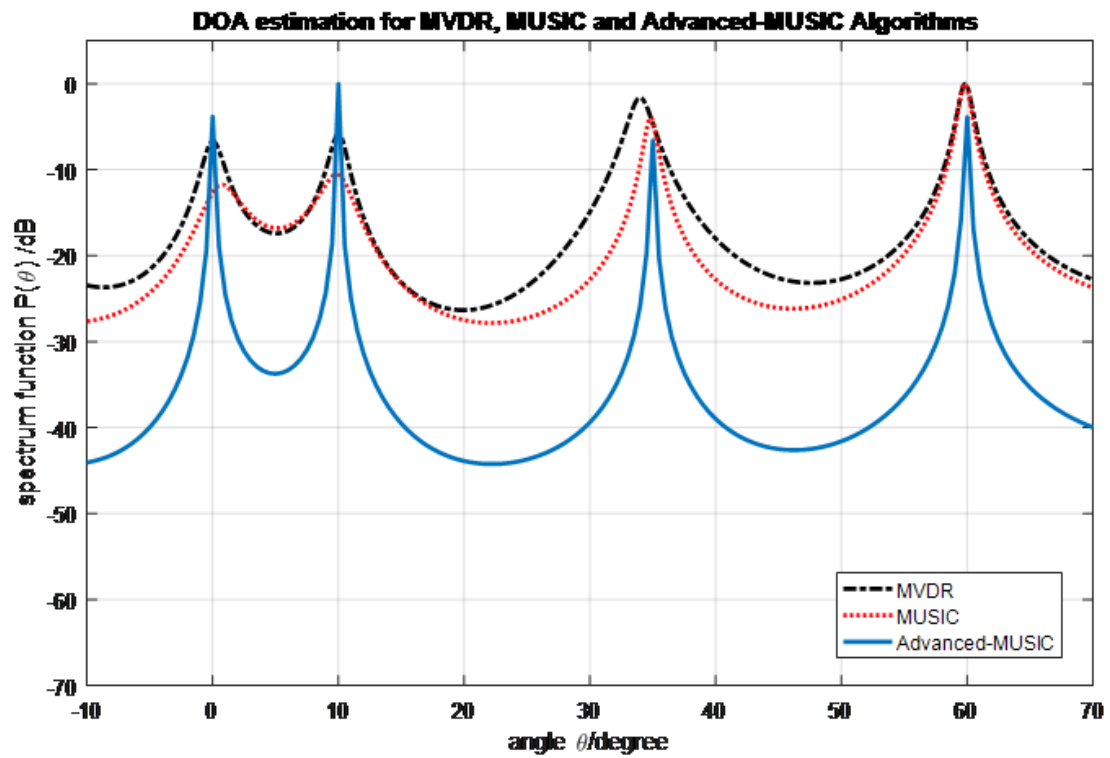
Fig. A.8: DOA estimation attenuation at shower rain rate  $r = 20\text{mm/hr}$  for  $N = 5$ .

To analyse the performance of the DOA algorithms and the proposed method, a simulation was done for four neighbouring signals and the results tabulated in Table A.4. The results depict the accuracy of the three DOA algorithms. There is a degradation in accuracy for the developed algorithm as the rain rate increases. From zero to  $20\text{mm/hr}$  the degradation of MVDR is 47%, for MUSIC is 33% and for A-MUSIC is 3.3% at reference point  $-20\text{dB}$ . Similarly, the results of Fig. A.9-A.12 shows the spatial output power spectrum in dB's of the three algorithms discussed in section 4 for different rain rates representing no rain, widespread, shower and thunderstorm rain conditions. However, the number of elements  $N = 15$  for 100 snapshots. Note that without rain the spectrum results for MVDR and MUSIC are similar to the ones in [26][27] respectively. The results reinforce the notion that the accuracy of DOA estimation reduces with increasing rain rate and the performance of the A-MUSIC is better than MUSIC followed by MVDR.

**Table A.4:** Spectrum Performance for actual DOA =  $[0^{\circ}, 10^{\circ}, 35^{\circ}, 60^{\circ}]$ .

<b>Fig. A5</b>	<b>Estimated DOA</b>	<b>Error %</b>
MVDR	$0.0201^{\circ}, 9.9^{\circ}, 35.01^{\circ}, 59.8^{\circ}$	3.372
MUSIC	$0.02^{\circ}, 10.001^{\circ}, 35.02^{\circ}, 60^{\circ}$	2.067
A-MUSIC	$0^{\circ}, 10^{\circ}, 35^{\circ}, 60^{\circ}$	0
<b>Fig. A6</b>	<b>Estimated DOA</b>	<b>Error %</b>
MVDR	$-0.032^{\circ}, 9.8^{\circ}, 34.0^{\circ}, 58.8^{\circ}$	10.057
MUSIC	$1.2^{\circ}, 10.5^{\circ}, 34.78^{\circ}, 60.1^{\circ}$	17.796
A-MUSIC	$0.001^{\circ}, 10^{\circ}, 35^{\circ}, 60^{\circ}$	0.1
<b>Fig. A7</b>	<b>Estimated DOA</b>	<b>Error %</b>
MVDR	$0.22^{\circ}, 9.5^{\circ}, 34.76^{\circ}, 62^{\circ}$	31.018
MUSIC	$0.1^{\circ}, 10.3^{\circ}, 34.8^{\circ}, 61.1^{\circ}$	15.404
A-MUSIC	$0.001^{\circ}, 10.002^{\circ}, 35.03^{\circ}, 60.01^{\circ}$	0.2217
<b>Fig. A8</b>	<b>Estimated DOA</b>	<b>Error %</b>
MVDR	$-0.32^{\circ}, 11.1^{\circ}, 35.7^{\circ}, 63.2^{\circ}$	50.33
MUSIC	$0.2^{\circ}, 10.2^{\circ}, 36.0^{\circ}, 63.0^{\circ}$	29.86
A-MUSIC	$0.01^{\circ}, 10.2^{\circ}, 35.1^{\circ}, 60.01^{\circ}$	3.303

**Fig. A.9:** DOA attenuation with rain rate  $r=0\text{mm/hr}$  for  $N=15$ .

Fig. A.10: DOA attenuation in light rain rate of  $r=2\text{mm/hr}$  for  $N=15$ .Fig. A.11: DOA attenuation in moderate rain rate of  $r=8\text{mm/hr}$  for  $N=15$ .

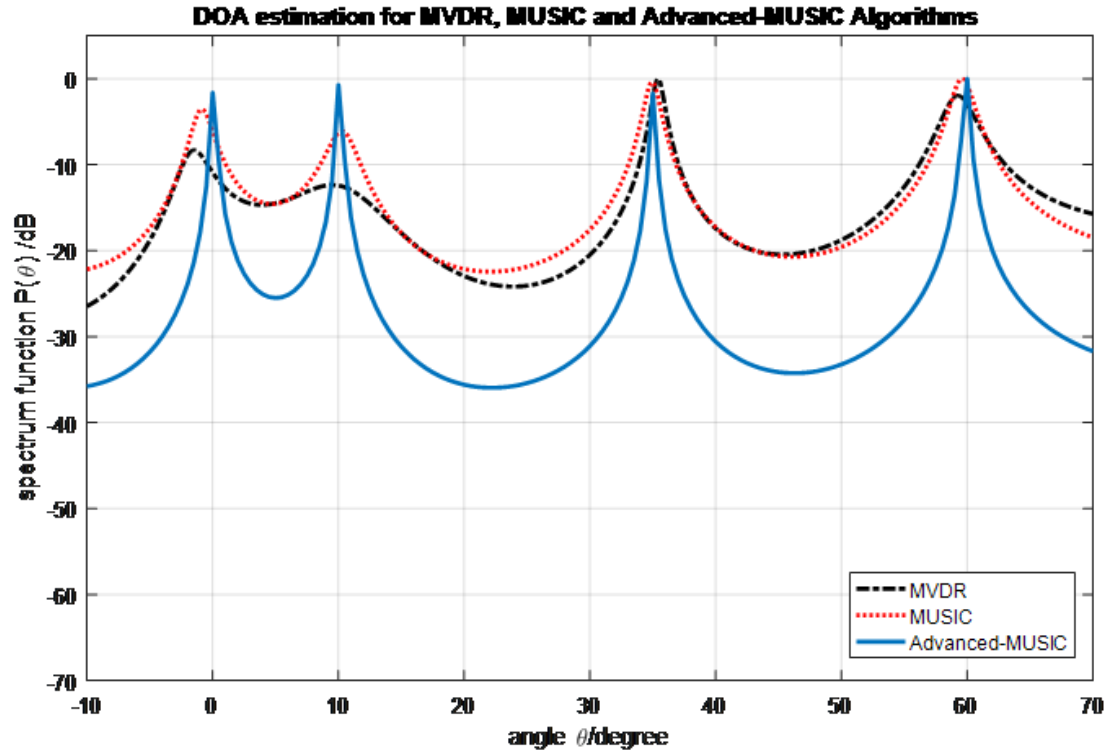
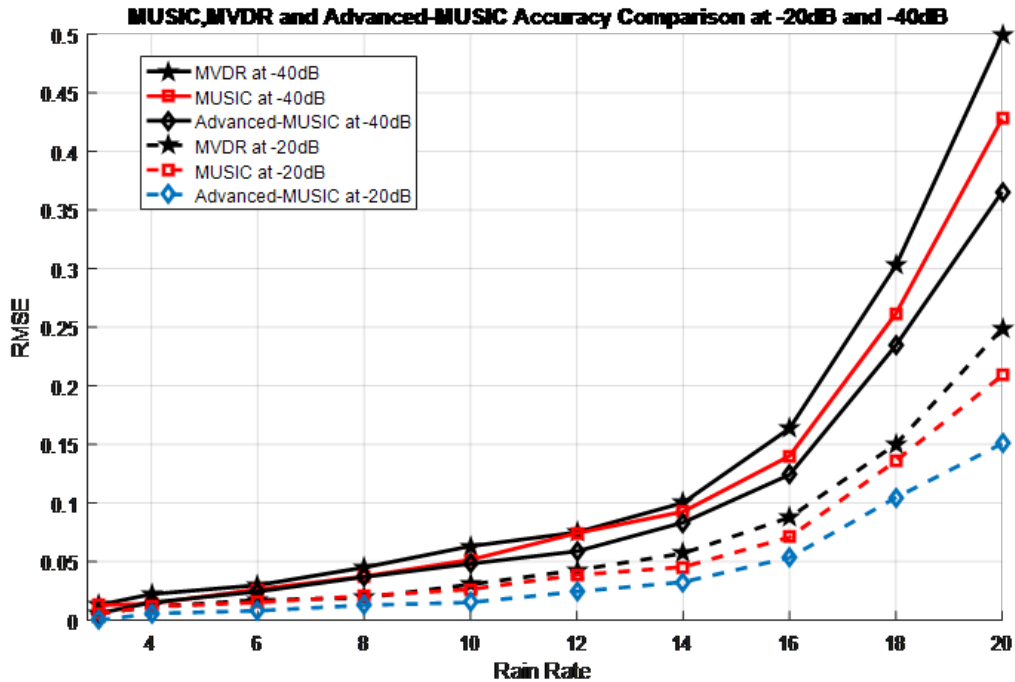


Fig. A.12: DOA attenuation in heavy rain rate of  $r=20\text{mm/hr}$  for  $N=15$ .

The results of estimated DOAs are tabulated in Table A.5. Similarly, the results depict the accuracy of the three DOA algorithms. There is a degradation in accuracy for the developed algorithm as the rain rate increases. From zero to  $20\text{mm/hr}$  the degradation of MVDR is 38%, for MUSIC is 23% and for A-MUSIC is 1.23%. at reference point  $-20\text{dB}$ . For different number of antennas, comparison of the results in Fig. A.5-A.8 for  $N = 5$  and Fig. A.9-A.12 for  $N = 15$  is done. We observe that DOA estimation improves with increasing the number of antenna elements. At the  $-40\text{dB}$  reference point we observe that the width of the spectrum function is wide and leading to high error estimation of the angle of arrival.

**Table A.5:** Spectrum Performance for actual DOA =  $[0^0, 10^0, 35^0, 60^0]$ .

Fig. A9	Estimated DOA	Error %
MVDR	$0^0, 10.001^0, 35.02^0, 60.01^0$	0.5977
MUSIC	$0.002^0, 10.01^0, 35.01^0, 60.02^0$	0.3623
A-MUSIC	$0^0, 10^0, 35^0, 60^0$	0
Fig. A10	Estimated DOA	Error %
MVDR	$0.2^0, 10.1^0, 33.7^0, 59.6^0$	25.381
MUSIC	$0.01^0, 10.2^0, 34.7^0, 60.1^0$	4.024
A-MUSIC	$0.001^0, 10.01^0, 35.01^0, 60^0$	0.2286
Fig. A11	Estimated DOA	Error %
MVDR	$0.23^0, 9.6^0, 35.3^0, 57.5^0$	32.024
MUSIC	$0.1^0, 10.2^0, 35.01^0, 60.01^0$	12.0453
A-MUSIC	$0.01^0, 10^0, 35^0, 60^0$	1.0
Fig. A12	Estimated DOA	Error %
MVDR	$-3^0, 9.5^0, 34.5^0, 58.5^0$	38.929
MUSIC	$-2^0, 10.2^0, 35.1^0, 59.5^0$	23.00
A-MUSIC	$0.002^0, 9.9^0, 35.01^0, 60^0$	1.2286



**Fig. A.13:** MUSIC, MVDR and A-MUSIC Accuracy Comparison at -20dB and -40dB with DOA =  $[20^0, 40^0, 50^0]$ .

The results of Fig. A.13 represent the RMSE value vs rain rate at a different angle of arrival  $[20^{\circ}, 40^{\circ}, 50^{\circ}]$  for two different reference spectrum function levels  $-20\text{dB}$  and  $-40\text{dB}$  with  $N = 10$ . As expected, the RMSE increases with an increase in rain rate. It is also higher at  $-40\text{dB}$  as compared to  $-20\text{dB}$ . The performance order of the algorithms is MVDR, MUSIC and A-MUSIC. Similarly, the results of Fig. A.14-A.16 represent the RMSE error comparison for different rain conditions albeit at variable antenna elements  $N = 5, N = 10$  and  $N = 20$  for  $SNR = 20\text{dB}$ . The RMSE increase with increase in rainfall and the proposed A-MUSIC performs better than the other models due to repeatedly reconstruction of the covariance matrix to obtain two noise and signal subspaces continuously that are averaged for several iterations. An additional deduction from the result is that the RMSE errors reduce with the increase in antenna elements.

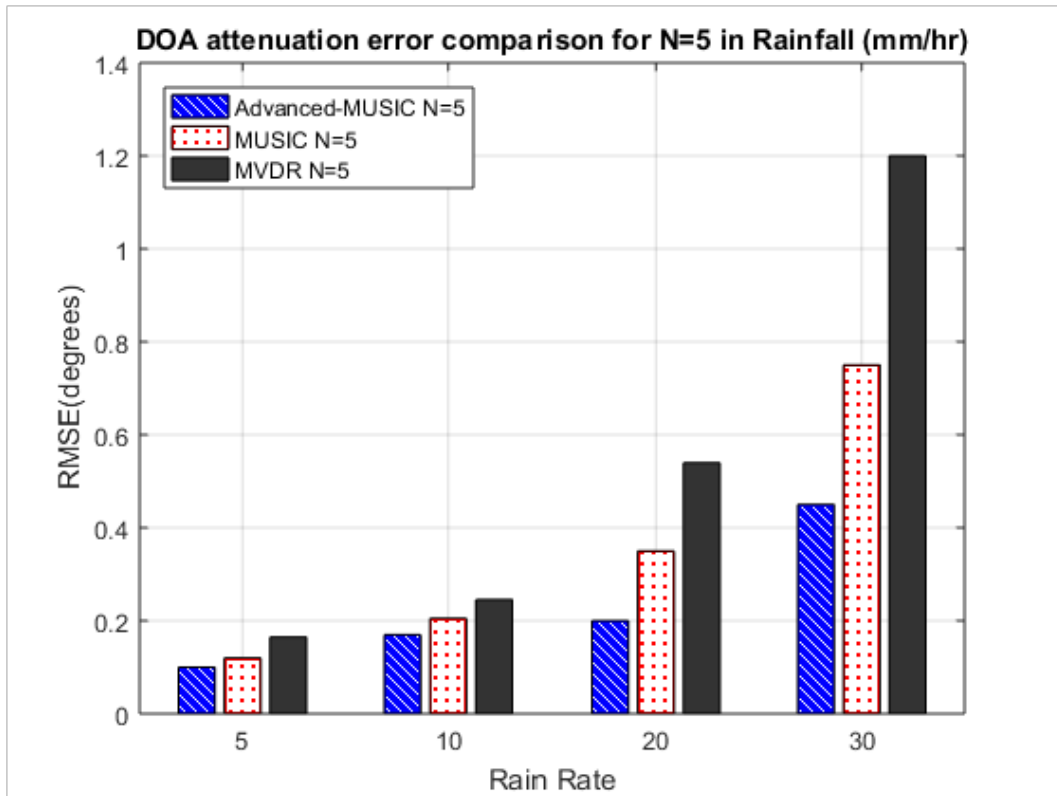


Fig. A.14: DOA estimation attenuation error comparison for N=5.

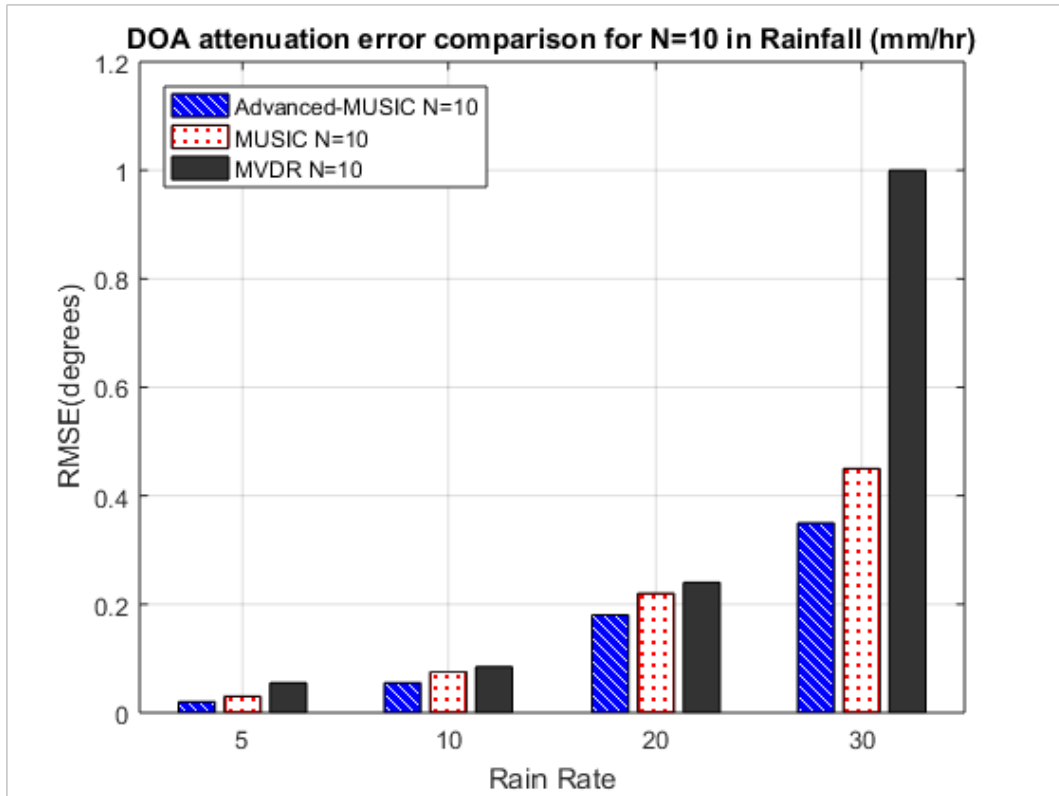


Fig. A.15: DOA estimation attenuation error comparison for N=10.

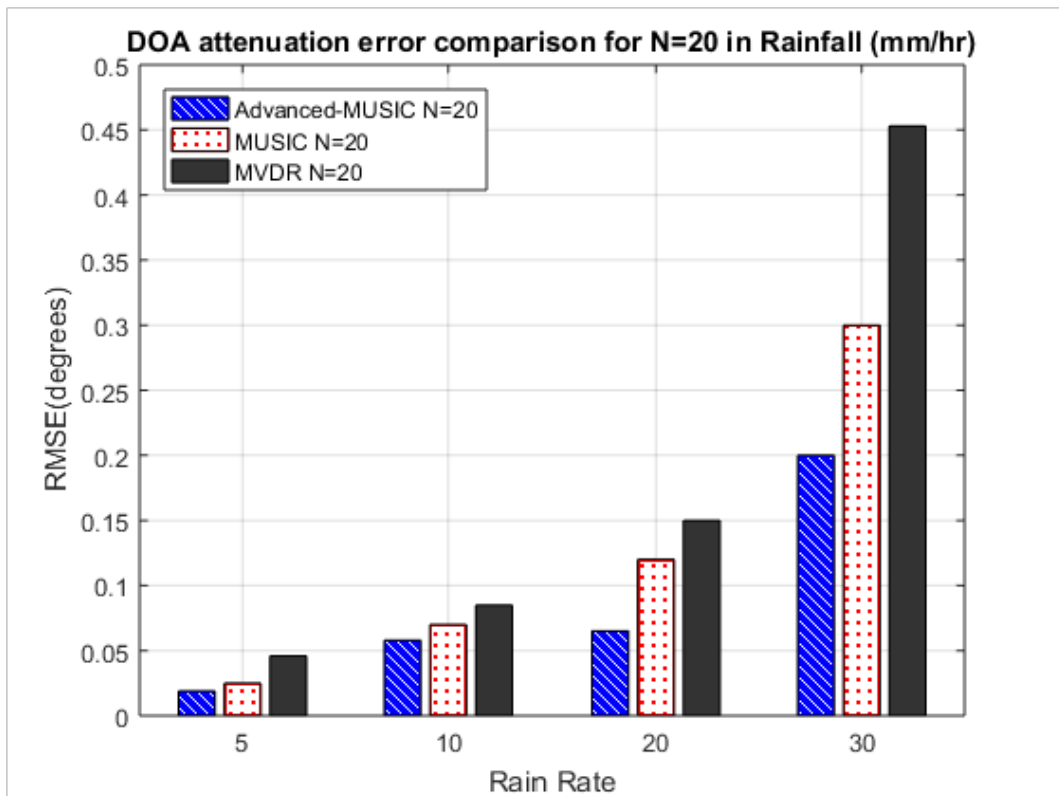


Fig. A.16: DOA estimation attenuation error comparison for N=20.

To reiterate the deduction from Fig. A.14-A.16, Fig. A.17 presents the results of the RMSE error vs the number of elements for no rain and the rate of 15mm/hr. It can be observed that as the number of elements increases the RMSE decreases. Still the proposed A-MUSIC outperforms MVDR and MUSIC algorithm in terms of error comparison. We conclude that the statistical channel model proposed in this paper is highly recommended in both rainfall and non-rainfall regions due to its excellent performance.

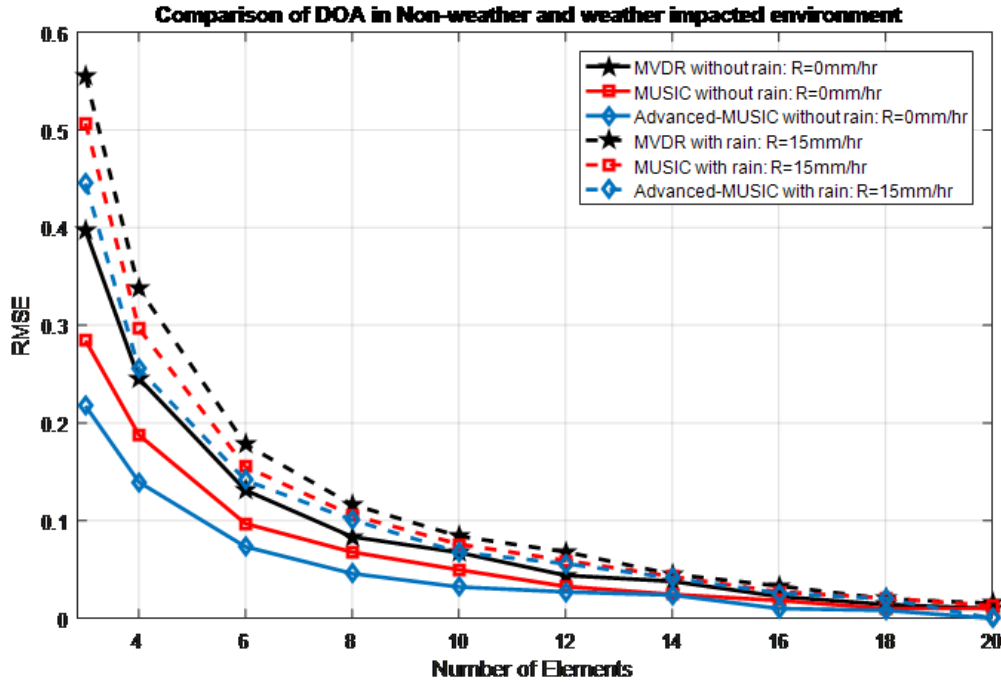


Fig. A.17: Comparison of DOA estimation algorithms in Non-weather and weather impacted environment.

To further investigate the performance of the system, the DOA estimation algorithms are tested at different rain rates leading to different SNR conditions and results presented in Fig. A.18 for  $N = 10$ . As expected the RMSE reduces with an increase in the values SNR and A-MUSIC outperforms MVDR and MUSIC making it highly recommended in estimation of DOA in both normal and rainfall environments.

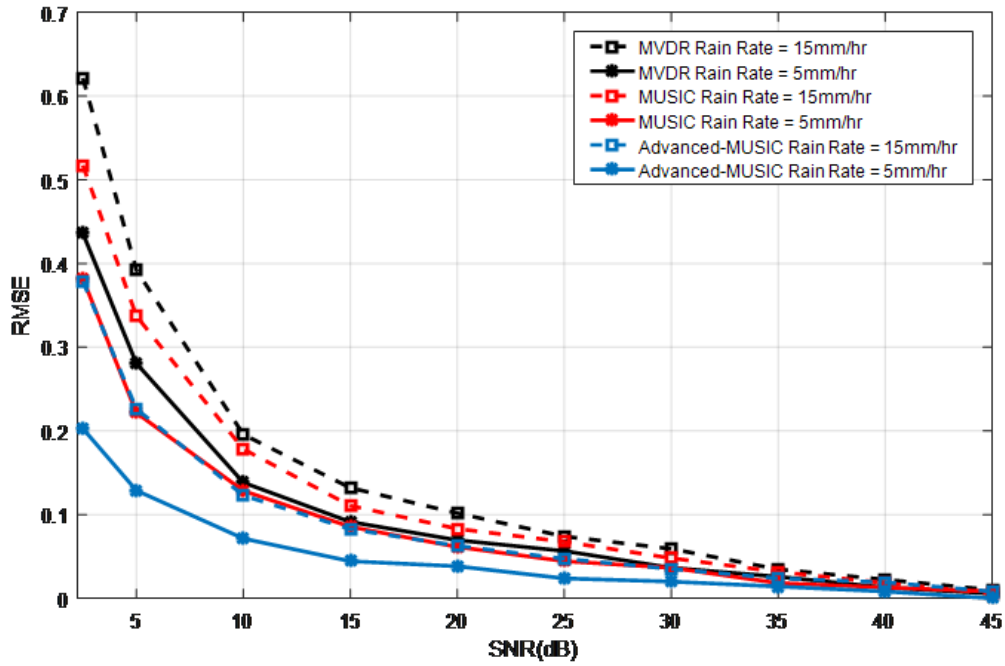


Fig. A.18: Error comparison in various rain rates vs SNR.

Fig. A.19 shows the performance comparison in rainfall for various number of snapshots at  $SNR = 20dB$ ,  $r = 20mm/hr$  and  $N = 5$ . As expected the RMSE decreases as we increase the number of trials from 100-500. Therefore increasing number of simulation trials can improve the performance of the algorithms. It can be intuitively observed that the proposed A-MUSIC surpasses the MVDR and classical MUSIC estimator over the range of the number of snapshots that we simulated.

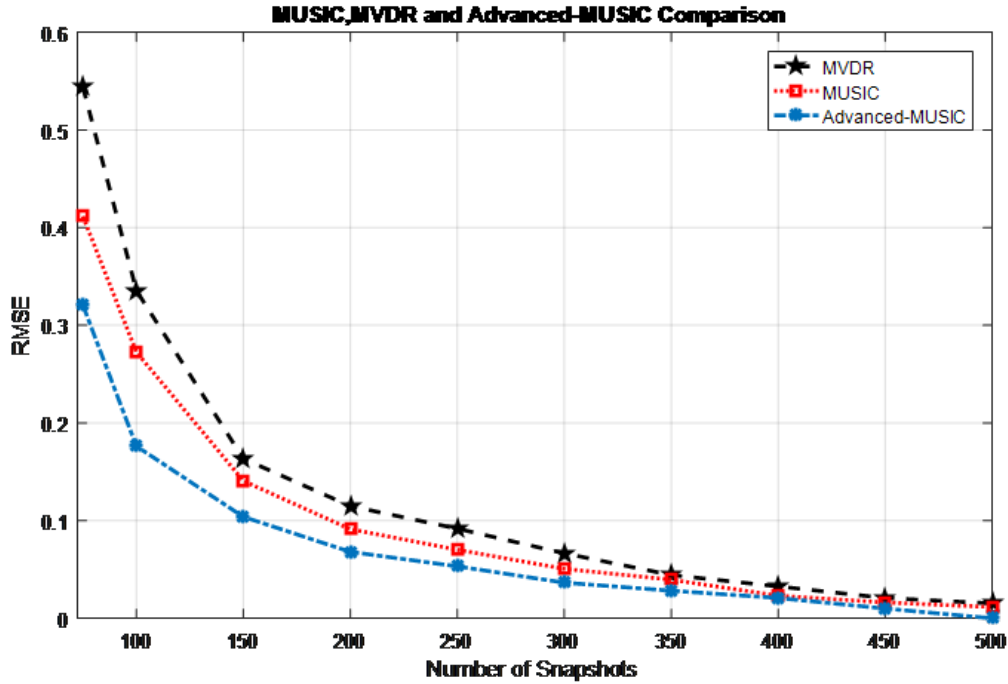


Fig. A.19: Error comparison in RMSE vs number of snapshots.

## 7 Conclusion

This work has investigated the performance of the existing DOA algorithms, MVDR and MUSIC compared with our proposed A-MUSIC on a weather-impacted network. The investigation is conducted for conditions of no rain, widespread, shower and thunderstorm rainfall. The deduction from the investigation indicates that the algorithms performance accuracy degrades by up to 43% and 28% for MVDR and MUSIC respectively from no rain condition to thunderstorm rainfall condition with MUSIC performing better than MVDR. The RMSE performance of the algorithms is shown to decrease by increasing the values of SNR and number of antenna elements. The work develops an A-MUSIC algorithm for the weather impacted conditions. The performance of the developed A-MUSIC is superior to the existing algorithm in terms of accuracy and RMSE parameters. The performance accuracy degrades by up to 2.3% from no rain condition to thunderstorm rainfall condition. However, its complexity is higher than the other algorithms. This work opens further investigation into the performance of DOA algorithms in weather impacted environment and the need for redesign of the existing algorithms. The accuracy of the investigation could be validated further by the derivation of the Cramer-Rao lower bounds and other statistical measures.

## References

- [1] Tsoulos, G. V., "Smart Antennas for Mobile Communication Systems: Benefits and Challenges," *IEE Electron. Commun Eng. Journal*, Vol. 11, No. 2, pp. 84–94, April, 1999.
- [2] Lavate, T. V., Kokate, V. K., Sakpal, A. M., "Performance Analysis of MUSIC and ESPRIT DOA Estimation Algorithms for Adaptive Array Smart Antenna in Mobile Communication," *Proc. of IEEE, Second Int. Conf. Computer and Network Technology*, 2010
- [3] Shaukat, S. F, Mukhtar, H., Farooq, R., Saeed, H. U, Saleem, Z., "Sequential Studies of Beamforming Algorithms for Smart Antenna Systems," *World Applied Sciences Journal*, Vol. 6, No. 6, pp. 754–758, 2009.
- [4] Balanis, C., *Antenna Theory: Analysis and Design*, John Wiley and Sons, Hoboken, New Jersey, 3rd edn. 2005.
- [5] Leon De, F. A., Marciano, S. J. J, "Application of MUSIC, ESPRIT and SAGE Algorithms for Narrowband Signal Detection and Localization," *TENCON, IEEE Reg. 10 Conf*, pp. 1–4, 2006.
- [6] Qian, C., Lei , H., So, H. C., "Computationally Efficient ESPRIT Algorithm for Direction-of-Arrival (DOA) Estimation Based on Nyström Method," *Signal Processing*, Vol. 94, pp. 74–80, 2014.
- [7] Roy, R., Kailath, T., "ESPRIT-a Subspace Rotational Approach to Estimation of Parameters of Cissoids in Noise," *IEEE Transactions on Acoustics, Speech, and Signal Processing*, Vol. 34, No. 10, pp. 1340–1342, 1986.
- [8] Xu, C., Krolik, J., "Space-delay Adaptive Processing for MIMO RF Indoor Motion Mapping," *IEEE. Int. Conf. on Acoustics, Speech and Signal Processing (ICASSP)*, Brisbane, QLD, pp. 2349–2353, April 2015.
- [9] Dhope, T., Simunic, D., Djurek, M., "Application of DOA Estimation Algorithms in Smart Antenna Systems," *Studies in informatics and Control*, Vol. 19, No. 4, pp. 445–452, Dec. 2010.
- [10] Schmidt, R., "Multiple Emitter Location and Signal Parameter Estimation," *IEEE Transactions on Antennas and Propagation*, Vol. 34, No. 3, pp. 276–280, 1986.
- [11] Zhang, Y., Wang, P., Goldsmith, "Rainfall Effect on The Performance of Millimeter-Wave MIMO Systems," *IEEE Transactions on Wireless Communications*, Vol. 14, No. 9, pp. 4857–4866, Sept. 2015.

- [12] Pi, Z., Khan, F., "An Introduction to Millimeter-wave Mobile Broadband Systems", *IEEE Commun. Mag.*, Vol. 49, No. 6, pp. 101–107, June 2011.
- [13] Ishimaru, A., "Wave Propagation and Scattering in Random Media," *IEEE Press*, Piscataway, NJ, USA, 1978.
- [14] Ishimaru, A., Jaruwatanadilok, S., Kuga, Y., "Multipel Scattering Effects on The Radar Cross Section (RCS) of Objects In a Random Medium Including Backscattering Enhancement and Shower Curtain Effects," *Waves Random Media*, Vol. 14, pp. 499–511, 2004.
- [15] Agber, J.U., Akura, J.M., "A High-Performance Model for Rainfall Effect on Radio Signals," *Journal of Information Engineering and Applications*, Vol. 3, No. 7, pp. 1–12, 2013.
- [16] Calla, O., Purohit, J., "Study of Effect of Rain and Dust on Propagation of Radio Waves at Millimeter Wavelength," *International Centre for Radio Science*, 'OM NIWAS' A-23 Shastri Nagar Jodhpur, pp. 1–4, January 1990.
- [17] Alonge, A.A., Afullo, T.J., "Fractal Analysis of Rainfall Event Duration for Microwave and Millimetre Networks: Rain Queueing Theory Approach," *IET Microwaves, Antennas and Propagation*, Vol. 9, No. 4, pp. 291–300, 2015.
- [18] Kedem, B., Chiu, L. S. "On The Lognormality of Rain Rate". *Proceedings of the National Academy of Sciences*, Vol. 84, No. 4., pp. 901–905, 1987.
- [19] Cho, H. K., Bowman, K. P., North, G. R. "A comparison of Gamma and Lognormal Distributions for Characterizing Satellite Rain Rates From The Tropical Rainfall Measuring Mission". *Journal of Applied Meteorology*, Vol. 43, No. 11, pp. 1586–1597, 2004.
- [20] I.T.U. Radiowave Propagation Series, "Specific Attenuation Model for Rain for Use In Prediction Methods," *Rec. P.838-3, ITU-R*, Geneva, Switzerland, 2005.
- [21] Oh, D., Ju, Y., Lee, J., "An Improved MVDR-Like TOA Estimation Without EVD for High-Resolution Ranging System," *IEEE Communications Letters*, Vol. 18, No. 5, pp. 753–756, May 2014.
- [22] El Gonnouni, A., Martinez-Ramon, M., Rojo-Alvarez, J.L., Camps-Valls, G., Figueiras-Vidal, A.R., Christodoulou, C.G., "A Support Vector Machine MUSIC Algorithm," *IEEE Transactions on Antennas and Propagation*, Vol. 60, No. 10, pp. 4901–4910, October 2012.

- [23] Balakrishnan, S., Ong, L.T., "GNU Radio Based Digital Beamforming System: BER and Computational Performance Analysis," *Proc. of the 2015 23rd European Signal Processing Conference (EUSIPCO)*, Nice, France, pp. 1596–1600, 31 August – 4 September 2015.
- [24] Stoeckle, C., Munir, J., Mezghani, A., Nossek, J.A., "DOA Estimation Performance and Computational Complexity of Subspace- and Compressed Sensing-Based Methods," *Proc. in WSA 2015 19th International ITG Workshop on Smart Antennas*, pp. 1–6, March 2015.
- [25] Bhaumik, B., "Performance Analysis of MUSIC Algorithm for DOA Estimation," *International Research Journal of Engineering and Technology (IRJET)*, Vol. 4, pp. 1667–1670, February 2017.
- [26] Khairy, A., Mahmoud, A., Hafez, A., Gaballa, A., "Minimum Variance Variable Constrain DOA Algorithm," *PIER Proceedings*, pp. 798–803, August 2014.
- [27] Kokare, R.G., Hendre, V.S., "Estimation of Direction of Arrival (DOA) Using MUSIC and ESPRIT Algorithm for Smart Antenna," *International Journal of Control Theory and Applications*, Vol. 10, No. 38, 2017.

# Paper B

## Performance Evaluation of DOA Algorithms for Non-uniform Linear Arrays in a Weather-Impacted Environment

Bongani Prudence Nxumalo and Tom Walingo

*Earth and Space Science Open Archive (ESSOAr)*

© 2021

*The layout has been revised.*

### **Abstract**

*Spectrum scarcity has necessitated the migration of radio frequencies from the lower to the higher frequencies. This has resulted in radio propagation challenges due to the adverse environmental elements otherwise unexperienced at lower frequencies. A re-design and re-evaluation of the performance of traditional lower frequency technologies and algorithms for implementation at higher frequencies especially for non-uniform linear antenna arrays are therefore necessary. Specifically, the performance of Direction of Arrival (DOA) algorithms for non-linear antenna arrays on weather impacted environments needs to be quantified and new algorithms developed to counteract the migration challenges. This work investigates the performance of Minimum Variance Distortionless Response (MVDR), Multiple Signal Classification (MUSIC) and the proposed Advanced-MUSIC (A-MUSIC) Non-uniform Linear Array (NLA) algorithms on a weather-impacted wireless channel. The results indicate that the developed NLA achieves better DOA estimation than the conventional NLA albeit at a reduced performance for both, in a weather-impacted scenario.*

### **1 Introduction**

Direction of Arrival (DOA) estimation is critical in antenna design for emphasizing the desired signal and minimizing interference. Smart antenna systems utilize DOA algorithms to estimate the beamforming vectors, to track and identify the antenna beam, making DOA estimation critical in smart antenna design and beamforming [1]. The accurate estimation of the DOA of the transmitted signals at the adaptive array antenna results in improved performance in the recovery of the transmitted signal and suppression of other interfering signals. The motivation for adopting Non-Uniform Linear Arrays (NLA) as opposed to the Uniform Linear Arrays (ULA) include the following [2] [3]: Firstly, the failure of any antenna sensor element(s) renders ULA to become NLA in harsh applications field and this could lead to data loss. Secondly, physical and geographical conditions may prohibit the construction of uniformly spaced sensors leading to NLA. Thirdly, the need to reduce the number of sensors to decrease the production cost and minimize the impact on performance, and finally the need to increase the aperture of an antenna using the same number of sensors in order to obtain better performance, among others. NLA allow better resolution for the same number of array elements compared to the ULA. Generally, NLA have larger antenna aperture, smaller main lobe width resulting in better performance in angle resolution, estimation precision, and other aspects. Therefore, the performance of NLA is of paramount importance especially with the

migration to higher frequencies that are more susceptible to the adverse weather environmental factors.

Estimation accuracy of a given array depends upon characteristics of the array geometry and the employed estimation algorithm; therefore, accurate DOA algorithms are required. DOA estimation for NLA is more critical. Their uneven number of source and receiver antennas leads to different degrees of freedom and irregular geometry. This results in different antenna sensor separation and aperture sizes. Furthermore, the migration to higher frequencies makes it worse due to the adverse effect of weather elements at these frequencies. New geometries requiring different degrees of freedom for NLA have been proposed [4] [5]. They involve the studying of the covariance matrix of the received signals among different sensors. Sparse arrays can be considered as a ULA where some sensors are omitted or irregular linear arrays where the inter-sensor separations are chosen in an arbitrary way [6]. The irregular spacing results in difficulties in covariance between the various elements because of the mutual coupling. These factors make DOA estimation for NLA challenging. NLAs give similar performance to ULA with a smaller number of physical elements. Co-prime array [4] [5] and array interpolation [7] [8] have become the most popular algorithms for evaluating NLA. A co-prime array comprises of two spatially under-sampled ULAs with co-prime spatial sampling rates [9]. Array interpolation maps the covariance matrix of a real array to a virtual array and enables the reduction of DOA estimation problems in NLA to much simpler virtual ULA problems. Both these algorithms are investigated in this work for NLA in a weather-impacted environment.

The most popular DOA algorithms used include the Minimum Variance Distortionless Response (MVDR) algorithm that enforces a unit response at the direction of the desired signal and places nulls in the directions of the interferences [10]. The Multiple Signal Classification (MUSIC) algorithm and its variants is applied directly to the NLA geometry resulting in high computational complexity due to the multiple search for the maximum [11]. This work proposes the Advanced-MUSIC (A-MUSIC) DOA algorithm that employs forward-backward averaging preprocessing technique on the cross correlation of array output to improve the performance of the DOA techniques for NLAs. The application of these techniques in a weather impacted radio propagation scenario for NLA is challenging and is the focus of this work.

The increasing demand on mobile broadband services has led to the scarcity of radio spectrum due to spectrum exhaustion [12]. This has led to migration to higher frequency millimetre-wave (mmW) bands, which range from 30 GHz to 300 GHz, for mmW communication with additional large bandwidths. Apart from the merits of increased bandwidth and high frequency reuse packing due to shorter wavelengths, mmW communication possesses its own challenges including large path loss

suffered by mmW signals and the effect of the weather effectors to signals in this band. Rainfall is a common weather phenomenon that affects signal transmission at this band. In link budget design at lower frequencies, rainfall is considered as a fixed propagation attenuation taken into account in the planning [13]. The signal suffers from absorption from the rain causing signal attenuation. Apart from attenuation, the signals undergo scattering when transmitted through rain leading to both amplitude attenuation and phase fluctuation [14]. Rain attenuation and scattering are a function of the rain rate, polarization, physical size of drops and operating frequency [15] [16]. Rainfall attenuation, frequency attenuation and phase distortion affect the received signal. It is therefore mandatory for DOA algorithms to consider weather effects for the systems. This has rarely been done in literature and therefore, addressed in this work.

The performance of the DOA algorithms for NLA in weather affected channels needs to be evaluated. Moreover, better DOA algorithms design is required to mitigate against the weather effects. This work investigates and compares the performance of the NLA DOA algorithms on a rainfall-impacted network and develops a hybrid algorithm to combat the weather effects. We employ realistic markovian rainfall channel model to accurately capture the rainfall variations in the following cases: widespread, shower and thunderstorm rain events.

The structure of this paper is organized as follows. Section 2 presents the NLA system model. Section 3 presents the evaluation of NLA as co-prime array or with array interpolation. In section 4, the weather impacted propagation channel is modelled. The proposed method for efficiently estimating the DOA and other conventional and subspace DOA estimation algorithms are presented in section 5. In section 6, the performance measures and overall performance evaluation algorithm are presented. The simulation results and discussion are presented in section 7 and the main conclusions drawn from them summarized in section 8.

Notation: The bold upper and lower-case letters represent the matrices and column vectors, respectively.  $I$  is an identity matrix. The following superscripts  $(\bullet)^*$ ,  $(\bullet)^H$ ,  $(\bullet)^{-1}$  and  $(\bullet)^T$  represent optimality, Hermitian, inverse and transpose operators, respectively and  $E(\bullet)$  is the mathematical expectation,  $d$  is the spacing difference between array elements,  $c$  is the speed of light and  $\lambda$  is the wavelength.

## 2 System Model

The system model consists of a source transmitting a signal  $s(t)$  that traverses through a weather-impacted environment to impinge on the antenna elements at an angle  $\theta$ . Assuming there are  $K$

uncorrelated narrowband plane-wave signals. The signals  $x(t)$  induced on the antenna arrays are multiplied by adjustable complex weights  $w$  and then summed to form the system output  $y(t)$ .

A sparse NLA is considered with  $L$  existing elements. The sensors are separated with a distance  $d_i$ , a multiple of a half wavelength from each other. As shown in Fig. B.1, the array has configuration,  $D = [d_1, d_2, \dots, d_{(L-1)}]$  such that  $d = 2 * [0, d_2, \dots, d_{(L-1)}]$ . The system is assumed to be confined to an azimuth-only system with isotropic sensors.

The received signal on the  $l^{th}$  element at the  $t^{th}$  snapshot is expressed as

$$x_l(t) = \sum_{i=1}^K \alpha_i s_i(t) a_i(\theta_i + \Delta\theta_i) + v_i(t), \text{ for } i = 1, 2, \dots, K \quad (\text{B.1})$$

where  $\alpha_i$  is the rainfall attenuation,  $\theta_i$  the angle of arrival,  $\Delta\theta_i$  the rainfall angle deviation,  $s_i(t)$  is signal associated with the  $i^{th}$  wave front and  $v_i(t)$  is the additive white Gaussian noise at the  $l^{th}$  element. The total received signal vector  $X$  is expressed as

$$X(t) = A(\hat{\theta})\tilde{S}(t) + V(t), \quad (\text{B.2})$$

where

$$\begin{aligned} X(t) &= [x_1(t), x_2(t), \dots, x_K(t)]^T, \\ A(\hat{\theta}) &= [a_1(\hat{\theta}_1), a_2(\hat{\theta}_2), \dots, a_K(\hat{\theta}_I)]^T, \\ \tilde{S}(t) &= [\tilde{s}_1(t), \tilde{s}_2(t), \dots, \tilde{s}_K(t)]^T, \\ V(t) &= [n_1(t), n_2(t), \dots, n_K(t)]^T. \end{aligned} \quad (\text{B.3})$$

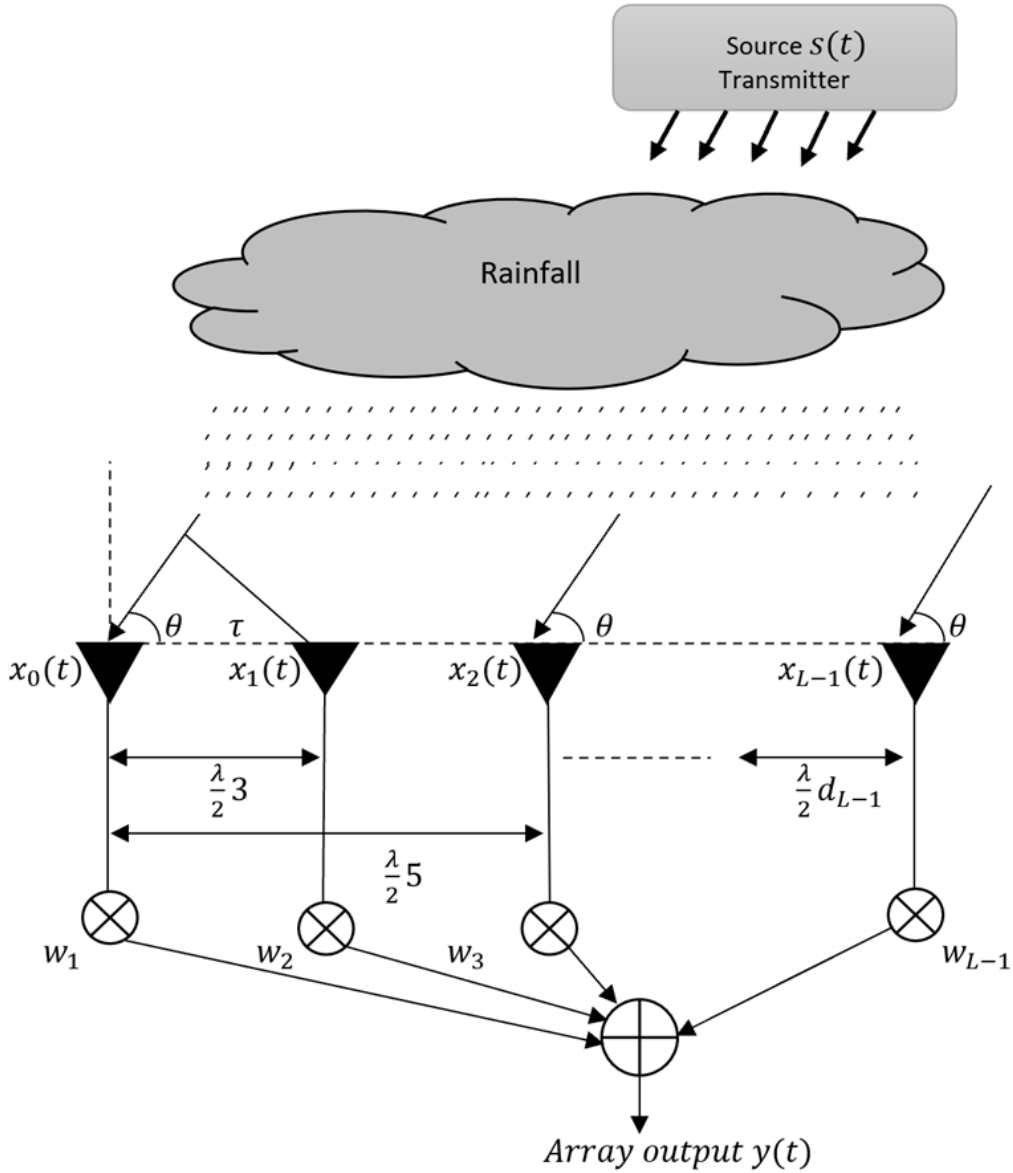


**Fig. B.1:** Non-uniform Linear Array (NLA).

where  $\tilde{S}(t) = \alpha_i s_i(t)$  and  $\hat{\theta} = \theta_i + \Delta\theta_i$ . The modelling and investigation of the rainfall attenuation  $\alpha_i$  and angle deviation  $\Delta\theta_i$  due to the weather impacted rainfall channel for NLA is the key focus on this work.

### 3 NLA methods

### 3.1 Co-prime Array Scheme

The NLA with  $L$  elements is divided into a co-prime array comprising of two spatially under sampled ULAs with co-prime spatial sampling rates [9]. This work utilizes the extended co-prime array configuration proposed in [9]. In this configuration, the array is a union of two ULAs, one with  $N$  sensors and spacing  $Md$  and the other with sensors  $2M - 1$  and spacing  $Nd$  as shown in the Fig. B.2, where  $d = \frac{\lambda}{2}$  to avoid spatial aliasing. The total number of physical elements is  $L = 2M + N - 1$ .

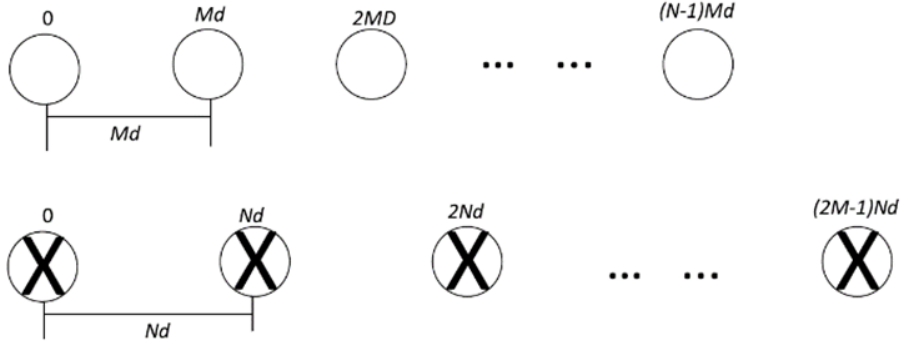


Fig. B.2: Co-prime array.

Denote  $d_i = \lambda/2 * [0, d_2, \dots, d_{(L-1)}]$  as the positions of the array sensors where  $i = 1, \dots, 2M + N - 1$ , the first sensor is assumed as the reference, i.e.,  $d_1 = 0$ . From equation B.1 the data vector received at the co-prime array is expressed as

$$x_l(t) = \sum_{i=1}^K \alpha_i s_i(t) a_i(\theta_i + \Delta\theta_i) + v_i(t), \quad (\text{B.4})$$

where

$$a_i(\theta_i) = [1, e^{\frac{(2\pi d_2)}{\lambda} \sin \hat{\theta}_i}, \dots, e^{\frac{(2\pi d_{2L})}{\lambda} \sin \hat{\theta}_i}]^T \quad (\text{B.5})$$

is the steering vector of the array corresponding to  $\hat{\theta}_i$ . The elements of the noise vector  $v(t)$  are assumed to be independent and identically distributed (i.i.d) random variables with a complex Gaussian distribution. The received signal vectors are similarly defined as in equation B.2 and B.3. The covariance matrix of data vector  $x_l(t)$  is obtained as [17]

$$\begin{aligned} \sigma(x, x) &= E[x_l(t)x_l^H(t)] \\ &= A\sigma(s, s)A^H + \vartheta^2 I \\ &= \sum_{i=1}^K \rho_i^2 a(\hat{\theta}_i)a^H(\hat{\theta}_i) + \vartheta^2 I \end{aligned} \quad (\text{B.6})$$

where  $\sigma(s, s) = E[s_l(t)s_l^H(t)] = \text{diag}([\rho_1^2, \dots, \rho_l^2])$  is the source covariance matrix,  $\text{diag}(\bullet)$  denotes a diagonal matrix that uses the elements of a vector as its diagonal elements,  $\rho_i^2$  denotes the input

signal power of the  $i^{th}$  signal,  $\vartheta^2$  denotes the noise variance and  $I$  is the identity matrix. In practice, the exact covariance matrix  $\sigma(x, x)$  is approximated by its sample estimate  $\hat{\sigma}(x, x)$  using the available  $Z$  snapshots, given by

$$\sigma(x, x) = \frac{1}{Z} \sum_{j=1}^Z x_l(t) x_l^H(t) \quad (\text{B.7})$$

The sample covariance matrix  $\hat{\sigma}(x, x)$  approaches the theoretical version  $\sigma(x, x)$  as the number of snapshots tends to infinity. The covariance matrix is utilised by the applied coprime DOA algorithms of section 5.

### 3.2 Modified Array Interpolation Scheme

The implemented interpolation considers an interpolation sector  $[\theta_b, \theta_f]$  with the source DOA's assumed to be inside the sector  $\hat{\theta} \in [\theta_b, \theta_f]$ . The interpolation sector is uniformly divided into  $\Delta\theta$  intervals such that  $\hat{\theta}_i = i\Delta\theta$ ,  $i = 0$  to  $\lfloor(\theta_f - \theta_b)/\Delta\theta\rfloor$ . With  $A(\hat{\theta})$  and  $\bar{A}(\hat{\theta})$  the manifold matrices of ULA and NLA respectively, the mapping matrix of the conventional interpolation array  $B$  is given by [18] [19]

$$B = (A(\hat{\theta})A(\hat{\theta})^H)^{-1}A(\hat{\theta})\bar{A}(\hat{\theta})^H \quad (\text{B.8})$$

Then an interpolation matrix  $B$  is designed to satisfy the least squares problem i.e.

$$\min_B \left\| B^H A(\hat{\theta}) - \bar{A}(\hat{\theta}) \right\|_F^2 \quad (\text{B.9})$$

where  $\|\bullet\|_F$  denotes the Frobenius norm of a matrix. The finite interpolation points results in interpolation mapping errors making the estimations not statistically optimal [20]. To alleviate this, the new transformation matrix  $G$  is reconstructed by projecting the transformational matrix with the sample array covariance matrix

$$G = (\bar{B}^H \bar{B})^{-\frac{1}{2}} \bar{B}^H \quad (\text{B.10})$$

where  $\bar{B} = \hat{\sigma}(x, x)B$ . The real antenna array steering vector  $a(\hat{\theta})$  and the virtual array steering vector  $\bar{a}(\hat{\theta})$  have the following relationship,  $Ga(\hat{\theta}) = (\bar{B}^H \bar{B})^{-\frac{1}{2}}\bar{a}(\hat{\theta}) = \hat{a}(\hat{\theta})$ . As a result of noise pre-whitening for cases where background noise becomes non-Gaussian after virtual transformation. The covariance matrix of the virtual antenna can be computed by using the transformation matrix  $G$  as [19] as

$$\hat{\sigma}(x, x) = G\sigma(x, x)G^H = \hat{A}\sigma(s, s)\hat{A}^H + \vartheta^2I \quad (\text{B.11})$$

with  $\hat{\sigma}(x, x)$  the covariance matrix and array manifold  $\hat{A}$  are the pre-whitened values of the virtual antenna array and  $\sigma(s, s) = E[s_l(t)s_l^H(t)]$ . The covariance matrix is utilised by the applied DOA algorithms of section 5.

## 4 Weather channel parameter modelling

### 4.1 Rainfall modelling

The signal attenuation magnitude largely depends on the rain intensity. Based on its intensity, rain event may be classified into drizzle (D), widespread (W), shower (S) and thunderstorm (T). Table B.1 presents the rain intensities of the four classes of rain. The rainfall is modelled by four or fewer states of a Markov Chain,  $R$ , given by

$$R = \{D, W, S, T\}, \quad (\text{B.12})$$

Table B.1 presents the rain event intensities. Practical rainfall, widespread, shower and thunderstorm

**Table B.1:** Rain Rates Categories.

Description	Rain rate (mm/hr)	Steady state ( $\pi_n$ )
Drizzle	1-5	$\pi_D$
Widespread	5-10	$\pi_W$
Shower	10-40	$\pi_S$
Thunderstorm	>40	$\pi_T$

events consist of a mix of the different rain events [21]. This work utilizes Markov models developed from actual rain data to model practical rain events, with the state transition diagram and state transition probabilities as given below:

i) Widespread rainfall: Consists of drizzle and widespread events. The markovian transition among states in this event is shown in Fig. B.3, with the transition probabilities,  $P_{i,j}^W$ , from state  $i$  to  $j$ , with  $i, j \in R$  given by equation B.13

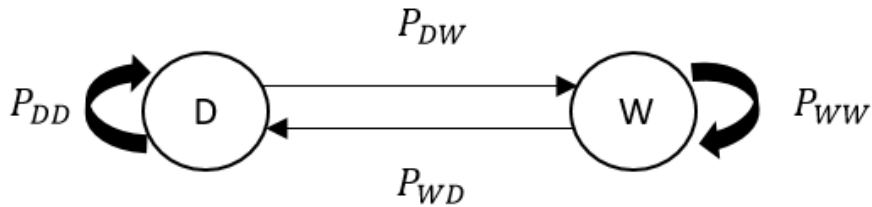


**Fig. B.3:** Widespread rainfall.

$$P_{i,j}^W = \begin{bmatrix} P_{DD} & P_{DW} \\ P_{WD} & P_{WW} \end{bmatrix}, \quad (\text{B.13})$$

where  $P_{DW}$  is the transition from drizzle to widespread,  $P_{WD}$  is the transition from widespread to drizzle,  $P_{DD}$  is the no transition from drizzle and  $P_{WW}$  is the no transition from widespread. ii) Shower rainfall consists of drizzle, widespread and shower events. The markovian transition among states in this event is shown in Fig. B.4, with the transition probabilities,  $P_{i,j}^S$ , from state  $i$  to  $j$ , with  $i, j \in R$  given by equation B.14

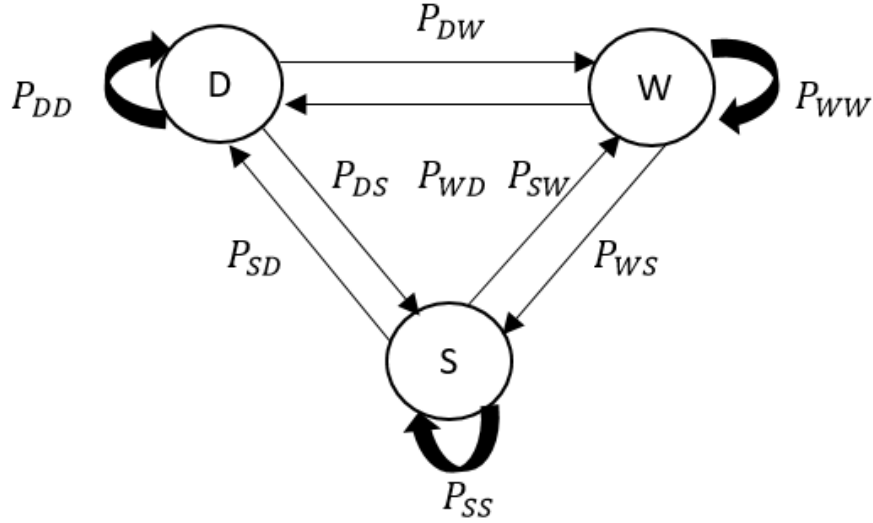


Fig. B.4: Shower rainfall.

$$P_{i,j}^S = \begin{bmatrix} P_{DD} & P_{DW} & P_{DS} \\ P_{WD} & P_{WW} & P_{WS} \\ P_{SD} & P_{SW} & P_{SS} \end{bmatrix}, \quad (\text{B.14})$$

where  $P_{DS}$  is the transition from drizzle to shower,  $P_{WS}$  is the transition from widespread to shower,  $P_{SD}$  is the transition from shower to drizzle,  $P_{SW}$  is the transition from shower to widespread and  $P_{SS}$  is the no transition from shower.

iii) Thunderstorm rainfall consists of drizzle, widespread, shower and thunderstorm events. The markovian transition among states in this event is shown in Fig. B.5, with the transition probabilities,  $P_{i,j}^T$ , from state  $i$  to  $j$ , with  $i, j \in R$  given by equation B.15

$$P_{i,j}^T = \begin{bmatrix} P_{DD} & P_{DW} & P_{DS} & P_{DT} \\ P_{WD} & P_{WW} & P_{WS} & P_{WT} \\ P_{SD} & P_{SW} & P_{SS} & P_{ST} \\ P_{TD} & P_{TW} & P_{TS} & P_{TT} \end{bmatrix}, \quad (\text{B.15})$$

where  $P_{DT}$  is the transition from drizzle to thunderstorm,  $P_{WT}$  is the transition from widespread to thunderstorm,  $P_{ST}$  is the transition from shower to thunderstorm,  $P_{TD}$  is the transition from

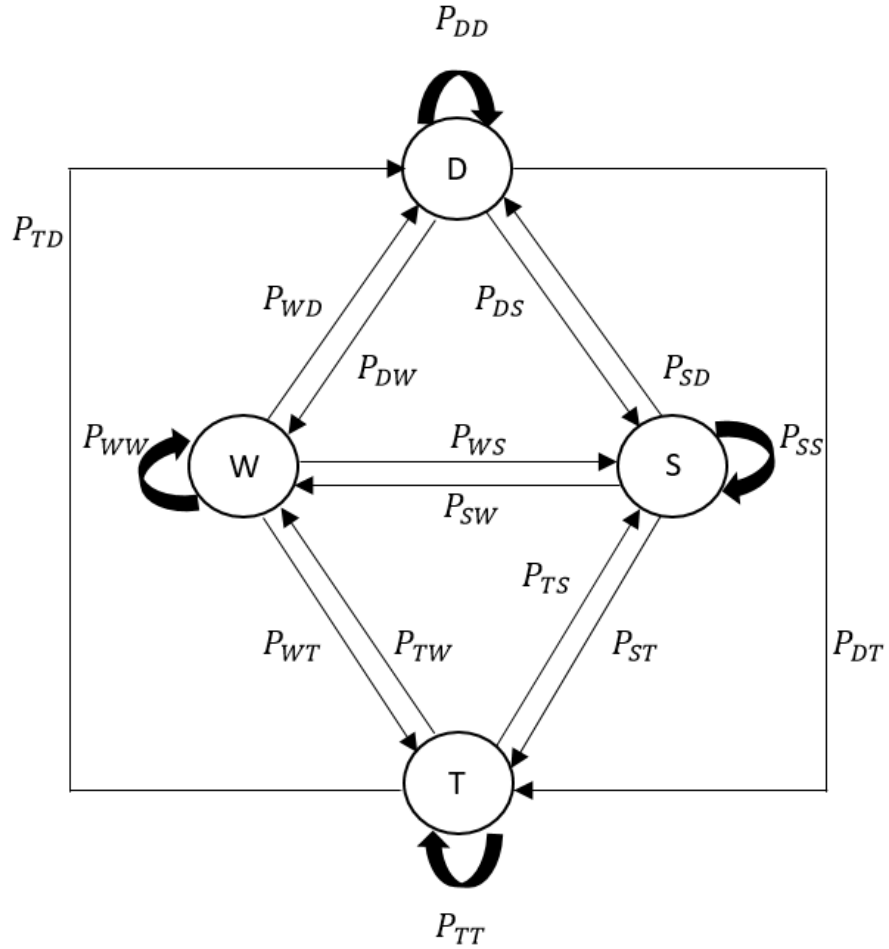


Fig. B.5: Thunderstorm rainfall.

thunderstorm to drizzle,  $P_{TW}$  is the transition from thunderstorm to widespread,  $P_{TS}$  is the transition from thunderstorm to shower and  $P_{TT}$  is the no transition from thunderstorm. The transition probabilities used are practically obtained as in [21]. The steady state probability of an event  $n$ ,  $\pi_n = \{\pi_D, \pi_W, \pi_S, \pi_T\}$ , is solved by the standard Markov chain solution methods. The expected rate for a rainfall occurrence is derived from the probabilities as

$$E[r] = \sum_n r_n \pi_n, \tag{B.16}$$

where  $r_n$  is the mean rain event and  $\pi_n$  is the steady state probability of the  $n^{th}$  state of the Markov model. The actual rain rate  $r$  is computed from a lognormal distribution with the given mean [22] [23].

## 4.2 Attenuation Model

We consider a radio propagation environment where the signal is affected by attenuation due to the weather-impacted factors. The total attenuation  $A_T$  is given by

$$A_T = \alpha_i + L_{fs}, \quad (\text{B.17})$$

where  $\alpha_i$  is the rain attenuation. The ITU rainfall model [24] is used for attenuation as

$$\alpha_i = kr^a, \quad (\text{B.18})$$

where  $r$  is the rain rate in mm/hr, of section 3.1. The constant parameter  $k$  and exponent  $a$  depend on the frequency  $f$ (GHz), the polarization state, and the elevation angle of the signal path. Free space loss attenuation,  $L_{fs}$ , is given by

$$L_{fs} = 20 * \log_{10} \frac{4\pi d}{\lambda}, \quad (\text{B.19})$$

where  $\lambda$  is the signal wavelength in metres, and  $d$  is the distance from the transmitter.

## 4.3 Angle Deviation Model

The weather related factors result in the delay and scattering of the transmitted signal as well as phase angle, and angle deviation change. The angle deviation,  $\Delta\theta_i$ , is modelled as a normal distributed random variable with a mean  $\mu_\theta$  bounded as follows

$$\Delta\theta_{min} \leq \Delta\theta_i \leq \Delta\theta_{max}, \quad (\text{B.20})$$

where  $\Delta\theta_{min}$  and  $\Delta\theta_{max}$  are the minimum and maximum angle deviations respectively. The mean  $\mu_\theta$  is derived from the normalised rain rate

$$\mu_\theta = \frac{r}{r_{max}}, \quad (\text{B.21})$$

and  $r_{max}$  is the maximum rain rate. The assumption is reasonable as the heavier the rain the more the scattering. Though the weather elements affect the mean and the standard deviation, we keep the standard deviation constant.

# 5 DOA Estimation Algorithms

## 5.1 MVDR Algorithm

### 5.1.1 MVDR Co-prime NLA

The MVDR algorithm minimizes the output power and constrains the gain in the direction of desired signal to unity as follows [10],

$$\min E\{|y_i(t)|^2\} = \min\{w^H \hat{\sigma}(x, x)w\}, \quad (\text{B.22})$$

subject to  $w.a(\hat{\theta}) = 1$  where  $y_i(t)$  is the output of the array system and is given by

$$y_i(t) = w^H \hat{\sigma}(x, x)w, \quad (\text{B.23})$$

The weight vector  $w$  is given by

$$w = \frac{(\hat{\sigma}(x, x))^{-1}a(\hat{\theta})}{a^H(\hat{\theta})(\hat{\sigma}(x, x))^{-1}a(\hat{\theta})}. \quad (\text{B.24})$$

where  $\hat{\sigma}(x, x)$  is covariance matrix of the received signal for the  $L$  number of elements given by equation B.7.  $H$  is the Hermitian matrix and  $a(\hat{\theta})$  is the steering vector. The MVDR spatial spectrum is defined by

$$P_{MVDR:Co-Prime}(\hat{\theta}) = \frac{1}{a^H(\hat{\theta})(\hat{\sigma}(x, x))^{-1}a(\hat{\theta})} \quad (\text{B.25})$$

The computational steps of MVDR algorithm using co-prime array are summarized in Algorithm 1.

---

#### Algorithm 5 MVDR Algorithm using Co-prime array

---

- 1: **Input:**  $x = \{x_i(t)\} = f(\alpha_i, \hat{\theta}_i)$ ,  $M, N, K, L, d, \lambda, Z$  and  $\mu \leftarrow$  step size
  - 2: Compute covariance matrix  $\hat{\sigma}(x, x)$  equation B.7
  - 3: Compute the weight vector  $w$ , equation B.24
  - 4: Compute the output array system  $y_i(t)$ , equation B.23
  - 5: **While**  $w.a(\hat{\theta}) \neq 1$
  - 6: **do** Minimize the output power, equation B.22,
  - 7:     Subject to  $w.a(\hat{\theta}) = 1$
  - 8: Compute MVDR spectrum for co-prime array, equation B.25
- 

### 5.1.2 MVDR Interpolation NLA

The spectrum of MVDR by array interpolation is given by [25]

$$P_{MVDR:AI}(\hat{\theta}) = \frac{1}{a^H(\hat{\theta})(\hat{\sigma}(x, x))^{-1}a(\hat{\theta})} \quad (\text{B.26})$$

where  $a(\hat{\theta})$  is the steering vector and  $\hat{\sigma}(x, x)$  is the covariance matrix of the virtual antenna derived in equation B.11. The computational steps of MVDR array interpolation algorithm are summarized in Algorithm 2.

**Algorithm 6** MVDR Algorithm using array interpolation

---

- 1: **Input:**  $x = \{x_i(t)\} = f(\alpha_i, \hat{\theta}_i)$ ,  $M, N, K, L, d, \lambda, Z$  and  $\mu \leftarrow$  step size
  - 2: Determine the ULA array manifold  $a(\hat{\theta})$
  - 3: Compute the real array covariance matrix  $\hat{\sigma}(x, x)$  equation B.7
  - 4: Compute the virtual array manifold  $\bar{A}(\hat{\theta})$  and the mapping matrix of the conventional interpolation array  $B$  using B.8 and the least squares problem B.9.
  - 5: Compute transformation matrix  $T$  in equation B.10.
  - 6: Compute the covariance matrix  $\hat{\hat{\sigma}}(x, x)$  in equation B.11 of the virtual array using the transformation matrix  $T$  in step 5.
  - 7: Compute the weight vector  $w$ , equation B.24, but using variance of step 6  $\hat{\hat{\sigma}}(x, x)$ .
  - 8: Compute the output array system  $y_i(t)$ , equation B.23.
  - 9: **While**  $w.a(\hat{\theta}) \neq 1$
  - 10: **do** Minimize the output power, equation B.22,
  - 11:     Subject to  $w.a(\hat{\theta}) = 1$
  - 12: Compute MVDR array interpolation spectrum for NLA, equation B.26.
- 

## 5.2 MUSIC Algorithm

### 5.2.1 MUSIC Co-prime NLA

For MUSIC, an estimate  $\sigma(x, x)$  of the covariance matrix is obtained and its eigenvectors decomposed into orthogonal signal and noise subspace [26] [27], where the DOA is estimated from one of these subspaces. The algorithm searches through the set of all possible steering vectors to find the ones orthogonal to the noise subspace. The diagonal covariance matrix  $\hat{\sigma}(x, x)$  given by equation B.7 is vectorized into

$$\hat{\sigma}(x, x) = Q\Lambda Q^H \quad (\text{B.27})$$

where  $a(\hat{\theta})$  is the steering vector corresponding to one of the incoming signals and  $Q_n$  is the noise subspace of the eigenvectors. The MUSIC technique for co-prime array is summarized in Algorithm 3.

---

**Algorithm 7** MUSIC Algorithm using co-prime

---

- 1: **Input:**  $x = \{x_i(t)\} = f(\alpha_i, \hat{\theta}_i)$ ,  $M, N, K, L, d, \lambda, Z$  and  $\mu \leftarrow$  step size
  - 2: Compute covariance matrix  $\hat{\sigma}(x, x)$  equation B.7
  - 3: Decompose  $\hat{\sigma}(x, x)$  into eigenvectors and eigenvalues in equation B.27
  - 4: Rearrange the eigenvectors and eigenvalues into the signal subspace and noise subspace.
  - 5: Compute the co-prime array MUSIC spectrum equation B.28 by spanning  $\hat{\theta}$  to acquire estimates of the angle of arrival
  - 6: Determine the substantial peaks of  $P_{(MUSIC:Co-Prime)}(\hat{\theta})$  to acquire estimates of the angle of arrival
- 

### 5.2.2 MUSIC Interpolation NLA

The autocorrelation matrix is decomposed into signal and noise subspaces. From equation B.11 the covariance matrix  $\hat{\sigma}(x, x)$  is decomposed as [19]

$$\hat{\sigma}(x, x) = U_S \Sigma_S U_S^H + U_N \Sigma_N U_N^H \quad (\text{B.28})$$

where  $U_S$  represents the signal subspace,  $U_N$  represents the noise subspace;  $\Sigma_S = \text{diag}(\lambda_1, \lambda_2, \dots, \lambda_M)$  is the signal eigenvalue;  $\Sigma_N = \text{diag}(\lambda_{(M+1)}, \lambda_{(M+2)}, \dots, \lambda_N)$  is the noise eigenvalue. The noise subspace  $\Sigma_N$  is orthogonal to all  $M$  signal steering vectors. The spectrum of the MUSIC, algorithm is given by

$$P_{(MUSIC_{AI})} \hat{\theta} = \frac{1}{a^H(\hat{\theta}) U_N U_N^H a(\hat{\theta})} = \frac{1}{\|U_N^H a(\hat{\theta})\|} \quad (\text{B.29})$$

If  $\hat{\theta}$  is equal to DOA, the noise subspace  $U_N$  is orthogonal to the signal steering vectors and  $\|U_N^H a(\hat{\theta})\|$  becomes zero when  $\hat{\theta}$  is a signal direction and the denominator is identical to zero. It is obvious that in practice,  $U_N^H a(\hat{\theta}) \neq 0$  due to finite samples. If this happens, the performance of MUSIC algorithm will not be optimal.

The MUSIC technique using array interpolation is summarized in Algorithm 4.

## 5.3 A-MUSIC Algorithm

### 5.3.1 A-MUSIC Co-prime NLA

The existing MVDR and MUSIC algorithms are adversely affected by the low SNR in rain-impacted systems and need modifications. The A-MUSIC algorithm [28] repeatedly reconstructs the covariance

**Algorithm 8** MUSIC Algorithm using array interpolation

---

- 1: **Input:**  $x = \{x_i(t)\} = f(\alpha_i, \hat{\theta}_i)$ ,  $M, N, K, L, d, \lambda, Z$  and  $\mu \leftarrow$  step size
  - 2: Determine the ULA array manifold  $A(\hat{\theta})$
  - 3: Compute the real array covariance matrix  $\hat{\sigma}(x, x)$  equation B.7
  - 4: Compute the virtual array manifold  $\bar{A}(\hat{\theta})$  and the mapping matrix of the conventional interpolation array  $B$  using B.8 and the least squares problem B.9.
  - 5: Compute transformation matrix  $G$  in equation B.10.
  - 6: Compute the covariance matrix  $\hat{\tilde{\sigma}}(x, x)$  in equation B.11 of the virtual array using the transformation matrix  $G$  in step 5.
  - 7: Decompose  $\hat{\tilde{\sigma}}(x, x)$  into eigenvectors and eigenvalues in equation B.29
  - 8: Rearrange the eigenvectors and eigenvalues into the signal subspace and noise subspace.
  - 9: Compute MUSIC array interpolation spectrum for NLA, equation B.30 by spanning  $\hat{\theta}$  to acquire estimates of the angle of arrival
  - 10: Determine the substantial peaks of  $P_{(MUSIC_{AI})}\hat{\theta}$  to acquire estimates of the angle of arrival.
- 

matrix to obtain two noise and signal subspaces continuously that are averaged for several iterations mitigating against the low SNR effects. From B.7, the covariance matrix  $\tilde{\sigma}(x, x)$  is reconstructed as

$$\tilde{\sigma}(x, x) = \hat{\sigma}(x, x) + J\hat{\sigma}(x, x)^*J \quad (\text{B.30})$$

where  $J$  is MATLAB constructions given as  $J = \text{fliplr}(\text{eye}(L))$  which returns columns flipped in the left-right direction and  $L$  is the number of elements. The eigen decomposition on reconstructed covariance matrix  $\tilde{\sigma}(x, x)$  is

$$\tilde{\sigma}(x, x) = \hat{Q}\Lambda\hat{Q}^H = Q_{S1}\Lambda_{S1}Q_{S1}^H + Q_{N1}\Lambda_{N1}Q_{N1}^H \quad (\text{B.31})$$

where  $\tilde{\sigma}(x, x)$  is divided into signal subspace  $Q_S$  and noise subspace  $Q_N$ . Using low rank of matrix instead of full rank matrix,  $\tilde{\sigma}(x, x)$  can be reconstructed into  $\omega_x$  as

$$\omega_x = Q_{S2}\Lambda_{S2}Q_{S2}^H + Q_{N2}\Lambda_{N2}Q_{N2}^H \quad (\text{B.32})$$

The average signal subspace, signal eigenvalue, noise subspace, and the noise eigenvalue are given by

$$\begin{aligned} Q_S &= \frac{(Q_{S1} + Q_{S2})}{2}, \\ Q_N &= \frac{(Q_{N1} + Q_{N2})}{2}, \\ \Lambda_S &= \frac{(\Lambda_{S1} + \Lambda_{S2})}{2}, \\ \Lambda_N &= \frac{(\Lambda_{N1} + \Lambda_{N2})}{2} \end{aligned} \quad (\text{B.33})$$

The A-MUSIC spectrum is then defined by

$$P_{Advanced-MUSIC}(\hat{\theta}) = \frac{a^H(\hat{\theta}) \left[ \frac{\check{\sigma}(s,s)\check{\sigma}(s,s)^H}{K} \right] a(\hat{\theta})}{a^H(\hat{\theta})\check{\sigma}(n,n)a(\hat{\theta})} \quad (\text{B.34})$$

where  $\check{\sigma}(s,s) = Q_S \Lambda_S^{-1} Q_S^H$  and  $\check{\sigma}(n,n) = Q_N \Lambda_N^{-1} Q_N^H$  are signal and noise subspace covariance matrix. The A-MUSIC technique using co-prime array is summarized in algorithm 5.

---

**Algorithm 9** Proposed A-MUSIC Algorithm using co-prime array

---

- 1: **Input:**  $x = \{x_i(t)\} = f(\alpha_i, \hat{\theta}_i)$ ,  $M, N, K, L, d, \lambda, Z$  and  $\mu \leftarrow$  step size
  - 2: Compute the covariance matrix  $\hat{\sigma}(x, x)$ , equation B.7
  - 3: Compute reconstructed covariance matrix  $\check{\sigma}$ , equation B.31
  - 4: Compute the eigen decomposition on reconstructed covariance matrix  $\check{\sigma}$ , equation B.32
  - 5: Compute reconstructed covariance matrix  $\omega_x$  in equation B.33
  - 6: Compute the average signal subspace, noise subspace, signal eigenvalues, and the noise eigenvalue,  $Q_S, Q_N, \Lambda_S, \Lambda_N$  in equation B.34.
  - 7: Determine signal and noise subspace averaged covariance matrix  $\check{\sigma}(s, s), \check{\sigma}(n, n)$
  - 8: Compute the spectrum function, equation B.35 spanning  $\hat{\theta}$
- 

### 5.3.2 A-MUSIC Interpolation NLA

In A-MUSIC array interpolation, we reconstruct the decomposed autocorrelation matrix into signal and noise subspaces. Using equation B.11, the reconstructed covariance matrix  $\vec{\sigma}(x, x)$  can be written as

$$\vec{\sigma}(x, x) = \hat{\sigma}(x, x) + J \hat{\sigma}(x, x)^* J \quad (\text{B.35})$$

with  $\hat{\sigma}(x, x)$  the covariance matrix of equation B.29. The eigen decomposition on reconstructed covariance matrix  $\vec{\sigma}(x, x)$  is

$$\vec{\sigma}(x, x) = \hat{\Phi} \Pi \hat{\Phi}^H = \Phi_{S1} \Pi_{S1} \Phi_{S1}^H + \Phi_{N1} \Pi_{N1} \Phi_{N1}^H \quad (\text{B.36})$$

where  $\vec{\sigma}(x, x)$  is divided into signal subspace  $\Phi_S$  and noise subspace  $\Phi_N$ . Using low rank of matrix instead of full rank matrix,  $\vec{\sigma}(x, x)$  can be reconstructed into  $\varpi_x$  as

$$\varpi_x = \Phi_{S2} \Pi_{S2} \Phi_{S2}^H + \Phi_{N2} \Pi_{N2} \Phi_{N2}^H \quad (\text{B.37})$$

The average signal subspace, signal eigenvalue, noise subspace, and the noise eigenvalue are given by

$$\begin{aligned}
 \Phi_S &= \frac{(\Phi_{S1} + \Phi_{S2})}{2}, \\
 \Phi_N &= \frac{(\Phi_{N1} + \Phi_{N2})}{2}, \\
 \Pi_S &= \frac{(\Pi_{S1} + \Pi_{S2})}{2}, \\
 \Pi_N &= \frac{(\Pi_{N1} + \Pi_{N2})}{2}
 \end{aligned} \tag{B.38}$$

The A-MUSIC spectrum is then defined by

$$P_{Advanced-MUSIC}(\hat{\theta}) = \frac{a^H(\hat{\theta}) \left[ \frac{\vec{\sigma}(s,s)\vec{\sigma}(s,s)^H}{I} \right] a(\hat{\theta})}{a^H(\hat{\theta})\vec{\sigma}(n,n)a(\hat{\theta})} \tag{B.39}$$

where  $\vec{\sigma}(s,s) = \Phi_S \Pi_S^{-1} \Phi_S^H$  and  $\vec{\sigma}(n,n) = \Phi_N \Pi_N^{-1} \Phi_N^H$  are signal and noise subspace covariance matrix. The A-MUSIC technique is summarized in Algorithm 6.

---

**Algorithm 10** Proposed A-MUSIC Algorithm using array interpolation

---

- 1: **Input:**  $x = \{x_i(t)\} = f(\alpha_i, \hat{\theta}_i)$ ,  $M, N, K, L, d, \lambda, Z$  and  $\mu \leftarrow$  step size
  - 2: Determine the ULA array manifold  $A(\hat{\theta})$
  - 3: Compute the covariance matrix  $\hat{\sigma}(x, x)$ , equation B.7
  - 4: Compute the virtual array manifold  $\bar{A}(\hat{\theta})$  and the mapping matrix of the conventional interpolation array  $B$  using B.8 and the least squares problem B.9.
  - 5: Compute transformation matrix  $G$  in equation B.10.
  - 6: Compute the covariance matrix  $\hat{\sigma}(x, x)$  in equation B.11 of the virtual array using the transformation matrix  $G$  in step 5.
  - 7: Compute reconstructed covariance matrix  $\vec{\sigma}(x, x)$  equation B.36
  - 8: Decompose  $\vec{\sigma}(x, x)$  into eigenvectors and eigenvalues, equation B.37
  - 9: Compute the average signal subspace, noise subspace, signal eigenvalues, and the noise eigenvalue  $\Phi_S, \Phi_N, \Pi_S, \Pi_N$ , equation B.39.
  - 10: Determine signal and noise subspace averaged covariance matrix  $\vec{\sigma}(s, s), \vec{\sigma}(n, n)$
  - 11: Compute the spectrum function  $P_{(Advanced-MUSIC)}(\hat{\theta})$  spanning  $\hat{\theta}$  equation B.40.
- 

## 6 Performance Measures

### 6.1 Root Mean Square Error (RMSE)

The performance of the DOA estimation algorithms is evaluated in terms of algorithms spectrum functions, equations B.25, B.26, B.28, B.30, B.35 and B.40, the Root Mean Square Error (RMSE) and the signal to noise ratios. The RMSE is given by

$$RMSE = \sqrt{\frac{1}{Z * K} \sum_{j=1}^Z \sum_{i=1}^K (\tilde{\theta}_{ij} - \theta_i)^2}, \quad (\text{B.40})$$

where  $Z$  is the number of simulation trials,  $K$  is the number of elements and the estimate of the  $i^{th}$  angle of arrival in the  $j^{th}$  trial is  $\tilde{\theta}_{ij}$ . Where utilised, the signal to noise ratio (SNR) is given by

$$SNR = 20 \log_{10}\left(\frac{x}{v}\right), \quad (\text{B.41})$$

where  $x$  is the received signal strength in dB and  $v$  is the noise strength in dB. The overall performance evaluation is done as in algorithm 7.

---

#### Algorithm 11 System Algorithm

---

- 1: **Choose an event**
  - 2: Compute expected rain rate, equation B.16 Compute the actual rain rate  $r$  from lognormal distribution with given mean
  - 3: **for**  $i$  number of antennas  $< L_{max}$
  - 4:     Compute the rain attenuation  $\alpha_r$ , total attenuation given
  - 5:      $A_T$  and the angle  $\hat{\theta}_i$ . Determine the angle deviation  $\Delta\theta_i$  as shown
  - 6:     in B.20 and the mean  $\mu_\theta$ .
  - 7: **end for**
  - 8: Determine the received signal  $x_i(t)$ .
  - 9: Compute DOA, Algorithm 1,2 and 3.
- 

### 6.2 Cramer Rao Bound (CRB)

To validate our DOA estimators, the Cramer Rao Bound (CRB) which shows the limit that can be achieved by an unbiased estimator is applied. The general CRB formula for the case of multiple DOA parameters per source and spatially uncorrelated white noise is developed in [29]. The following compact matrix expression for the stochastic CRB was derived in [30] and is applied in our case with the few required modification,

$$CRB = \frac{\sigma^2}{2T} \left( \text{Re}(H \odot G^T) \right)^{-1} \quad (\text{B.42})$$

where  $T$  is the number of data snapshots,  $H = D^H[I - A(A^H A)^{-1}A^H]D$ ,  $G = \sigma(s, s)A^H(\sigma(x, x))^{-1}A\sigma(s, s)$ ,  $D = [d(\theta_1), \dots, d(\theta_K)]$ ,  $d(\theta_i) = \frac{da(\theta)}{d\theta} |_{\theta=\theta_i}$ ,  $\sigma(x, x) = E[x(t)x^H(t)] = A\sigma(s, s)A^H + \vartheta^2 I$ ,  $\sigma(s, s) = E[s(t)s^H(t)]$ ,  $I$  is the identity matrix,  $\vartheta^2$  is the noise variance, and  $E(\bullet)$  denotes the expectation.

### 6.3 DOA Estimation Algorithm complexity

The complexity of MVDR and MUSIC algorithm has been derived and shown in Table B.2 [31]. For A-MUSIC, there are three major computational steps needed to estimate the DOA. The complexity of the first step is the covariance function and reconstruction of the covariance matrix,  $\mathcal{O}(L^2K)$ . The second step is the eigenvalue decomposition operation, which has a complexity of  $\mathcal{O}(L^3)$ . The third step is obtaining the spatial pseudo spectrum, which has a complexity of  $\mathcal{O}(J_\theta \dots J_{\Delta\theta}(L+1)(L-K)/2)$ , with  $J$  being the number of spectral points of the total angular field of view. Therefore, the total complexity of A-MUSIC is given by  $\mathcal{O}(L^2K + L^3) + \mathcal{O}(J_\theta \bullet J_{\Delta\theta}(L+1)(L-K)/2)$ .

Note that the complexity of deriving the covariance matrix for co-prime and array interpolation, and the complexity of deriving the weather effectors is same for all the algorithms and is not included in the derivation.

**Table B.2:** Computational Complexity of DOA Estimation Algorithms.

DOA algorithm	Computational Complexity
MVDR	$\mathcal{O}(L^2K + L^3 + (2L^2 + 3L))$
MUSIC	$\mathcal{O}(L^2K + L^3 + JL)$
A-MUSIC	$\mathcal{O}(L^2K + L^3) + \mathcal{O}(J_\theta \bullet J_{\Delta\theta}(L+1)(L-K)/2)$

## 7 Simulation Results

An investigation into the performance of MVDR, MUSIC and the proposed A-MUSIC DOA algorithms for NLA is presented in this section. The performance investigation is based on co-prime array and array interpolation methods of a pair of sparse NLAs for different number of array elements, rain rates and SNR. The developed results are for a case where signals impinge on the NLA sensors from the same signal source. It is assumed that the signals are mutually independent and that

## 7. SIMULATION RESULTS

---

noise is additive white Gaussian noise (AWGN) with a zero mean. Unless explicitly stated, the simulation parameters are as in Table B.3.

**Table B.3:** Simulation parameters

Simulation Parameters	Values
Input $\theta$	$[5^0, 25^0, 25^0, 65^0]$
Number of elements	$L = 10$
Spacing difference	$d = \frac{\lambda}{2} * [0, 3, 5, 6, 9, 10, 12, 15, 20, 25]$
Signal-to-noise ratio	$SNR = 20dB$
Snapshots	$Z = 300$
Rain rate in (mm/hr)	$[0, 2.5, 6, 15, 40]$
$a$ at f(GHz)	0.7103
$k$ at f(GHz)	1.16995
$\Delta\theta_{min}, \Delta\theta_{max}$	$[0^0 - 60^0]$
$M, N$	3, 5

The results of Fig. B.6-B.9 and Fig. B.10-B.13 show co-prime array and array interpolation based spatial output spectrum of the MVDR, MUSIC and the proposed A-MUSIC for different rain rates; no rain, widespread, shower and thunderstorm rain conditions. Note that without rain, the spectrum results for MVDR and MUSIC are similar to the ones in [26] [27] respectively. From the results, the following can be observed, the accuracy of DOA estimation reduces with increasing rain rate due to the high signal distortion at higher rain rates. The performance of the A-MUSIC is better than MUSIC followed by MVDR. This is because of the multiple averaging nature of the A-MUSIC algorithm. It can further be observed that at higher rain rates in the thunderstorm events, MVDR and MUSIC do not estimate the Direction of Arrival (DOA) accurately.

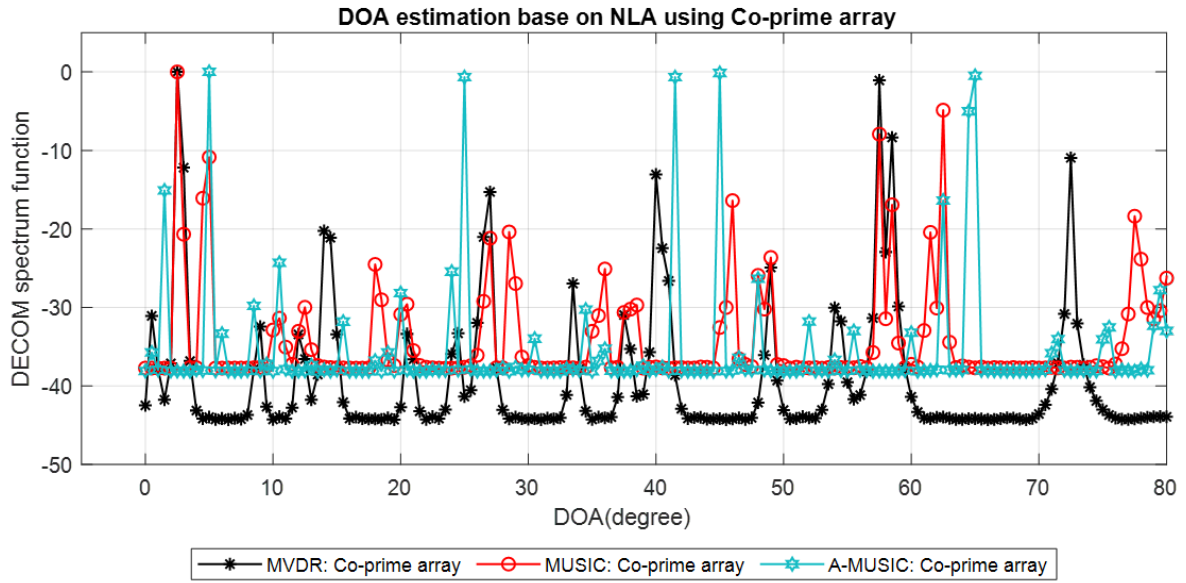


**Fig. B.6:** DOA estimation attenuation using Co-prime array with no rain.

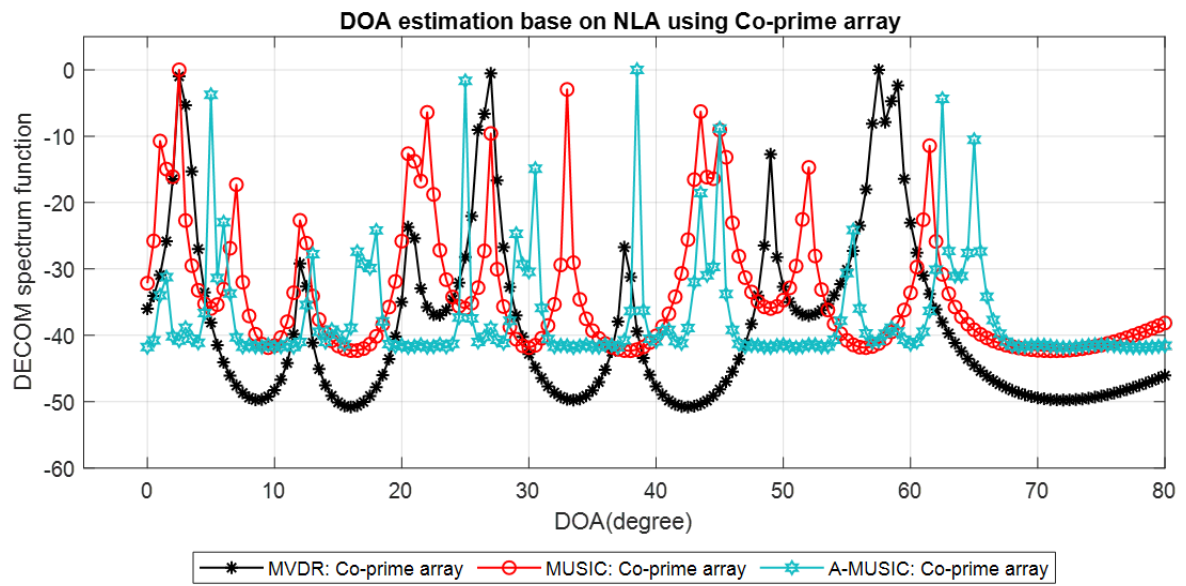


**Fig. B.7:** DOA estimation attenuation using Co-prime array for widespread rainfall.

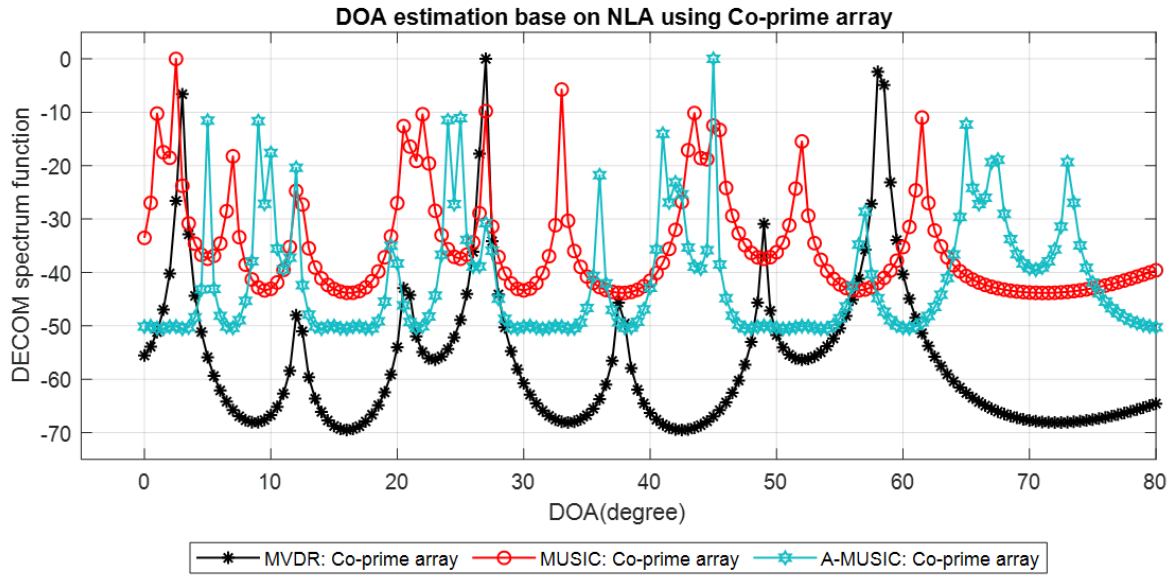


Fig. B.8: DOA estimation attenuation using Co-prime array for shower rainfall.

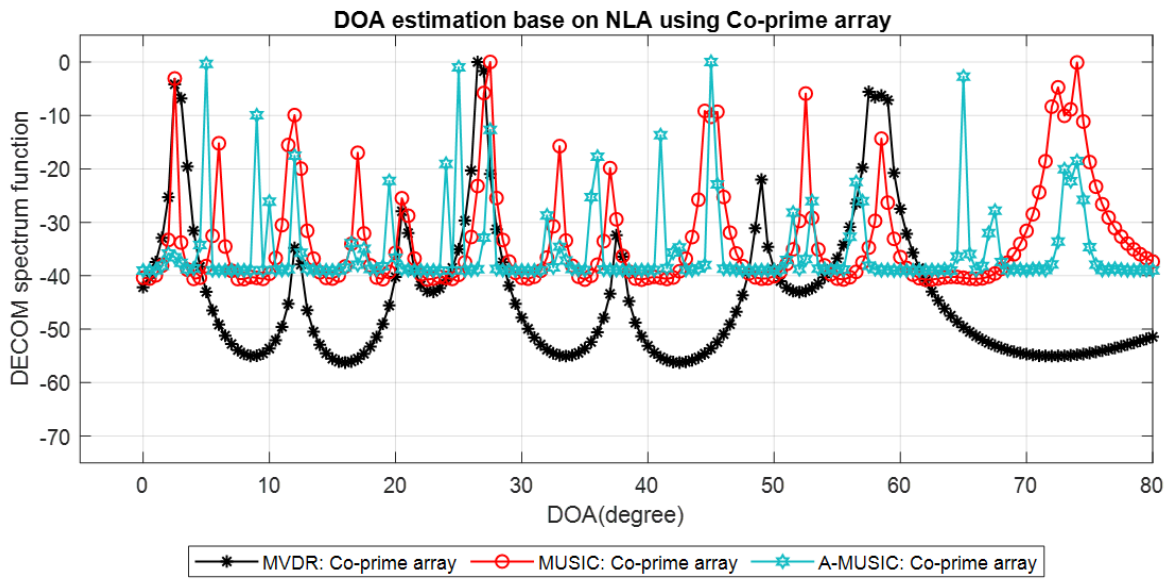


Fig. B.9: DOA estimation attenuation using Co-prime array for thunderstorm rainfall.

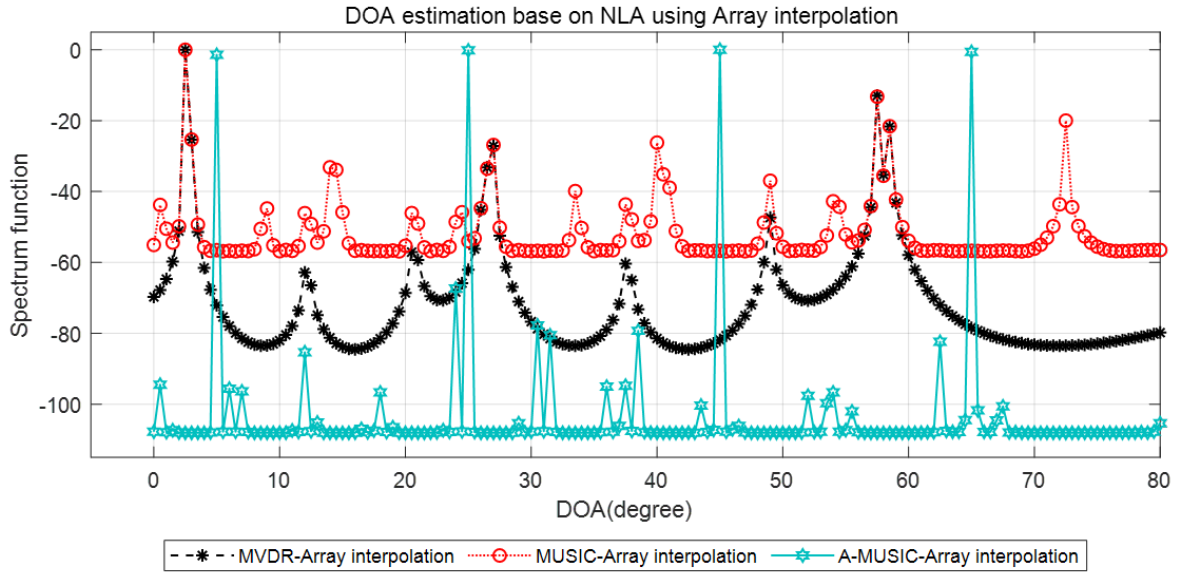


Fig. B.10: DOA estimation attenuation using array interpolation with no rain.

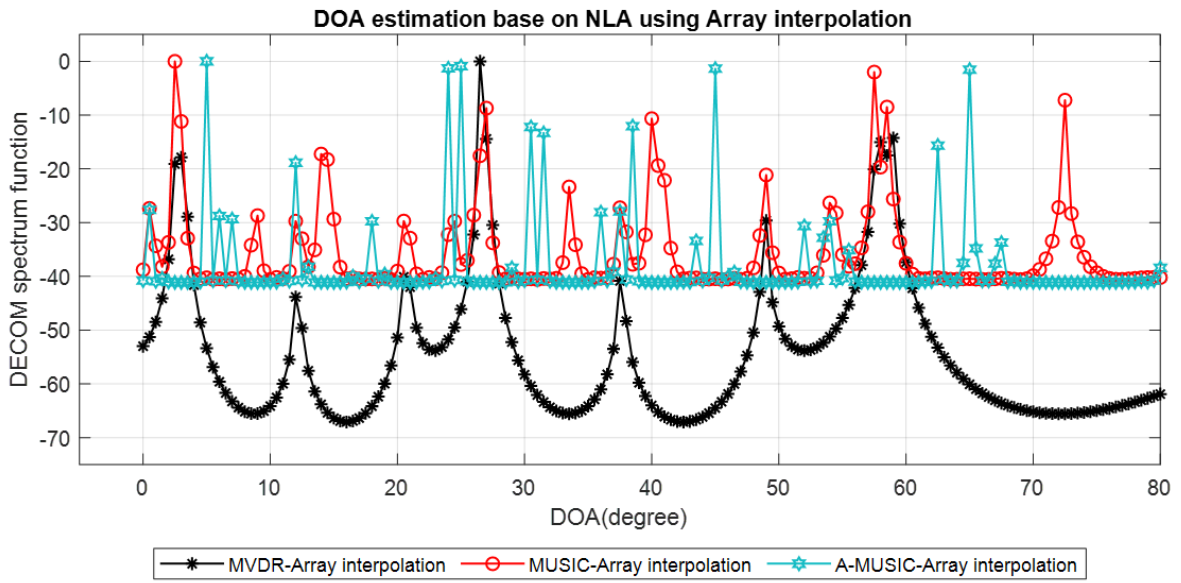


Fig. B.11: DOA estimation attenuation using array interpolation for widespread rainfall.

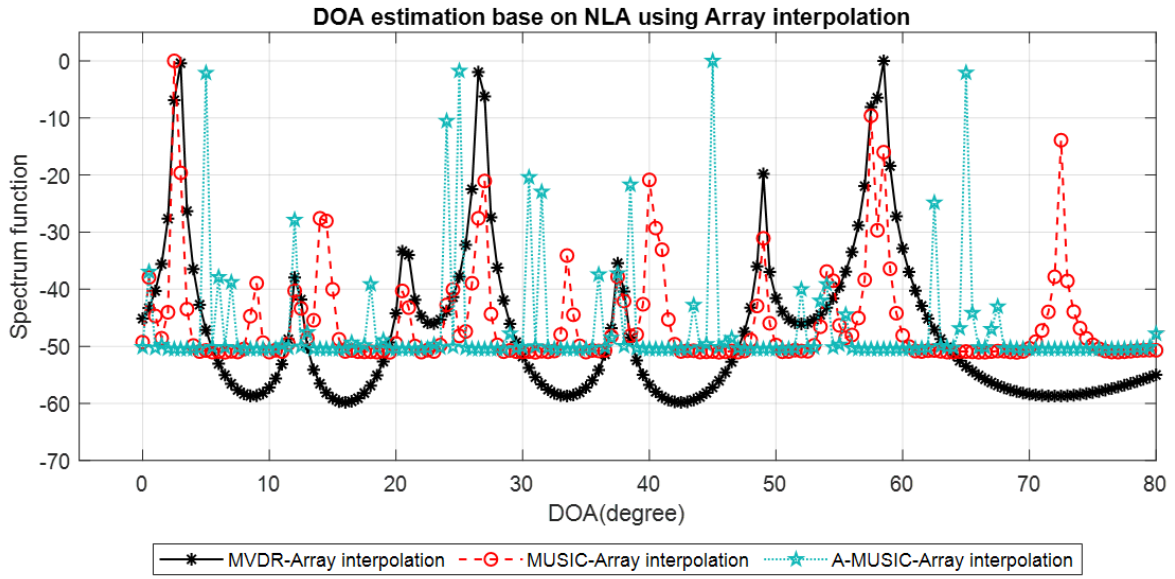


Fig. B.12: DOA estimation attenuation using array interpolation for shower rainfall.

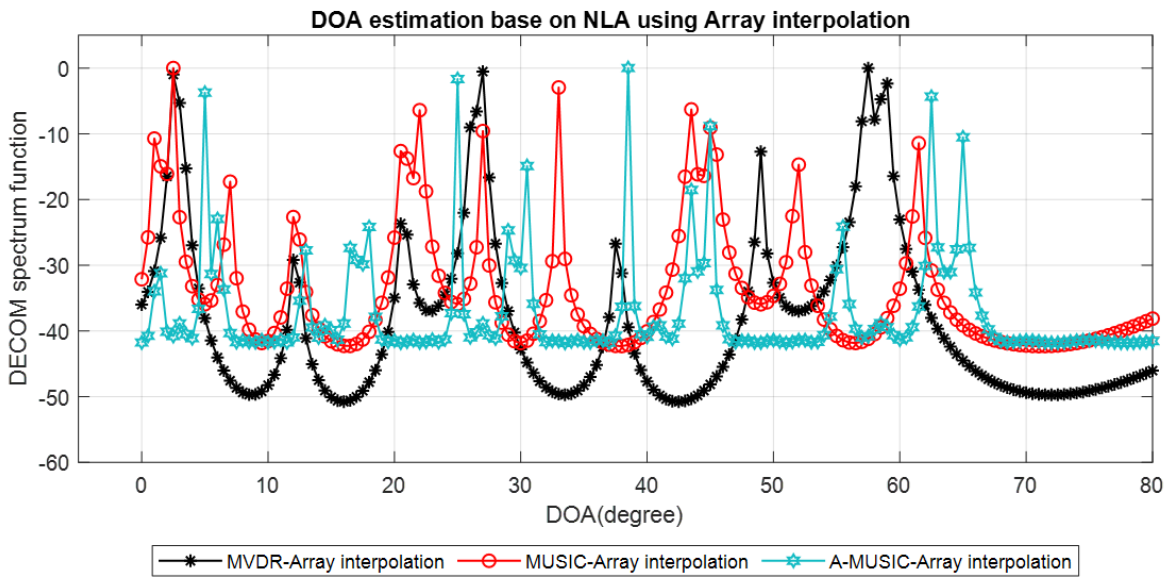


Fig. B.13: DOA estimation attenuation using array interpolation for thunderstorm rainfall.

The results of Fig. B.14-B.16 represent the RMSE value vs rain rate comparison of co-prime array and array interpolation of DOA algorithms for different number of elements. As expected, the RMSE increases with increasing rain rates while the error reduces with an increase in the number of antenna elements. A noticeable difference in performance is when the rain rate exceeds 10 mm/hr. It can also be observed that the co-prime array configuration results in a higher error than the array interpolation method.

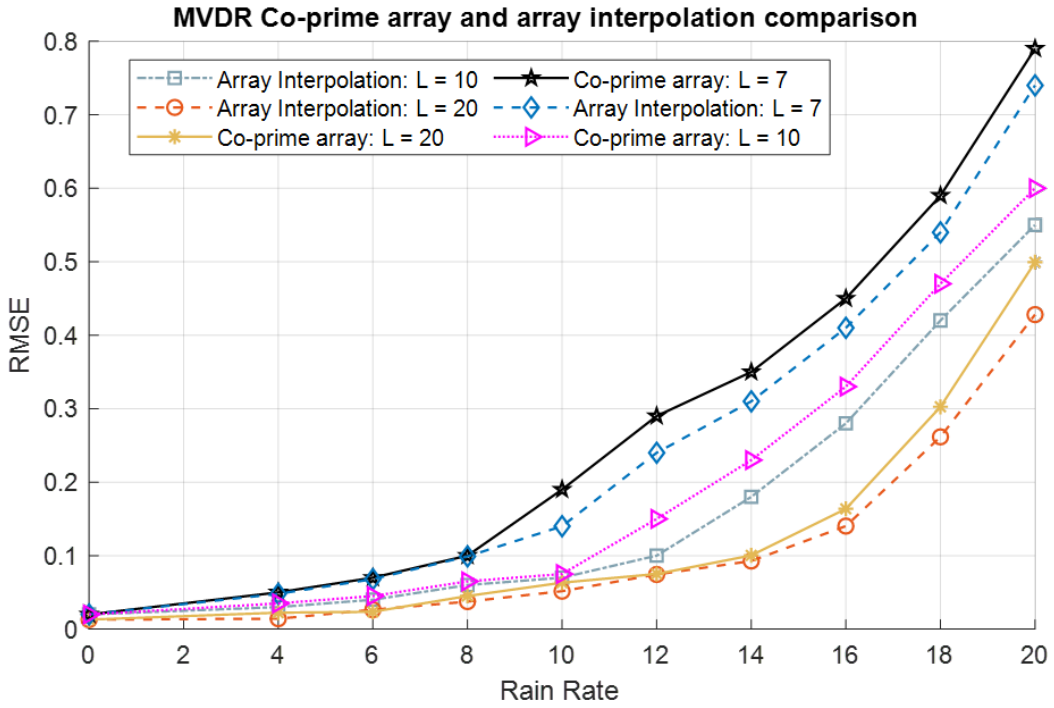


Fig. B.14: MVDR RMSE vs rain rate for coprime and array interpolation at L=7, 10, 20.

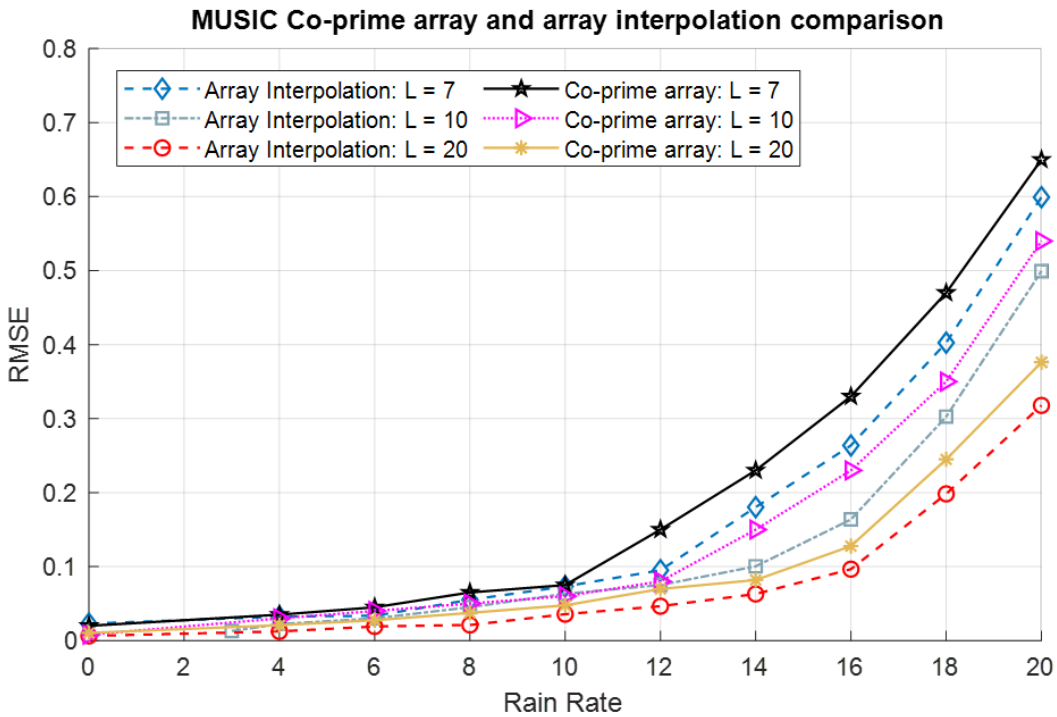


Fig. B.15: MUSIC RMSE vs rain rate for coprime and array interpolation at L=7, 10, 20.

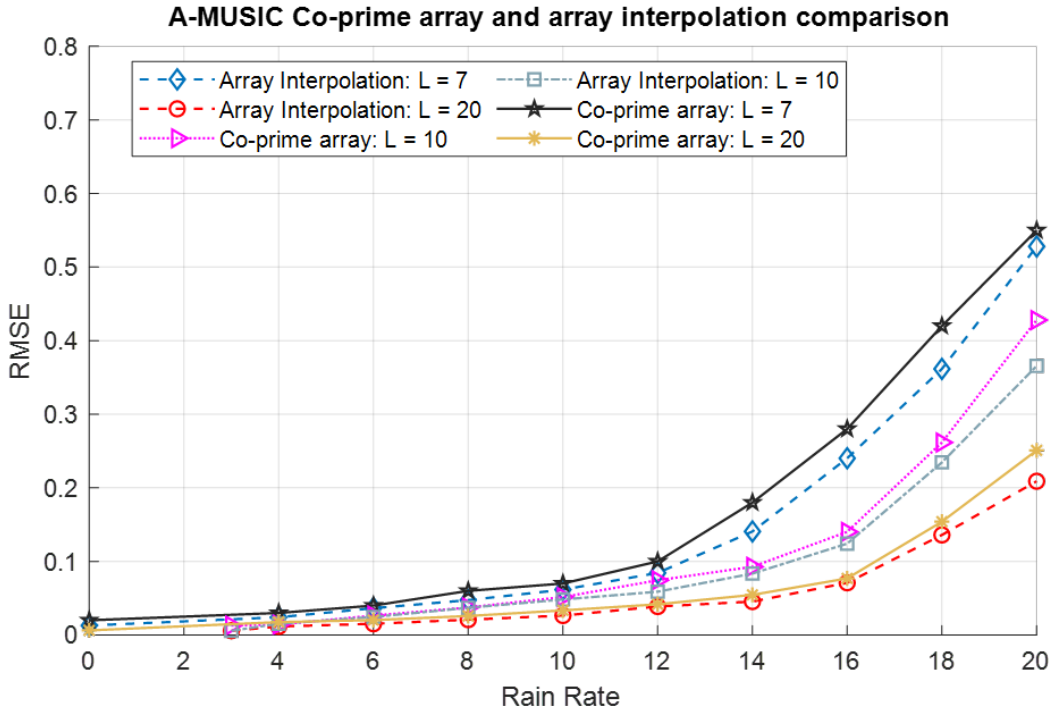


Fig. B.16: A-MUSIC RMSE vs rain rate for coprime and array interpolation at L=7, 10, 20.

The results of Fig. B17-B.19 represent a comparison of the three DOA algorithms for different rain rates at different antenna elements. As observed above, the RMSE increases with increase in rainfall and reduction in number of antenna elements. The proposed A-MUSIC performs better than MUSIC and MVDR in that order. This can be attributed to the repeated reconstruction of the covariance matrix to obtain two noise and signal subspaces continuously that are averaged for several iterations.

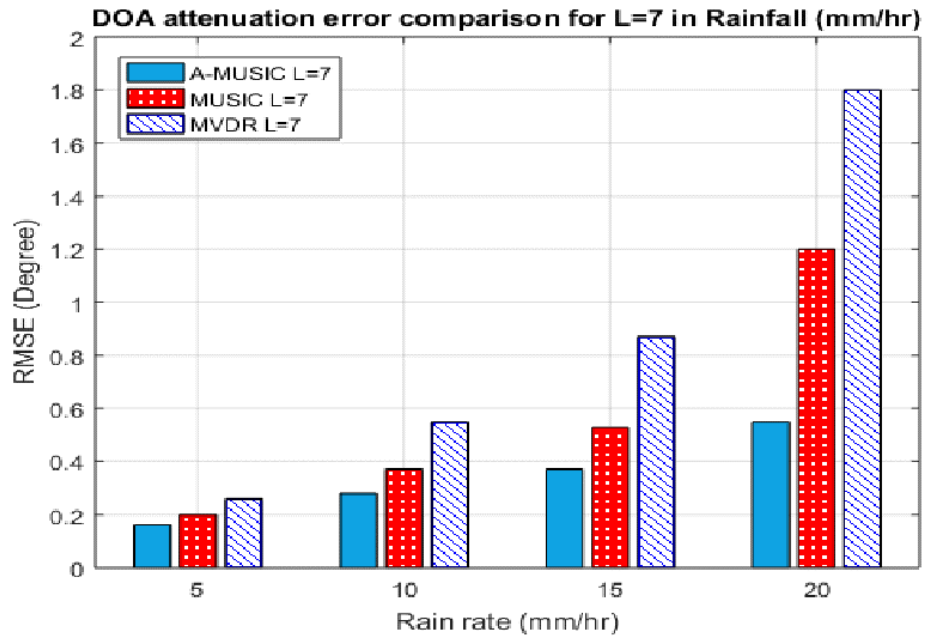


Fig. B.17: DOA estimation attenuation error comparison for L = 7.

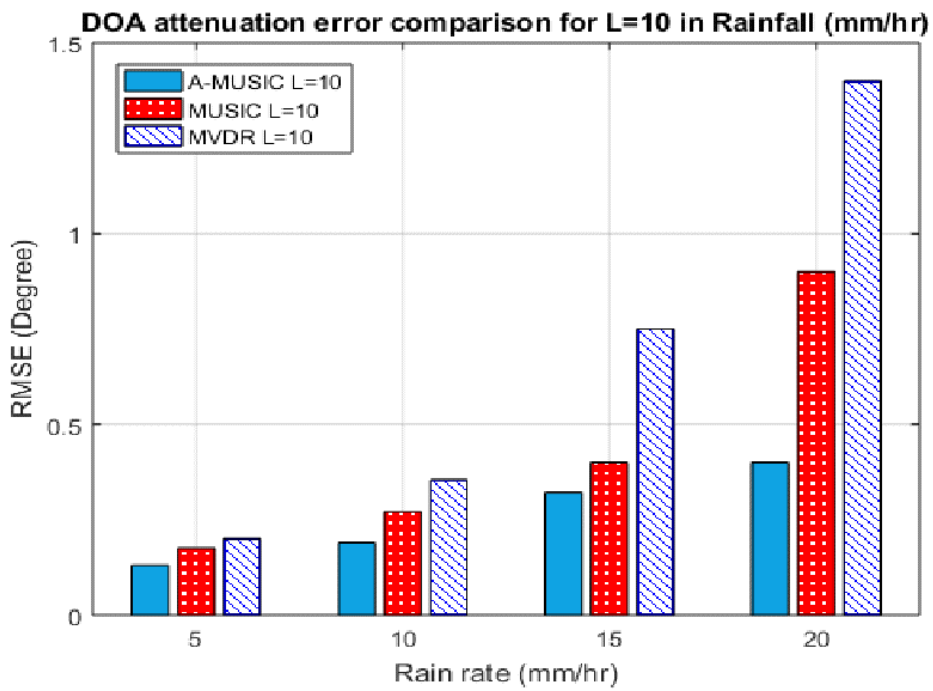
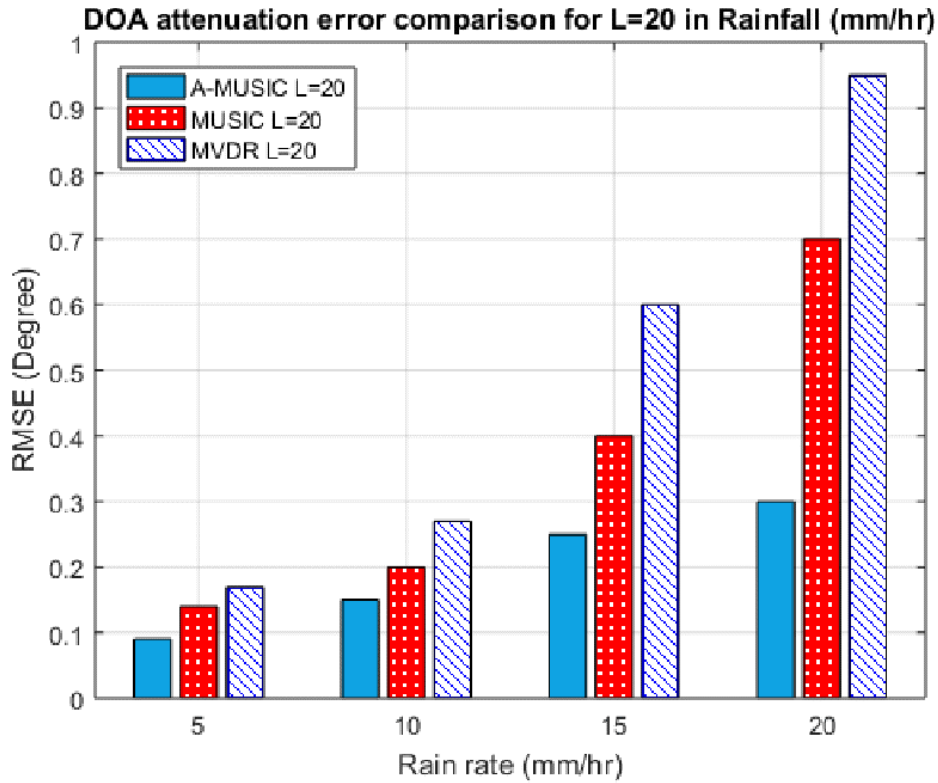


Fig. B.18: DOA estimation attenuation error comparison for L = 10.



**Fig. B.19:** DOA estimation attenuation error comparison for L = 20.

The performance of the system is investigated further at different SNR conditions for a co-prime configuration in Fig. B.20 and array interpolation in Fig. B.21 At  $r = 10$  mm/hr. It is observed that as the SNR increases, the RMSE decreases. The A-MUSIC co-prime array-based algorithm outperforms the MVDR and MUSIC algorithm, and its performance trend is within the CRB bounds. This demonstrates that the proposed method can still achieve satisfactory performance at lower SNR conditions.

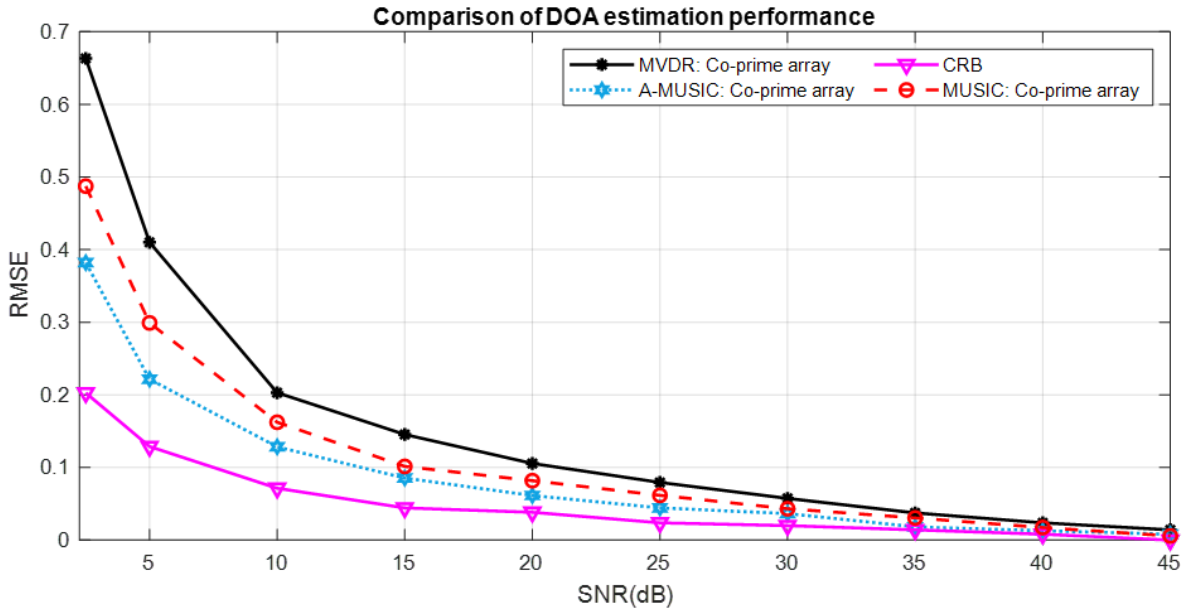


Fig. B.20: DOA estimation using co-prime array error comparison vs SNR.

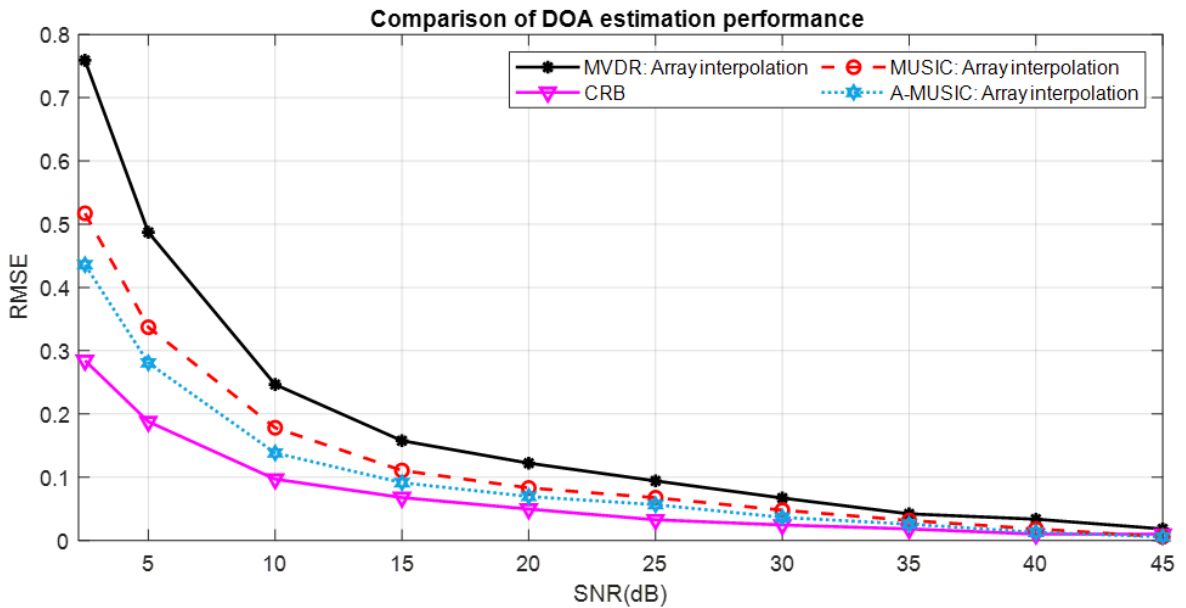


Fig. B.21: DOA estimation using array interpolation error comparison vs SNR.

In Fig. B.22, the systems error performance at various number of snapshots is presented for condition where  $r = 10$  mm/hr and  $SNR = 20$  dB. As expected, the RMSE decreases as we increase the number of trials from 100 to 500. Therefore, this shows that by increasing the number of simulation trials, the algorithm's performance can be greatly improved. Furthermore, one can intuitively observe that the performance of the proposed A-MUSIC surpasses the classical MUSIC and the MVDR estimator over the range of the number of snapshots simulated.

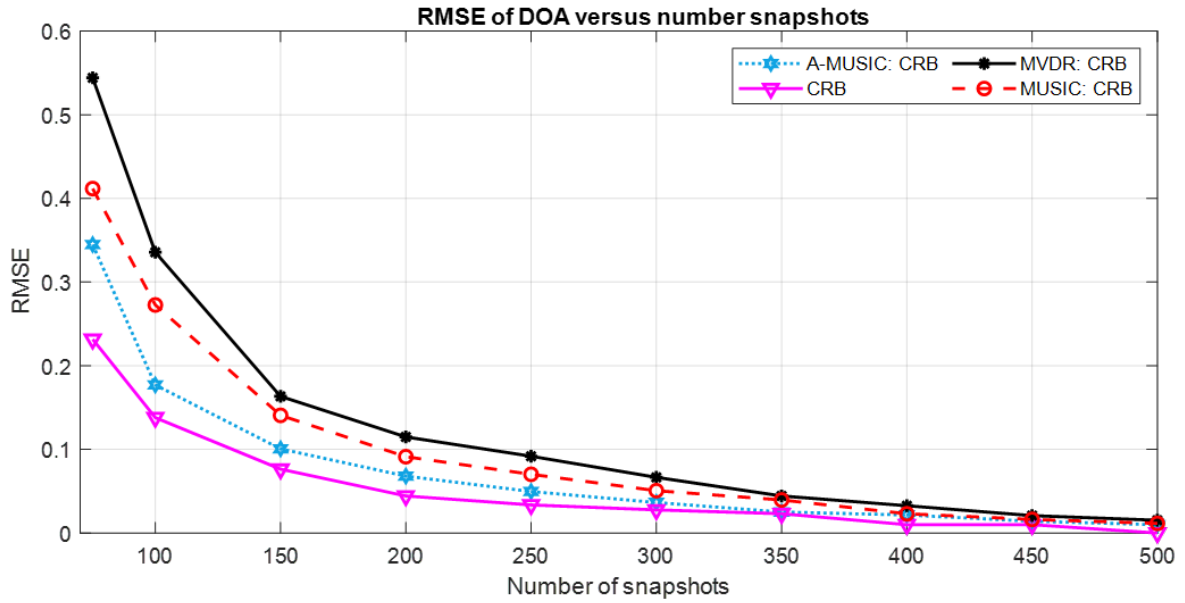


Fig. B.22: DOA estimation CRB error comparison vs number of snapshots.

In Fig. B.23, the computational complexity of A-MUSIC and the other DOA estimation algorithms is compared at different antenna elements. Although A-MUSIC algorithm have high performance in estimating the DOA, its computational complexity is high compared to MVDR and MUSIC estimations. This is because of the multiple averaging nature of A-MUSIC algorithm.

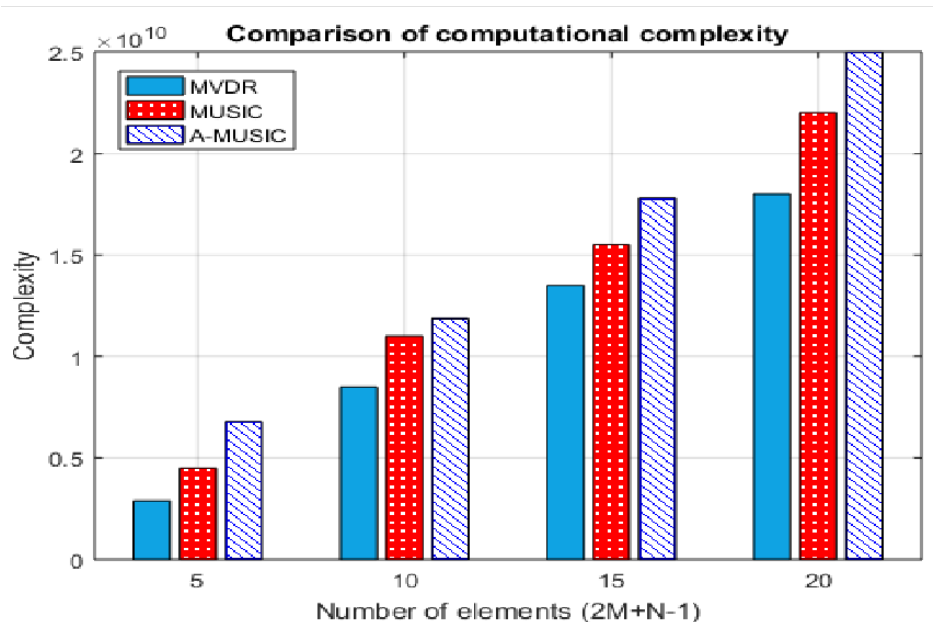


Fig. B.23: Comparison of computational complexity.

## 8 Conclusion

This work has investigated and evaluated the performance of DOA algorithms for Non-uniform Linear Arrays (NLA) in weather-impacted environment. The investigation is conducted with no rain, widespread, shower and thunderstorm rainfall events. From the investigation, the algorithm's performance accuracy significantly reduce from no rain condition to thunderstorm rainfall condition with MUSIC performing better than MVDR. In terms of RMSE, the algorithm's performance decline as the SNR values and number of snapshots are increased. The work develops an A-MUSIC algorithm for the weather impacted conditions in NLA. The performance of the developed A MUSIC is superior to the existing algorithm in terms of accuracy and RMSE parameters. This work opens further investigation of performance of DOA algorithms in weather-impacted environment and the need for a re-design of the existing algorithms. The accuracy of the investigated algorithms needs to be validated further while considering other statistical, analytical and computational measures.

## References

- [1] H. Krim and M. Viberg, "Two Decades of Array Signal Processing Research: The Parametric Approach," *IEEE Signal Processing Magazine*, vol. 13, no. 4, pp. 67–94, 1996.
- [2] C. E. Kassis, J. Picheral, and C. Mokbel, "Advantages of Non-uniform Arrays Using Root-MUSIC," *Signal Processing*, vol. 90, no. 2, pp. 689–695, 2010.
- [3] Z. M. Saric, D. D. Kukulj, and N. D. Teslic, "Acoustic Source Localization in Wireless Sensor Network," *Circuits, Systems and Signal Processing*, vol. 29, no. 5, pp. 837–856, 2010.
- [4] P. P. Vaidyanathan and P. Pal, "Sparse Sensing With Co-Prime Samplers and Arrays," *IEEE Transactions on Signal Processing*, vol. 59, no. 2, pp. 573–586, 2011.
- [5] Z. Tan, A. Nehorai, and Y. C. Eldar, "Continuous Sparse Recovery for Direction of Arrival (DOA) Estimation with Co-prime Arrays," in *2014 IEEE 8th Sensor Array and Multichannel Signal Processing Workshop (SAM)*, 2014, pp. 393–396.
- [6] Y.-H. Choi, "ESPRIT-Based Coherent Source Localization With Forward and Backward Vectors," *IEEE Transactions on Signal Processing*, vol. 58, no. 12, pp. 6416–6420, 2010.
- [7] T. Bronez, "Sector Interpolation of Non-uniform Arrays for Efficient High Resolution Bearing Estimation," *ICASSP-88., International Conference on Acoustics, Speech, and Signal Processing*.
- [8] B. Friedlander, "The Root-MUSIC Algorithm for Direction Finding With Interpolated Arrays," *Signal Processing*, vol. 30, no. 1, pp. 15–29, 1993.
- [9] P. Pal and P. P. Vaidyanathan, "Coprime Sampling and The Music Algorithm," in *2011 Digital Signal Processing and Signal Processing Education Meeting (DSP/SPE)*, 2011, pp. 289–294.
- [10] L. Yu, Y. Wei, and W. Liu, "Adaptive Beamforming Based on Non-uniform Linear Arrays (NLA) With Enhanced Degrees of Freedom," in *TENCON 2015 - 2015 IEEE Region 10 Conference*, 2015, pp. 1–5.
- [11] Y. Abramovich, N. Spencer, and A. Gorokhov, "Resolving Manifold Ambiguities in Direction-of-Arrival (DOA) Estimation for Non-uniform Linear Antenna (NLA) Arrays," *IEEE Transactions on Signal Processing*, vol. 47, no. 10, pp. 2629–2643, 1999.
- [12] Y.-P. Zhang, P. Wang, and A. Goldsmith, "Rainfall Effect on the Performance of Millimeter-Wave MIMO Systems," *IEEE Transactions on Wireless Communications*, vol. 14, no. 9, pp. 4857–4866, 2015.
- [13] Z. Pi and F. Khan, "An Introduction to Millimeter-wave Mobile Broadband Systems," *IEEE Communications Magazine*, vol. 49, no. 6, pp. 101–107, 2011.
- [14] A. Ishimaru, S. Jaruwatanadilok, and Y. Kuga, "Multiple Scattering Effects on The Radar Cross Section (RCS) of Objects in A Random Medium Including Back-Scattering Enhancement and Shower Curtain Effects," *Waves in Random Media*, vol. 14, no. 4, pp. 499–511, 2004. [Online]. Available: <https://doi.org/10.1088/0959-7174/14/4/002>

## REFERENCES

---

- [15] J. Agber and M. Akura, "A High Performance Model for Rainfall Effect on Radio Signals," vol. 3, 01 2013.
- [16] O. N. Calla and J. Purohit, "Study of Effect of Rain and Dust on Propagation of Radio Waves at Millimeter Wavelength," 01 1990.
- [17] Y. D. Zhang, S. Qin, and M. G. Amin, "DOA Estimation Exploiting Co-prime Arrays with Sparse Sensor Spacing," in *2014 IEEE International Conference on Acoustics, Speech and Signal Processing (ICASSP)*, 2014, pp. 2267–2271.
- [18] T. E. Tuncer, T. K. Yasar, and B. Friedlander, "Direction of Arrival (DOA) Estimation for Non-uniform Linear Arrays (NLA) by Using Array Interpolation," *Radio Science*, vol. 42, no. 04, pp. 1–11, 2007.
- [19] W. Li, X. Mao, W. Yu, and C. Yue, "An Effective Technique for Enhancing Direction Finding Performance of Virtual Arrays," *International Journal of Antennas and Propagation*, vol. 2014, pp. 1–7, 2014.
- [20] F. Belloni, A. Richter, and V. Koivunen, "DOA Estimation Via Manifold Separation for Arbitrary Array Structures," *IEEE Transactions on Signal Processing*, vol. 55, no. 10, pp. 4800–4810, 2007.
- [21] A. A. Alonge and T. J. Afullo, "Fractal Analysis of Rainfall Event Duration for Microwave and Millimetre Networks: Rain Queueing Theory Approach," *IET Microwaves, Antennas Propagation*, vol. 9, no. 4, pp. 291–300, 2015.
- [22] B. Kedem and L. S. Chiu, "On The Lognormality of Rain Rate," *Proceedings of the National Academy of Sciences*, vol. 84, no. 4, pp. 901–905, 1987.
- [23] H.-K. Cho, K. P. Bowman, and G. R. North, "A Comparison of Gamma and Lognormal Distributions for Characterizing Satellite Rain Rates from the Tropical Rainfall Measuring Mission," *Journal of Applied Meteorology*, vol. 43, no. 11, pp. 1586–1597, 2004.
- [24] I. T. U. ITU-R, "Specific attenuation Model for Rain for Use in Prediction Methods," *Recommendation*, pp. 838–3, 2005.
- [25] B. Friedlander and A. Weiss, "Direction Finding Using Spatial Smoothing with Interpolated Arrays," *IEEE Transactions on Aerospace and Electronic Systems*, vol. 28, no. 2, pp. 574–587, 1992.
- [26] Z. Tan and A. Nehorai, "Sparse Direction of Arrival (DOA) Estimation Using Co-Prime Arrays with Off-Grid Targets," *IEEE Signal Processing Letters*, vol. 21, no. 1, pp. 26–29, 2014.
- [27] Z. Li, C. Zhou, Y. Jia, G. Wang, C. Yan, and Y. Lv, "DOD and DOA Estimation for Bistatic Co-Prime MIMO Array Based on Correlation Matrix Augmentation," *2019 International Conference on Control, Automation and Information Sciences (ICCAIS)*, 2019.
- [28] B. P. Nxumalo and T. Walingo, "Direction Of Arrival (DOA) Estimation For Smart Antennas In Weather Impacted Environments," *Progress In Electromagnetics Research C*, vol. 95, pp. 209–225, 2019.
- [29] A. Nehorai and E. Paldi, "Acoustic Vector-Sensor Array Processing," *IEEE Transactions on Signal Processing*, vol. 42, no. 9, pp. 2481–2491, 1994.

## REFERENCES

---

- [30] P. Stoica and A. Nehorai, "Performance Study of Conditional and Unconditional Direction-of-Arrival (DOA) Estimation," *IEEE Transactions on Acoustics, Speech, and Signal Processing*, vol. 38, no. 10, pp. 1783–1795, 1990.
- [31] Z. Meng and W. Zhou, "Direction-of-Arrival (DOA) Estimation in Co-prime Array Using the ESPRIT-Based Method," *Sensors*, vol. 19, no. 3, pp. 707–721, 2019.

## **Part III**

# **Conclusion**

# Conclusion

We conclude this dissertation by summarizing the contributions and present potential future research trends that are related to our accomplished work.

The introduction detailed the evolution of communication networks, Direction of Arrival (DOA) estimation algorithms and the modelling of radio propagation in rainfall environment, the research motivation, methodology, and contributions were also clearly stated in the introduction. The DOA plays a very big role in wireless communication systems particularly in array signal processing. It has many application in engineering fields such as radar, sonar, weather forecasting, tracking targets, ocean and geological exploration, seismic survey and biomedical, and communications in general. The main idea in the DOA estimation is to use an array of antennas to receive a narrowband signal from a far field sources in the diverse directions. The signal received is then processed using a sub-space method that has a high resolution and an accurate DOA estimation. Thus, the investigation for efficient solutions to encourage improvement in DOA estimation performance are the main objective this of research. The summary of the research contributions is comprehensively outlined in the section below, which sets the direction for the future works.

## 1 Summary of research contribution

In paper A, we studied the Direction of Arrival (DOA) estimation for smart antennas in weather impacted environments. The investigated DOA, included: MVDR, MUSIC, and our proposed DOA method the A-MUSIC that addressed the issues signal attenuation in weather impacted environment and improved system-capacity. The investigation was carried in various rainfall condition such as drizzle, shower, widespread and thunderstorm. The simulation results show performance degradation in a rainfall impacted communication network with the developed algorithm showing better performance degradation.

In paper B, we study the performance evaluation of DOA algorithms for non-uniform linear arrays in a weather impacted environment. The performance of Minimum Variance Distortionless Response

(MVDR), Multiple Signal Classification (MUSIC) and our proposed Advanced-MUSIC (A-MUSIC) non-uniform linear array (NLA) algorithms on a weather impacted wireless channel is investigated. The co-prime and array interpolation NLA configurations are investigated on a markovian rainfall channel model capturing widespread, shower and thunderstorm rain events. The results indicate that the algorithms experience severe performance degradation in a weather affected environment. However, the developed NLA algorithm achieves better Direction of Arrival (DOA) estimation than the conventional NLA.

## 2 Possible Future Work

This section provides some insight on possible future trends that could extend to this work and other contributions related to DOA, radio propagation signal and rainfall attention. The Direction of Arrival (DOA) estimation methods, theory and other technologies in smart array antennas have become well established some further investigations can be conducted as:

1. In future, one can work on the other geometry of antenna used in array signal processing like L shape and 2L shape parametric estimation.